2017

# Oral squamous cancer cell-bone interactions and resistance to alendronate (Fosamax) drug therapy in 3D-live bone-microenvironment

BOSTON UNIVERSITY

HENRY M. GOLDMAN SCHOOL OF DENTAL MEDICINE

THESIS

# ORAL SQUAMOUS CANCER CELL-BONE INTERACTIONS AND RESISTANCE TO ALENDRONATE (FOSAMAX) DRUG THERAPY IN 3D-LIVE BONE-MICROENVIRONMENT

by

**MELODY YA-DI HWANG**

B.A. University of California, Berkeley, 2005

D.M.D. University of Nevada, Las Vegas, 2012

Submitted for the partial fulfillment of the requirements for the degree of

Master of Science in Dentistry

In the Department of Periodontology

2017

## Reader's Approval

First Reader

**Erdjan Salih, Ph.D.**

Research Associate Professor, Department of Periodontology

_____ _____

Date Signature

Second Reader

**Wayne Gonnerman**

Assistant Professor, Department of Periodontology

_____ _____

Date Signature

**Department Approval**

**Serge Dibart**

Director and Chairman, Department of Periodontology

| | |
|---|---|
| _____ | _____ |
| Date | Signature |

## Dedication

I will like to thank my father, Dr. James Hwang, and my mother, Emily Hwang, for their continuous support, guidance and their unconditional love. Without them, I would not be where I am today. Thank you to my sister, Dr. Lillian Hwang, for sharing not only the journey of this residency, but also her life with me. Thank you to my younger sister, Nina Hwang, for always believing in me and seeing my strength and potential.

## Acknowledgements

First and foremost, I would like to thank Dr. Serge Dibart, Director and Chairman of Department of Periodontology at Boston University, Henry M. Goldman School of Dental Medicine, for giving me the opportunity to be a part of this program.

I would like to thank my advisor, Dr. Erdjan Salih, for all of his guidance and encouragements. He has been a great mentor and without his support my thesis project would not be completed.

Thank you to Dr. Taisuke Ohira, my co-resident in the Department of Periodontology, who has spend numerous hours with me analyzing data and giving me valuable insights.

Lastly, I would like to thank staffs in the Department of Periodontology at Boston University who assisted me through this year of research.

**ORAL SQUAMOUS CANCER CELL-BONE INTERACTIONS AND RESISTANCE TO ALENDRONATE (FOSAMAX) DRUG THERAPY IN 3D-LIVE BONE-MICROENVIRONMENT**

**MELODY YA-DI HWANG**

Boston University, Henry M. Goldman School of Dental Medicine, 2017

Erdjan Salih, Ph. D. Research Associate Professor, Department of Periodontology

## ABSTRACT

Bisphosphonates (BPs) have been used clinically as anti-resorptive/cancer agents with confounded clinical outcomes and uncertain/conflicting biological understanding. This study was designed to evaluate the impact of clinically used anti-resorption drug alendronate (ALN) on cancer-bone metastasis and bone biology using novel 3D cancer-bone interaction model systems.

To test the effects of ALN on the cancer-bone metastasis/interactions and bone biology we have utilized a novel 3D Co-cultures of live mouse neonatal calvarial bone organs with oral squamous cancer cells in a roller tube model systems (Curtin et al, 2012) in the absence and presence of ALN. These model systems under bone resorption and formation conditions were evaluated by chemical, biochemical, and histological analyses of the used media and calvarial bones. At the end of 8 days, the calvarial bones co-cultured with oral cancer cell lines in the absence and presence of ALN were processed for histological

observations, TRAP and ALP enzyme activities, and neutral red staining. These studies were complemented by the effects of ALN on oral cancer cells under 2D classic cell culture conditions.

In 3D-bone organ cultures under resorption conditions, oral cancer cells induce differentiation of osteoclasts and bone resorption and inclusion of ALN inhibited cancer-induced bone resorption. However, in both bone resorption and formation models the oral cancer cells colonized the bone and while treatment with ALN inhibits bone resorption, no effect on bone colonization was evident. Contrary to those under 2D cell culture conditions exposure to ALN of confluent and non-confluent oral cancer cells in the absence of live bone impacted oral cancer cells significantly in a dose dependent manner.

Our studies using live bone organ cultures with oral cancer cells under specific dissociated bone remodeling stages, viz., resorption or formation only, revealed major and significant biological events which led to the conclusions that: (a) In the absence of bone in 2D cultures oral cancers are sensitive to ALN treatment whereas in the 3D live bone microenvironment tumors are resistant to ALN drug therapy, and (b) oral cancer-bone metastasis is independent of bone remodeling stage.

## Table of Content

## List of Figures

## List of Table

## List of Abbreviations

ASC: Ascorbic acid
ALN: Alendronate
ALP: Alkaline phosphate
ATP: Adenosine triphosphate
BMP: Bone morphogenetic protein
BMU: Basic multicellular unit
BP: Bisphosphonate
BPT: Bisphosphonate treatment
BRONJ: Bisphosphonates-related osteonecrosis of the jaws
BSA: Bovine serum albumin
DMEM: Dulbecco's Modified Eagle Medium
DXA: Dual X-ray absorptiometry
FCS: Fetal calf serum
FPP: Farnesyl diphosphate
FPPS: Farnesyl pyrophosphate synthase
GGPP: Geranylgeranyl diphosphate
H&E: Hematoxylin & eosin
HA: Hydroxyapatite
HPV: Human papilloma virus
HSV: Herpes simplex virus
IPP: Isopentenyl pyrophosphate
MNOC: Multi-nucleated Osteoclast
NBP: Nitrogen-containing bisphosphonate
NR: Neutral Red
OB: Osteoblast
OC: Osteoclast
OPG: Osteoprotegrin
p-NP: p-nitrophenol
p-NPP: p-nitrophenyphosphate
PTH: Parathyroid hormone
RA: Resorption Area
RANK: Receptor activator of nuclear factor kappa-B
RANKL: Receptor activator of nuclear factor kappa-B ligand
SCC: Squamous cell carcinoma
TC: Tumor Cells;
TRAP: Tartrate resistant acid phosphatase

# 1. Squamous Cell Carcinoma

## *1.1 Epidemiology*

Squamous cell carcinoma (SCC) is the most common intraoral malignancy, accounting for 94% of all oral malignancies. In the United State it is the 8$^{th}$ most common cancer in males and 15$^{th}$ most common in females; its highest incidence rate is in middle-age males of African ancestry. (Neville, 2008)

## *1.2 Risk Factors of Oral Cancer*

The cause of SCC is multifactorial including both extrinsic and intrinsic factors. Some of the extrinsic factors include tobacco smoke, alcohol, syphilis and sunlight/UV exposure. Systemic intrinsic factors include factors such as malnutrition ad iron-deficiency anemia.

### *1.2.1 Tobacco Smoke*

Smokers have 2-3 times greater risk of developing SCC than the non-smoking general population. Patients who continue to smoke after diagnosis have 2-6 times greater risk of developing a second primary carcinoma. Furthermore, people smoking a pipe or cigars have a greater risk of developing oral cancer than cigarette smokers and the risk increase with dosage and smoking duration. (Neville, 2008)

### *1.2.2 Alcohol*

Alcohol consumption in combination with tobacco smoking is a significant risk factor for SCC development. This risk is dose- and time-dependent, and can increase a person's risk for oral cancer by 15 times or more (Neville, 2008).

### *1.2.3 Syphilis*

Tertiary stage syphilis has a strong association with the development of dorsal tongue SCC. However, syphilis-associated oral cancer is rare today because syphilis is typically diagnosed and treated before the infection progresses to the tertiary stage.

### *1.2.4 Radiation Exposure*

Prolonged exposure to ultraviolet radiation can increase the risk of developing SCC of the lips. Furthermore, radiation therapy of the head and neck area can increase the risk of later development of a new primary oral malignancy, and this effect is dose dependent.

### *1.2.5 Iron Deficiency*

Iron deficiency is associated with increased risk of SCC of the esophagus, oropharynx, and posterior mouth. People who suffer from iron deficiency tend to have impaired cell-mediated immunity and their epithelial cells have a higher turnover rate which can lead to atrophic or immature mucosa.

### 1.2.6 *Oncogenic Viruses*

No virus has been proven to cause oral cancer, but herpes simplex viruses (HSVs), retroviruses, and human papilloma viruses (HPVs) have all been suggested to play a role in the development of SCC. HPV subtypes 16, 18, 31,

and 33 are the strains that have been found to associate with dysplasia and SCC. (Neville, 2008)

### *1.3 Clinical and Radiographic Features*

SCC can vary in its clinical presentation and it can present as: exophytic (mass forming, irregular, papillary), endophytic (depressed, ulcerated, rolled border of red/white mucosa), leukoplakic (white patch), erythroplakic (red patch), or erythroleukoplakic (red-and-white patch).

Extraorally, SCC can be found at either upper/lower lips or the lip vermillion. Almost 90% of the extraoral lesions are located on the lower lip. Carcinoma of the lip vermillion is usually found on people with long-term UV radiation exposure and is usually associated with actinic cheilosis. SCC on the vermillion is typically a crusted, non-tender ulceration less than 1cm in diameter when discovered. It is characterized by slow growth rate. (Neville, 2008)

Intraorally, the most common sites for SCC include the lateral/ventral surfaces of tongue (50% of intraoral cancer) and floor of the mouth (35% of intraoral cancer). Other possible sites of development include the hard/soft palate, buccal mucosa, and gingival tissue. If the tumor is adjacent to a tooth it may mimic periodontal disease or pyogenic granuloma. (Neville, 2008)

SCC found at the soft palate or oropharyngeal mucosa is generally greater in size and is usually accompanied by symptoms such as dysphagia or referred pain to the ear.

When destruction of underlying bone is present, symptoms may be painful or completely painless. Radiographically it will appear as a “moth-eaten” radiolucency with ill-defined margins. (Neville, 2008)

### *1.4 Metastasis*

Metastatic spread of oral SCC is largely through the lymphatic system to the ipsilateral cervical lymph nodes. When the lymph node is affected it is usually firm to touch, non-tender and enlarged. If the malignant cells have perforated the capsule of the lymph node then the node will feel fixed. Extracapsular invasion is associated with poor prognosis, increased risk of recurrence, distant metastasis and lower survival rate. (Neville, 2008)

Most common sites of SCC distant metastasis are lung, liver, and bone. The incidence rate of distant metastasis can range from 3.8% to 23% (Takahama et al, 2014). Most distant metastases are asymptomatic and are discovered and diagnosed only during autopsy. In a retrospective study (Carlson & Ord, 2002), 4 out of 597 patients diagnosed with SCC had vertebral metastases accounting for 0.7% of the series. Each of the patients experienced severe pain, hypercalcemic somnolence, and flaccid paralysis of the lower extremities (Carlson & Ord, 2002). Takahama et al (2013) reported a case of SCC with metastasis to the calvarias 1 year after initial diagnosis. Important predictive factors for SCC distant metastasis include the site of the primary tumor (hypopharyngeal tumor has the greatest risk), advanced T/N classification, histological grade, and ability to achieve local regional disease

control (Takes et al, 2012). Median survival rate is 8.9 months for patient with lung metastasis, and 1.8 month for bone metastasis (Kowalski et al, 2005).

### *1.5 Staging*

The most commonly used staging protocol is the tumor-node-metastasis (TNM) system. This protocol depends on these three clinical features: T (size of primary tumor in centimeters); N (involvement of local lymph nodes); and M (distant metastasis). Higher the stage classification indicates a poor prognosis.

**Figure 1 – SCC at the Lateral Border of Tongue.** An ulcerated, exophytic SCC of the posterior lateral border of the tongue**.** Reproduced from (Neville, 2008).

**Figure 2 – SCC at the Lower Lip Vermillion.** A SCC that manifested as a small crusted ulcer on the lower lip vermillion. Reproduced from (Neville, 2008)

| **Primary Tumor Size (T)** | |
|---|---|
| TX | No available information on primary tumor |
| T0 | No evidence of primary tumor |
| Tis | Only carcinoma *in situ* at primary site |
| T1 | Tumor 2 cm or less in greatest diameter |
| T2 | Tumor more than 2 cm but not more than 4 cm in greatest diameter |
| T3 | Tumor more than 4 cm in greatest diameter |
| T4a | (Lip) Tumor invades through cortical bone, inferior alveolar nerve, floor of mouth, or skin of face (i.e., chin, nose) |
| | Tumor is resectable |
| T4a | (Oral cavity) Tumor invades through cortical bone, into deep extrinsic tongue muscles (genioglossus, hyoglossus, palatoglossus, and styloglossus), maxillary sinus, or skin of face |
| | Tumor is resectable |
| T4b | Tumor involves masticator space, pterygoid plates, or skull base and/or encases internal carotid artery |
| | Tumor is unresectable |
| **REGIONAL LYMPH NODE INVOLVEMENT (N)** | |
| NX | Nodes could not be or were not assessed |
| N0 | No regional lymph node metastasis |
| N1 | Metastasis in a single ipsilateral node 3 cm or less in greatest diameter |
| N2 | Metastasis in a single ipsilateral node more than 3 cm but not greater than 6 cm in greatest diameter; multiple ipsilateral nodes, none more than 6 cm in greatest diameter; or bilateral or contralateral nodes, none more than 6 cm in greatest diameter |
| N2a | Metastasis in a single ipsilateral node more than 3 cm but not greater than 6 cm in greatest diameter |
| N2b | Metastasis in multiple ipsilateral nodes, none more than 6 cm in greatest diameter |
| N2c | Metastasis in bilateral or contralateral nodes, none more than 6 cm in greatest diameter |
| N3 | Metastasis in a node more than 6 cm in greatest diameter |
| **Involvement by Distant Metastases (M)** | |
| MX | Distant metastasis was not assessed |
| MO | No evidence of distant metastasis |
| M1 | Distant metastasis is present |

**Figure 3 – Tumor-Node-Metastasis (TNM) Staging System for Oral SCC**. Tumor (T) refers to the size of the primary tumor; Node (N) refers to presence of regional lymph node metastasis; and Metastasis (M) refers to the presence of distant metastasis. Reproduced from (Neville, 2008)

| | | Five-Year Relative Survival Rate | |
|---|---|---|---|
| **Stage** | **TNM Classification** | **Oral Cavity** | **Lip** |
| Stage I | T1 N0 M0 | 68% | 83% |
| Stage II | T2 N0 M0 | 53% | 73% |
| Stage III | T3 N0 M0, or T1, T2, or T3 N1 M0 | 41% | 62% |
| Stage IV | | 27% | 47% |
| IVA | T4a N0 or N1 M0, or T1, T2, T3, or T4a N2 M0 | | |
| IVB | Any T N3 M0, or T4b any N M0 | | |
| IVC | Any M1 lesion | | |

**Figure 4 – TNM Clinical Staging Criteria for SCC.** The staging criteria of SCC based on the TNM classification, and the 5-year relative survival rate for each stage. Reproduced from (Neville, 2008)

### *1.6 Histopathologic Features*

SCC is characterized by invasive islands of malignant squamous epithelial cells with irregular extensions of epithelium through the basement membrane and into the sub-epithelial connective tissue. The invading cells may extend deeply into the underlying adipose tissue, muscle, or bone, and destroy the original tissue. Strong inflammatory responses can often be noted along with focal areas of necrosis. Some of the common histologic features include hyperchromatic nuclei, increased nuclear-to-cytoplasmic ratio, and keratin pearls, which are concentrically layered keratinized cells. The histopathologic evaluation of the degree to which the tumors resemble their original tissue is called grading. Less differentiated tumors receive higher grades. A well-differentiated SCC that closely resembles its parental tissue is called *low-grade*, and in general it grows at a slower rate and tends to metastasize later in its course.

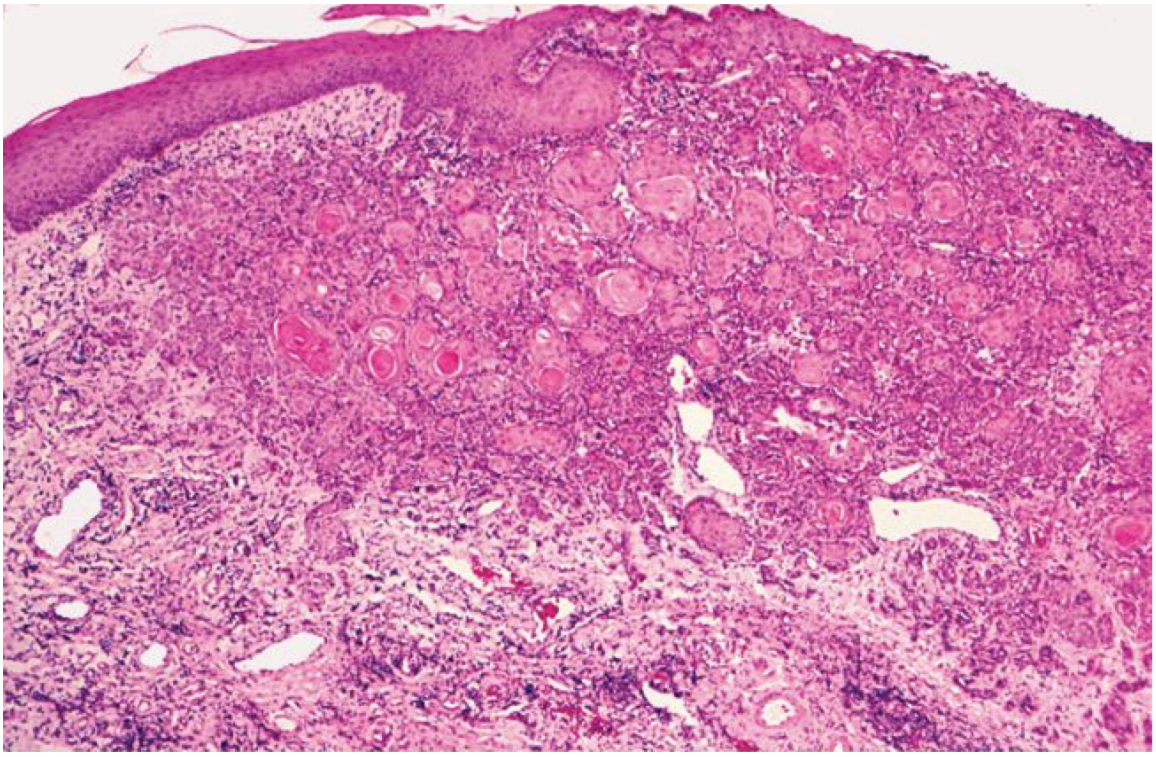

**Figure 5 – Photomicrograph of A Well-Differentiated SCC.** Islands of squamous epithelium are shown invading the lamina propria. Reproduced from (Neville, 2008)

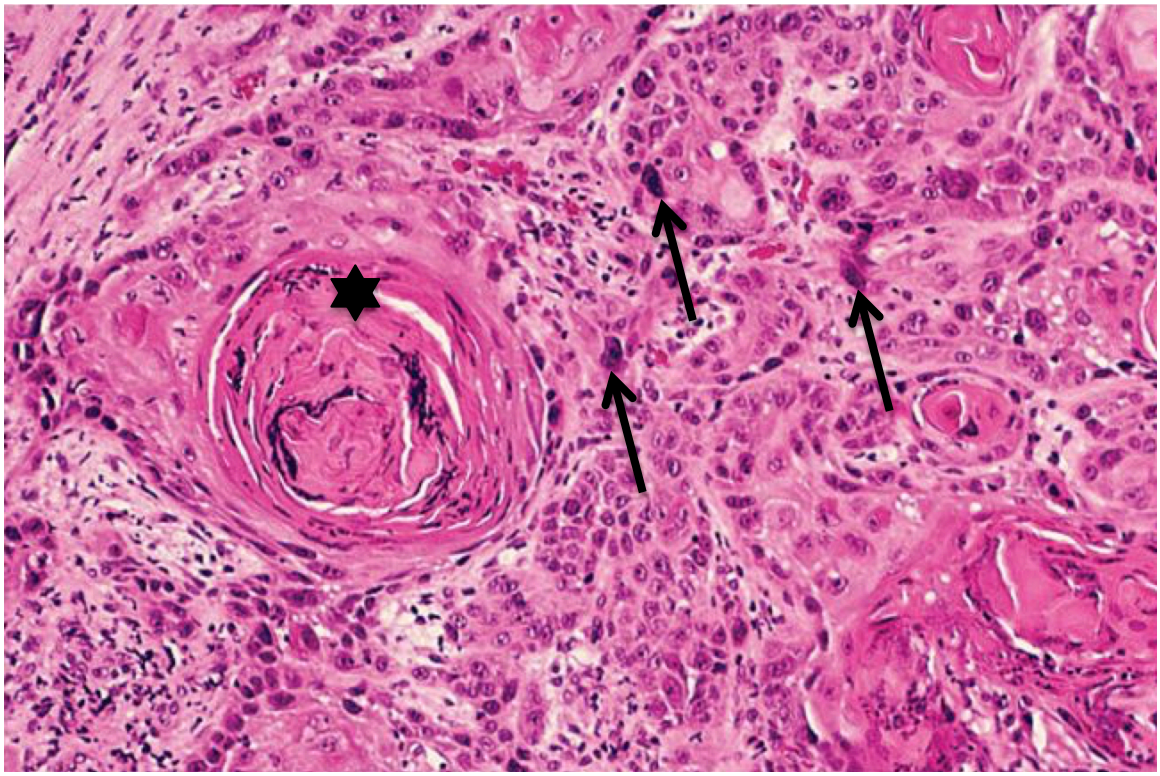

**Figure 6 – Photomicrograph of A Well-Differentiated SCC with Keratin Pearls.** Epithelial cells with hyperchromatic nuclei (arrows) are present along with keratin pearl formation (star). Reproduced from (Neville et al, 2008)

### *1.7 Treatment and Prognosis*

SCC of the vermillion is usually treated with surgical wedge resection, with 5-year survival rates of 95%-100%. SCC of the upper lip is less common than lower lip or vermillion SCC, and has 5-year survival rate of 58% (Neville, 2008).

Treatments for intraoral SCC is dictated by the clinical stage of the disease, and may include radical surgical excision, radiation therapy, or a combination of surgery with radiation therapy. Indications for radiation therapy include oropharyngeal lesions, regional metastasis, and high-grade histopathologic features. When local lymph nodes metastasis is suspected radical neck dissection can be performed.

Chemotherapy is generally administered concurrently with radiation therapy or by itself as palliative therapy. Some of the commonly used chemotherapy agents include platinum-containing compounds, 5-fluorouracil, and paclitaxel/docetaxel.

The prognosis for SCC depends on the tumor stage; stage I and II patients have 53%-68% 5-year survival rates while stage III and IV patients have 27%-41% 5-year survival rates. Therefore, early diagnosis is important for improving treatment outcomes.

## 2. Bone biology

### *2.1 Bone Structure*

Bone is a mineralized connective tissue whose functions include support, protection, mineral storage, and hemopoiesis. Bone can be classified as either

long or flat bone. Long bones include bones of the extremities, such as femur, tibia, radius, ulna and humerus. Flat bones include the skull, sternum, scapula, and pelvis. All bones are composed of a dense outer compact bone and a central medullary cavity which is filled with red or yellow bone marrow and a network of trabecular bone.

Histologically, compact bone is composed of lamellae which can be classified as circumferential (forming the outer and inner perimeter of bone), concentric (forming the osteon), and interstitial (fragments of pre-existing concentric lamellae that are interspersed between adjacent concentric lamellae). The osteon, also called the haversian system, is the basic unit of bone. It is a cylinder of bone that is usually 0.2mm in diameter and 2mm in length and is oriented parallel to the long axis of bone. At the center of the osteon is the haversian canal which houses a capillary, and adjacent haversian canals are interconnected by Volkmann canals that create a vascular network throughout compact bone. (Nanci, 2008)

Trabecular , or spongy, bone is a network of thin plates of bone within the bone marrow cavity. The bone marrow contains progenitor cells for white blood cells, red blood cells, and platelets and plays a role in hemopoiesis.

The outer aspect of every compact bone is covered by the periosteum which is a connective tissue membrane that consists of an outer and inner layer. The outer layer of periosteum consists of a dense, irregular connective tissue and fibroblasts, while the inner layer consists of osteoprogenitor cells and fibroblasts. The internal surface of compact and trabecular bone is covered by

the endosteum composed of loose connective tissue, osteoprogenitor cells, osteoblasts (OB), and occasionally osteoclasts (OC).

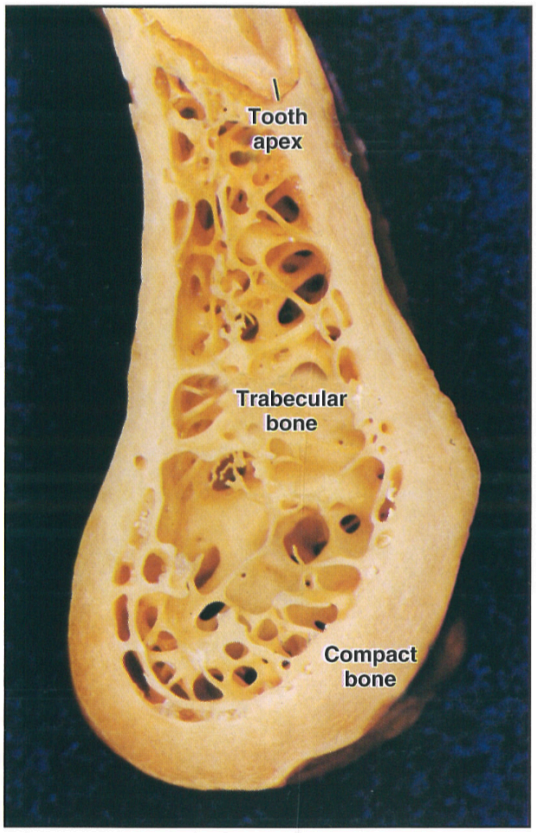


**Figure 7 – Compact Bone and Trabecular Bone**. An image of the body of the mandible, demonstrating the outer layer of compact bone and inner network of trabecular bone. Reproduced from (Nanci, 2008)

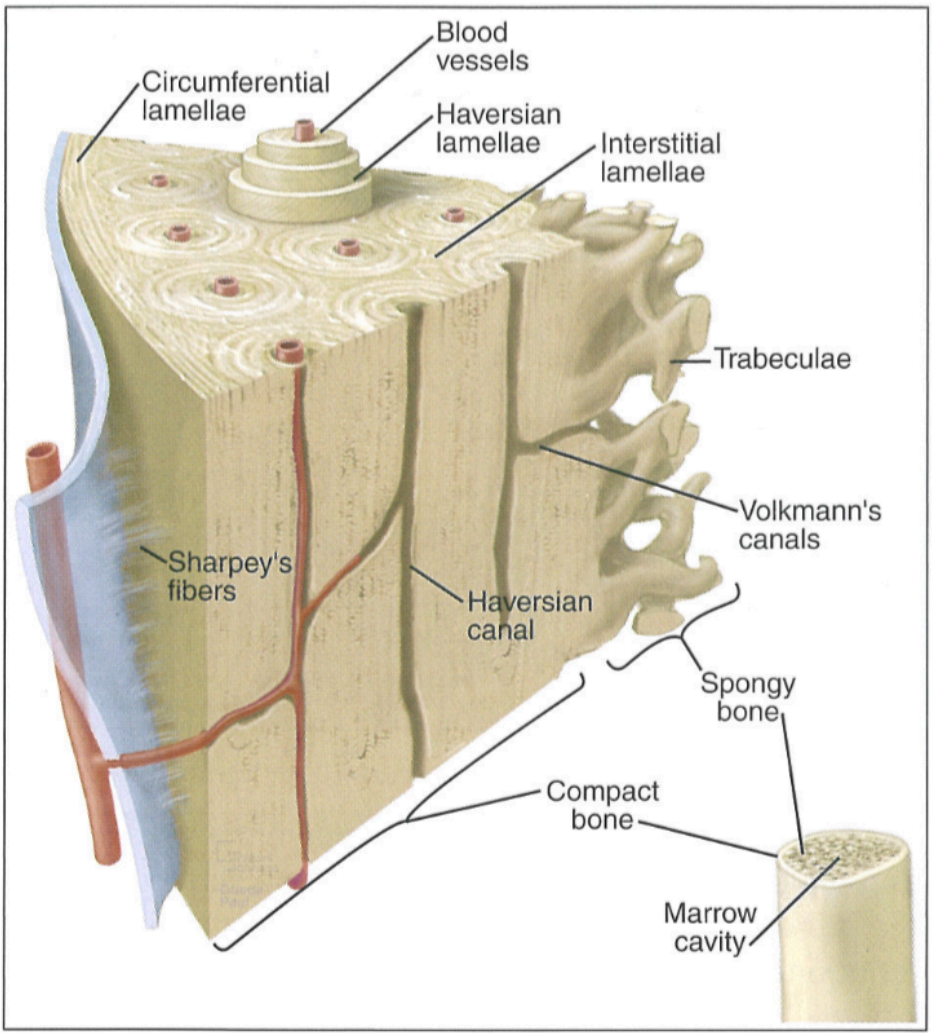


**Figure 8 – Structural Organization of Bone.** Cross-section depicting organizational components of bone, including circumferential lamellae, osteon, interstitial lamellae, Haversian canal, and Volkmann's canal. Reproduced from (Nanci, 2008)

## *2.2 Bone Composition*

### *2.2.1 Extracellular Composition*

The extracellular matrix of bone accounts for about 90% of the weight of bone. The inorganic component accounts for 65% of the dry weight of bone, while the organic component accounts for the other 35% (Buckwalter et al, 1996)

The inorganic component of the extracellular matrix is composed primarily of hydroxyapatite (HA), which contributes to the compressive strength of bone. HA is a naturally occurring mineral composed of calcium, phosphate, and hydroxide ions with a chemical formula of $Ca_{10}(PO_4)_6(OH)_2$. The unit cell of HA is hexagonal, and when stacked together they form a crystalline lattice. (Nanci, 2008)

Type 1 collagen produced by OB makes up 90-95% of the organic component of the extracellular matrix. The remainder contains hyaluronic acid, as well as non-collagenous proteins such as osteocalcin, osteopontin, and bone sialoprotein. Collagen fibers are composed of basic subunits called tropocollagen molecules which are made of two α1 and one α2 polypeptide chains wound into a triple helix (Bornstein, 1985). They aggregate into fibrils in a one-quarter stagger configuration leaving a gap between the tail of one tropocollagen molecule and the head of the succeeding molecule of a single row, Tails of tropocollagen molecules overlap the heads of tropocollagen molecules in adjacent rows. This arrangement allows formation of covalent cross links which contributes to the bone strength. (Nanci, 2008)

### *2.2.2 Cellular Composition*

There are at least two different cell lineages present in bone: 1) osteogenic cells that form and maintain bone, and 2) osteoclasts that resorb bone. Osteogenic cells include osteopregenitors, osteoblasts, osteocytes, and bone lining cells all of which are derived from mesenchymal stem cells. OCs are derived from hemopoietic stem cells. OBs, OCs and bone lining cells can be found on the surfaces of the bone while osteocytes are found in the interior of bone. (Nanci, 2008; Buckwalter et al, 1996)

#### *2.2.2.1 Osteoblasts*

Osteoblasts are mononucleated cells that arise from mesenchymal stem cells in the axial skeleton and from ectomesenchymal stem cells in the head (Buckwalter et al, 1996). Osteoblasts can be cuboidal or slightly flattened in shape. They are primarily responsible for synthesizing type 1 collagen and noncollagenous bone matrix proteins. Collagen molecules can assemble extracellularly to form fibrils, and accumulate as an uncalcified matrix called osteoid which will act as scaffold for the deposition of the apatite crystals. (Nanci, 2008)

In addition, osteoblasts also secrete cytokines and growth factors that help to regulate bone formation and cellular function. They include transforming growth factor β (TGF- β), platelet-derived growth factor (PDGF), and insulin-like growth factor (IGF-I and IGF-II), which are members of the bone morphogenic protein (BMP) superfamily (Fleisch, 2000).

Osteoblasts form a layer of cells connected by gap junctions over the forming surface of bone. When bone formation ceases osteoblasts flatten substantially and become bone lining cells. These inactive OBs are elongated in shape and contain fewer protein synthetic organelles. Bone lining cells cover most of the surface of the adult skeleton and it has been postulated that by retaining the gap junctions they create a network that functions to control mineral homeostasis (Nanci, 2008).

#### *2.2.2.2 Osteocytes*

Osteocytes are osteoblasts that become trapped within the extracellular matrix during bone formation. The number of osteocytes depends on the rate of bone formation. If bone formation is rapid then more osteocytes are present per unit volume. The space that the osteocyte occupies in the extracellular matrix is called a lacuna. Extensions of these lacunae form canaliculi which are channels that house radiating osteocytic cytoplasmic processes. Through canaliculi osteocytes can maintain contact with adjacent osteocytes or osteoblasts on the bone surface. This mechanism enables osteocytes to sense their surrounding biochemical and mechanical environments and to respond to or transduce signals to maintain bone integrity and vitality. (Buckwalter et al, 1996).

#### *2.2.2.3 Osteoclasts*

Osteoclasts are multinucleated cells derived from hemopoietic stem cells. They are responsible for bone resorption and are often found against the bone surface in hollow depressions called Howship's lacunae; morphometric measurement of the area of Howship's lacunae can be used to reflect the activity

of osteoclasts. Use of the electron microscope permitted discovery of several morphologic characteristics of osteoclast, including the “ruffled border” of the cellular membrane that creates a sealing zone that not only attaches osteoclasts to the bone surface but also creates an isolated microenvironment on the bone surface and cytoplasm enriched in actin, vinculin, and talin. The mechanism of bone resorption will be discussed in a greater detail in later section. (Nanci, 2008)

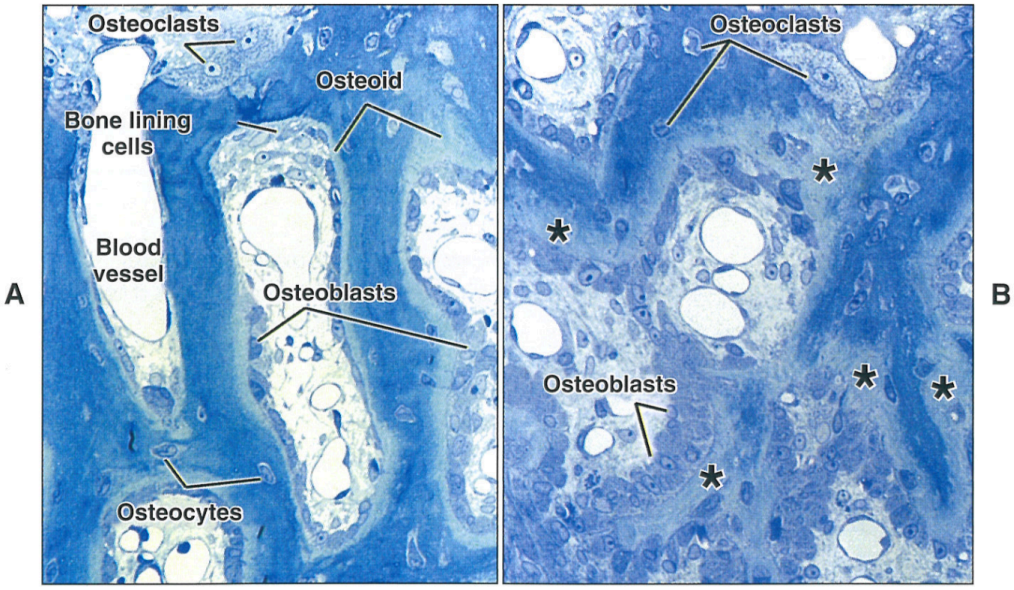


**Figure 9 – Photomicrograph of Mandibular Bone.** Cuboidal osteoblasts are noted along bone-forming surfaces. Osteocytes are observed within the calcified matrix and osteoid (asterisks). Osteoclasts are found opposite of active bone-forming surfaces. Reproduced from (Nanci, 2008)

### *2.3 Mechanism of Bone Formation*

Bone formation can occur through either endochondral or intramembranous ossification. In intramembranous ossification bone develops directly within the soft connective tissue. This bone formation process occurs at the cranial vault, maxilla, and body of mandible. The mesenchymal stem cells proliferate, differentiate into OB and produce the bone matrix which mineralizes (Nanci, 2008).

Endochondral ossification takes place for all long bones, vertebrae, ribs, and at the articular extremity of the mandible and base of the skull. It starts with differentiation of mesenchymal cells into chondroblasts which proliferate and produce a cartilage matrix containing type II and X collagen. The cartilage matrix is then the template for shape and position of the future bone. Later, vascularization increases within the midshaft of the diaphysis, and the perichondrium converts to a periosteum through the development of osteoprogenitor cells and osteoblasts, with OB producing a collar of bone through intramembranous formation. In the middle of the cartilage, chondroclasts resorb the mineralized matrix making room for further vascular ingrowth. The mesenchymal cells differentiate into osteoblasts and begin to deposit osteoid on the mineralized cartilage columns and then mineralize it. Bone matrix surrounds and entraps some of the osteoblasts and these become osteocytes. As the developing bone grows longer, osteoclasts remove the core of the mineralized cartilage and expand the marrow cavity. In the long bones of the extremities, a secondary invasion of blood vessels into the head of the bones

creates a secondary ossification center, resulting in formation of the epiphyseal growth plate. Longitudinal bone growth then occurs through cell division and interstitial growth in the plate. The process ceases when chondroblast stop proliferating and the growth plate disappears (Brighton et al, 1973).

### *2.4 Mechanism of Bone Resorption*

Bone resorption occurs in an isolated acidic microenvironment created by the sealed zone between OC and the bone surface. As OCs become active part of its cellular membrane becomes infolded creating a region known as the "ruffled border". Bone sialoprotein and osteopontin facilitate osteoclast adhesion and formation of the sealing zone. An integrin receptor for $\alpha_v\beta_3$ on osteoclast cell membranes recognizes and binds to the RGD (arg-gly-asp) sequence of osteopontin and bone sialoprotein (Franzen et al, 1985).

Proton pumps in the ruffled border of osteoclast pump hydrogen ions into the sealed zone creating an acidic microenvironment that can demineralize the bone surface and expose the organic matrix. Active osteoclasts contain an extensive Golgi apparatus, numerous mitochondria, a rough endoplasmic reticulum (RER), and numerous vesicles located between the Golgi apparatus and resorption surface. The enzymes acid phosphastase and proteases (i.e. cathepsin K, collagenases, matrix metalloproteinase) are synthesized in the RER, transported to the Golgi apparatus and packaged into vesicles that move to the ruffled border. The vesicles then release degradative enzymes into the sealed zone to degrade the exposed organic matrix. During degradation the

byproducts such as calcium and protein fragments are endocytosed at the ruffled border, and transported in vesicles to be released into extracellular fluid. (Zou & Teitelbaum, 2010)

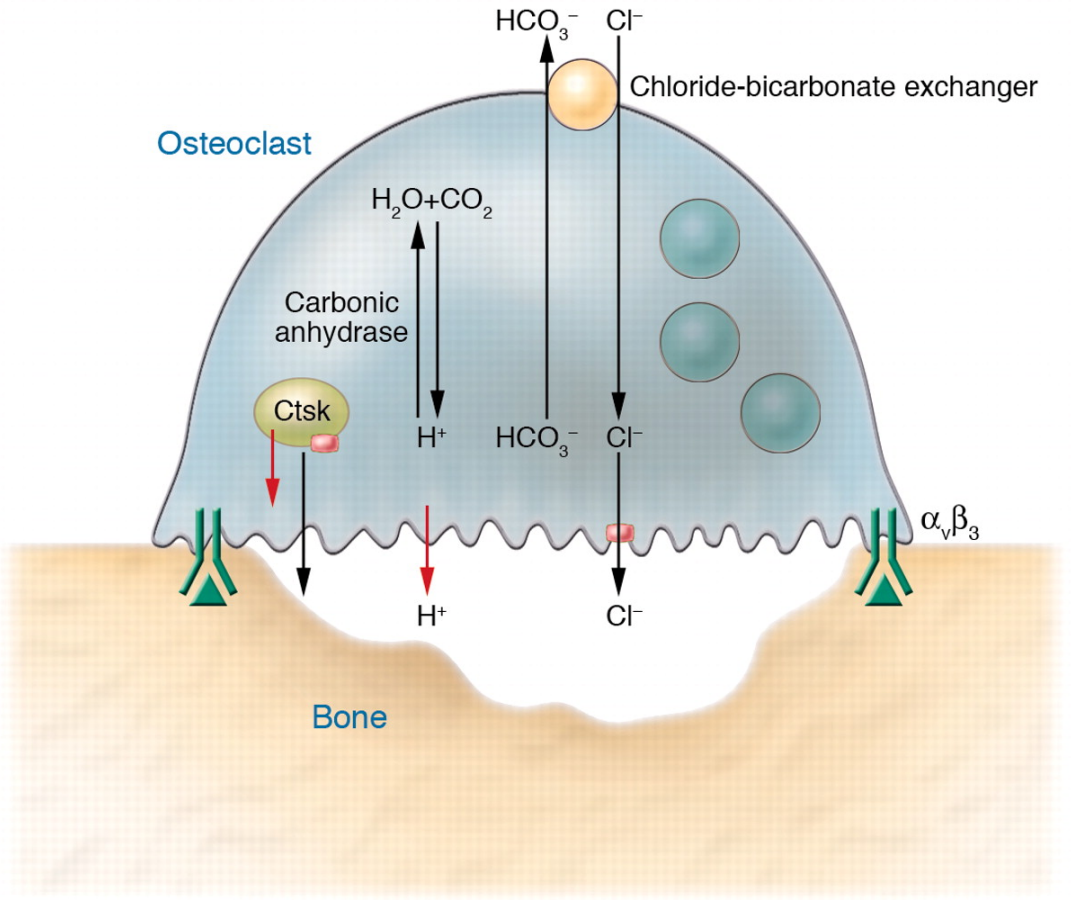


**Figure 10 – Mechanism of Osteoclast Resorption.** The binding of integrin $\alpha_v\beta_3$ receptor to RGD protein of osteopontin leads to attachment of osteoclast to bone surface creating the sealing zone. Proton pump moves hydrogen ions into the isolated space and secretion of cathepsin K and other proteases begin the bone resorption process. Reproduced from (Ross et al, 2006)

### *2.5 Modulation of Bone Resorption*

The process of bone resorption can be modulated by stromal cells in the marrow and OBs through secreted molecules and direct cell-to-cell interaction. The signaling pathway of receptor-activated nuclear factor kappa-B (RANK) and its ligand (RANKL) plays a major role in controlling osteoclastogenesis. RANKL is expressed on the plasma membrane of stromal cells and OB binds to RANK on the plasma membrane of osteoclast progenitor cells. This interaction then induces the differentiation of OC progenitor cells and promotes activity of osteoclasts. OB also secretes osteoprotegrin (OPG) which is a decoy of RANKL and interferes with OC formation by blocking the interaction between RANKL and RANK.

Bone resorption is also modulated by parathyroid hormone (PTH), vitamin $D_3$ ($1,25(OH)_2,D$) and calcitonin. PTH and vitamin $D_3$ increase bone resorption by stimulating OC formation while calcitonin decreases bone resorption (Tatevossian 1973). In addition, interleukins 1, 3, 6, and 11 and tumor necrosis factor α and β stimulate bone resorption while interleukins 4 and 13 have inhibitory effect on bone resorption.

### *2.6 Bone Modeling and Remodeling*

Bone modeling is a process through which the overall size and shape of bones are established, and it extends in time from embryonic bone development to pre-adult period of human growth. During this phase, bone is being formed rapidly on the periosteal surface while being simultaneously destroyed along the

endosteal surface resulting in the change of shape of the bone. Because bone increases in length and thickness during growth bone formation occurs at a greater rate than bone resorption. This process is essential for the growth of bone during development as well as modulation of bone structure under different mechanical conditions.

Replacement of old bone by new bone without a change in the overall shape of bone is called bone remodeling. Bone turnover continues even after adulthood is reached and the adult skeleton is continuously degraded and reformed through the coordinated and coupled action of OBs and OCs. In a healthy individual the amount of bone lost is balanced by the amount of bone formed. But in disease such as osteoporosis the resorption can exceeds formation resulting in overall loss of bone.

# 3 Metabolic Bone Diseases

## *3.1 Osteoporosis*

Osteoporosis is a metabolic bone disease characterized by low bone density and deterioration of the micro-architecture of bone tissue, resulting in bone fragility and increased risk of bone fracture (Eastell et al, 2016). A quantified definition was given by a study group of the World Health Organization, defining the disease as being present when the bone mineral density (BMD) or bone mineral content (BMC) is over 2.5 standard deviations below the young adult reference mean (Fleisch, 2000). Osteoporosis is diagnosed and assessed quantitatively by techniques that can measure bone

mineral density. The most common clinical measurement uses dual X-ray absorptiometry (DXA).

Osteoporosis in post-menoapusal women is mainly due to lack of estrogen, while in men it is possibly due to reduction in testosterone. In post-menopausal women both the cortical and trabecular bone become thinner with increased porosity while the overall chemical composition of the bone remains the same. A second possible cause of osteoporosis is failure to achieve optimal peak bone mass during adolescence, which can be affected by malnutrition, calcium deficiency or lack of exercise. As people age bone resorption gradually becomes greater than bone formation. The net loss of bone will reach a point where the overall bone structure becomes fragile and fractures can occur.

The mechanisms leading to bone loss in osteoporosis are still under investigation. Chronic lack of dietary calcium and vitamin D deficiency due to lack of sun exposure may play a role in the overall bone loss. In addition bone loss might be related to the general muscle atrophy that accompanies with aging, which can lead to decreased mechanical forces on the skeleton. For post-menopausal women decreased estrogen level induces formation of new basic multicellular unit (BMU) which increases bone remodeling and amplifies bone loss.

The clinical symptoms of osteoporosis include bone fractures and related consequences. For middle-aged men and women the most common site of fracture is the forearm while fractures in the vertebrae and hip become more prominent later in life.

Treatment protocols for osteoporosis can be divided into those that inhibit bone loss, and those that increase bone formation. Estrogen replacement therapy has been found to be effective in inhibiting bone loss and can even lead to some increase in bone density but long-term therapy is required as its effect on bone stops after discontinuation of treatment. BP has been found to be an effective treatment for osteoporosis. BPs such as ALN, risedronate, ibandronate and zoledronic acid have shown to decrease bone resorption and increase bone density. Treatment options for increasing bone formation include increased calcium and vitamin D intake and administration of parathyroid hormone (PTH).

### *3.2 Paget's Disease*

Paget's disease is a bone disorder characterized by increased bone remodeling, bone hypertrophy and abnormal bone structure. It is usually diagnosed in patients over 40 years of age and who may have a genetic predisposition for the disease. The initial course of disease is marked by an increase in bone resorption leading to a compensatory increase in bone formation and consequently a positive bone balance. The disease is often asymptomatic and is usually discovered during a routine x-ray or measure of serum alkaline phosphatase. The most common symptoms include pain, bone deformity, bone fracture, and neurovascular symptoms.

Laboratory tests may show elevated level of biochemical markers for both bone resorption (urinary pyridinium crosslinks) and bone formation (serum alkaline phosphatase). This finding is correlated with histologic studies which

often show a mosaic structure of areas of resorption (large number of osteoclast) and bone formation (osteoblasts with increased bone matrix).

Treatments for Paget's disease include use of BPs or calcitonin. Calcitonin can decrease bone turnover, however relapses can occur after discontinuation of treatment. BPs are now considered the treatment of choice for Paget's disease and ALN, clodronate, etidronate, pamidronate and risedronate have been shown to be effective in treating Paget's disease. BPs can decrease the rate of bone resorption which can then reduce the rate of bone formation due to the coupling effect between the two processes. BPs can improve the bone morphology as the new bone formed under BPs administration is lamellar rather than woven.

### *3.3 Tumor Induced Osteolytic Bone Disease*

Osteolytic tumor-induced bone disease is a condition in which tumors of various origins induce bone destruction leading to bone fracture, pain, and hypercalcemia. Bone destruction can be induced by local invasion or by secretion of bone resorbing factors, such as PTH-related protein, into the bloodstream.

Local bone destruction is often seen in breast and lung cancer metastases. The mechanism of cancer-associated bone resorption is still not well understood but it appears that tumor cells can either secrete or induce other cells to secrete bone-resorbing cytokines, such as PTH-related protein, TGFα, TNFα, TNFβ, IL-1α, IL-1β, and IL-6 which can induce osteoclasts to resorb bone.

Localized bone resorption can lead to pathological bone fracture, pain, and hypercalcemia.

Malignancies of the lung, breast, head and neck, kidney and ovary can also induce generalized bone destruction through systemic production and release of osteolytic factors such as cytokines and PTH-related protein into the bloodstream.

The main focus for treatment of osteolytic tumor-induced bone disease includes pain, bone fracture, and serum/urinary calcium level. Initial treatments of tumor-induced hypercalcemia include surgical excision of the primary tumor, chemotherapy, and radiation therapy. BPs are effective in preventing hypercalcemia when it is due to local invasion of carcinomas into bone. They are less effective in treating hypercalcemia caused by circulating factors produced by cancers outside the skeleton. *In vitro* BPs can induce apoptosis of myeloma and other cancer cells and inhibit their proliferation (Berenson, 2011). Further study is required to gain a clearer understanding of BPs' effect on tumor cells.

## 4 Bisphosphonates

Pyrophosphate is a normal byproduct of the anabolic process that is rapidly hydrolyzed into two phosphate groups once produced. Pyrophosphate has been considered to be an endogenous regulator of bone mineralization as it rapidly binds to bone minerals and inhibits dissolution of hydroxyapatite (Russell et al, 1970; Fleisch et al, 1966, Fleisch, 2000). However, rapid degradation of inorganic pyrophosphate makes it difficult to utilize pyrophosphate clinically.

Bisphosphonates were discovered to be inorganic pyrophosphate analogues with similar regulatory effects on bone dissolution (Russell et al, 1970). Instead of the P-O-P backbone that is seen in regular inorganic pyrophosphate, BP is characterized by a P-C-P central structure and a variable side chain (Coelman et al, 2008). The P-C-P backbone promotes binding of BP to mineralized bone matrix and renders BP resistant to phosphatase activity.

### *4.1 Chemical Features of BP*

As mentioned previously, BP is characterized by a stable P-C-P backbone and can form two covalent bonds with carbon, oxygen, sulfur or nitrogen atoms. The P-C-P backbone is crucial to the binding of BP to mineralized bone matrix as an oxygen atom from each of the phosphonate groups coordinate with a divalent cation such as $Ca^{2+}$ in a bidentate manner. If the hydroxyl (-OH) group on the two phosphonate groups of the P-C-P backbone is substituted by a methyl ($-CH_3$) group, BP loses its ability to bind to hydroxyapatite (Sunberg, 1991).

The chemical properties of BP can be altered with changes in the composition of the two side chains attached to the carbon center. The shorter side chain ($R_1$) is responsible for the chemical characteristics and pharmacokinetics of BP while the longer side chain ($R_2$) determines the mode of action and potency of BP. For example, increasing the length of the alkyl side chain will increase BP's potency while an incorporation of an amino ($-NH_2$) group to the $R_2$ side chain can increase BP's antiresorptive potency up to 1000-fold (Schenk et al, 1986).

### *4.2 Classification of BP*

BP can be divided into a non-nitrogen containing group and a nitrogen-containing group. Members of both groups share the same general structure of P-C-P backbone; but difference in the chemical composition of the two side chains provides each class with a different mechanism of inhibiting OC-mediated bone resorption.

The non-nitrogen containing class includes members such as clodronate and etidronate and they contain relatively short $R_1$ and $R_2$ side chains. The nitrogen containing group include members whose $R_2$ side chain contain an amino ($-NH_2$) group that is either in the terminal end of the side chain or within a heterocyclic ring. Members of the nitrogen-containing group include alendronate (ALN), pamidronate and zoledronate.

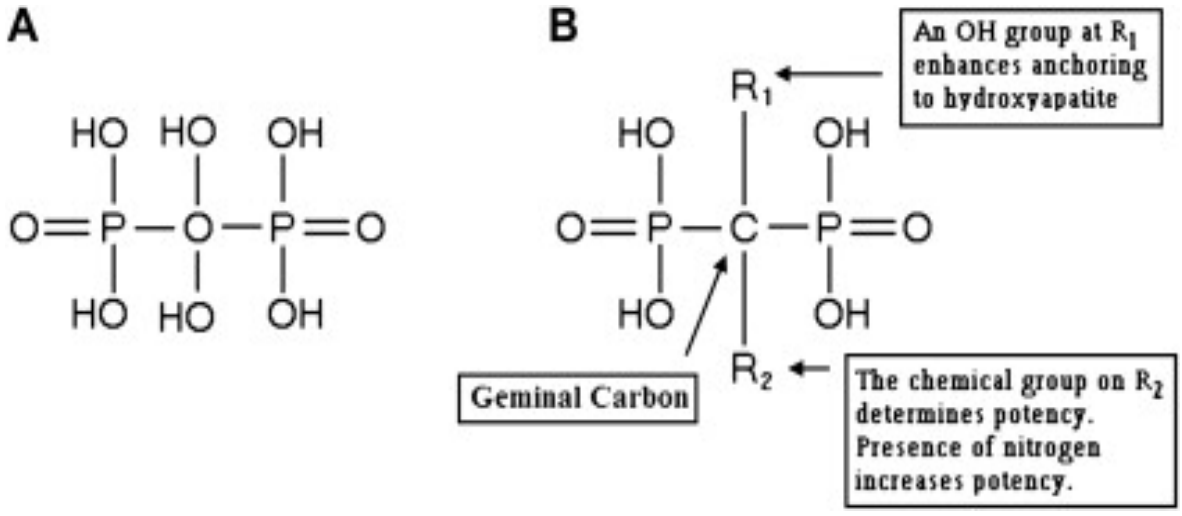


**(A)**

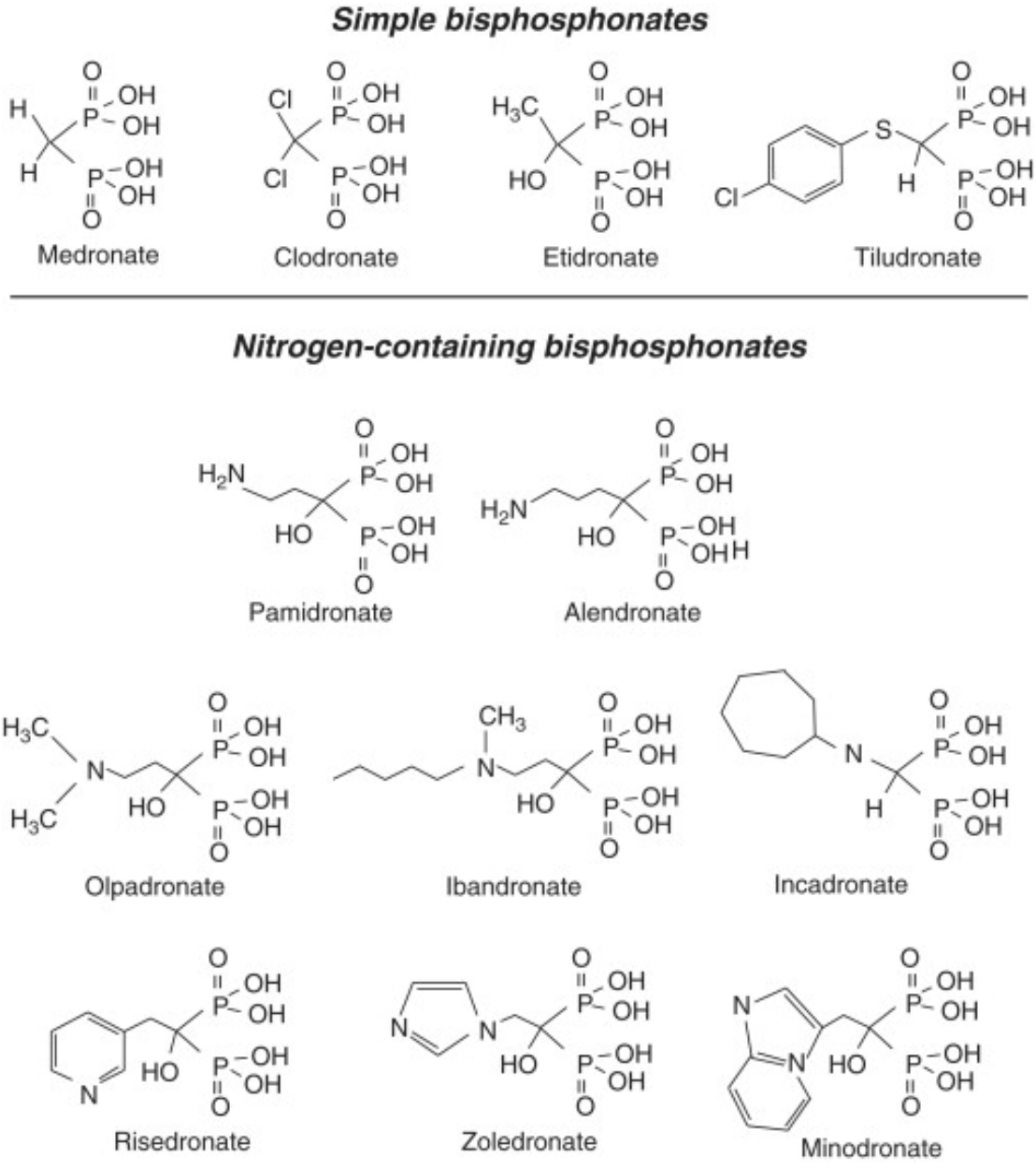
Simple bisphosphonates
Medronate
Clodronate
Etidronate
Tiludronate
Nitrogen-containing bisphosphonates
Pamidronate
Alendronate
Olpadronate
Ibandronate
Incadronate
Risedronate
Zoledronate
Minodronate

**(B)**

**Figure 11 – BP Structure and Classification.** (A) The difference in structure between inorganic pyrophosphate which has a P-O-P back bone and BP which has a P-C-P backbone. The $R_1$ side chain affect BP's binding to hydroxyapatite while the $R_2$ side chain affects BP's potency. (B) Members of the non-nitrogen containing BP include clondronate, and etidronate. Members of the nitrogen-containing BP include ALN, pamidronate and risedronate. Reproduced from (Fan, 2007) and (Roelofs et al, 2008)

### *4.3 Mechanism of Action of Non-Nitrogen Containing BP*

Non-nitrogen containing BPs can be incorporated by aminoacyl-tRNAsynthetase into methylene-containing analogues of adenosine triphosphate (ATP). This results in an analogue of ATP such as App$CH_2$p which replaces the pyrophosphate (P-O-P) moiety of ATP with the P-C-P moiety of BP. App$CH_2$p resembles ATP but is resistant to hydrolytic breakdown and release of phosphate. As a result of the non-hydrolysable nature of the ATP analogues their increased intracellular concentration is likely to inhibit numerous intracellular metabolic enzymes that are ATP-dependent and have detrimental effect on cell function, including inducing apoptosis. One of the enzymes affected is the adenine nucleotide translocase (ANT), which translocate ATP across the inner mitochondrial membranes. Consequently, there is breakdown of the mitochondrial membrane potential and activation of Caspase-2 and subsequent caspase-mediated cleavage of MSt-1, which is an apoptosis-promoting kinase (Rogers et al, 2011).

### *4.4 Mechanism of Action of Nitrogen Containing BP*

The NBPs are more potent than non-nitrogen containing BPs in inhibiting bone resorption and they exert their effect through a different mechanism. NBPs such as alendronate and pamidronate inhibited cholesterol synthesis but did not inhibit squalene synthase (Amin et al, 1996). This suggested that NBPs inhibited farnesyl pyrophosphate synthase (FPPS), an enzyme further upstream in the mevalonate pathway. (Rogers et al, 2011). The main function of the

mevalonate pathway is the production of cholesterol as well as isoprenoid lipids such as farnesyl diphosphate (FPP) and geranylgeranyl diphosphate (GGPP). The inhibition of FPPS leads to reduced synthesis of FPP and GGPP both of which are essential for post-translational (prenylation) of small GTPase such as Ras, Rab, and Rac, and accumulation of isopentenyl pyrophosphate (IPP), which is the metabolite immediate upstream of FPPS in the mevalonate pathway. These small GTPase enzymes are important signaling proteins that regulate processes necessary for osteoclast function such as cytoskeletal arrangement, membrane ruffling, trafficking of intracellular vesicles and apoptosis (Ridley et al, 1992; Marshall 1993; Zerial et al, 1993). IPP can be converted into a toxic ATP analog, ApppI, which inhibits the mitochondrial ANT and can cause osteoclast apoptosis. Therefore, loss of prenylation of GTPase and accumulation of unprenylated proteins can lead to loss of signaling required for osteoclast function and inappropriate activation of downstream signaling pathways.

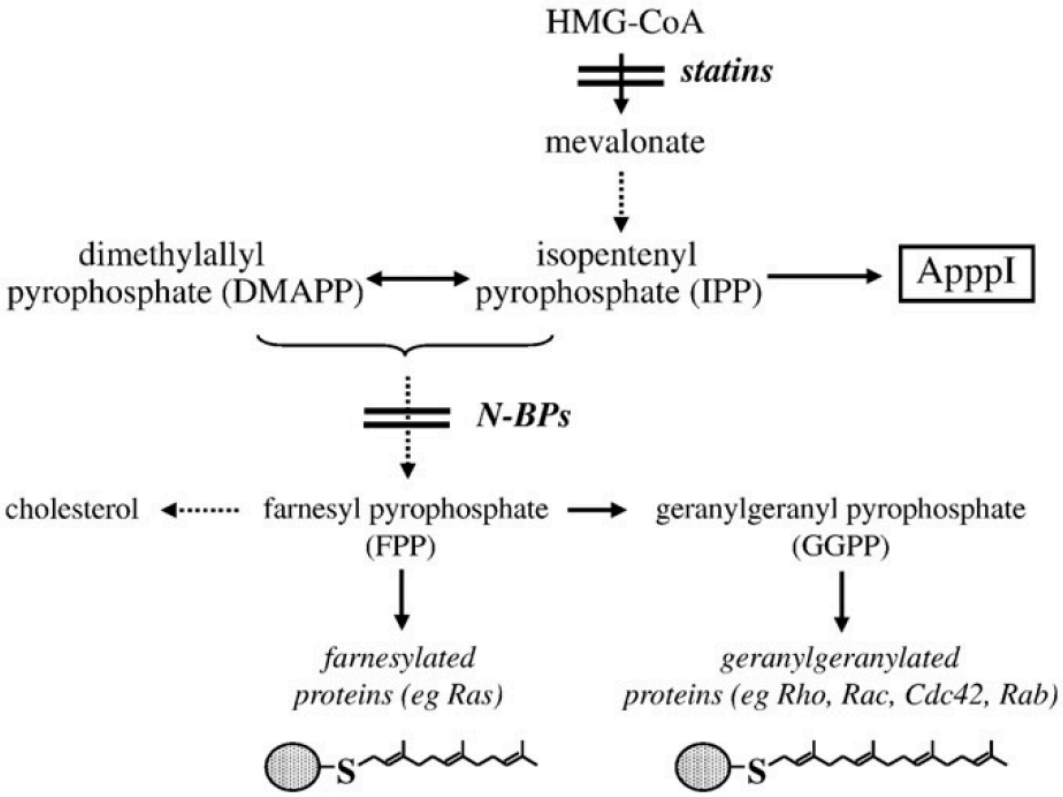


**Figure 12 – NBP's Effect on Mevalonate Pathway.** NBP are potent inhibitors of FPP Synthase preventing the synthesis of FPP and GGPP which are required for the prenylation of proteins that are crucial for osteoclast function and survival. Reproduced from (Rogers et al, 2011)

### *4.5 Bisphosphonate and Osteoclast*

The preferential binding of BP to bone matrix brings them into close contact with osteoclasts. During osteoclast-mediated bone resorption the acidic pH in the resorption lacuna causes BP to be dissociated from the bone mineral surface followed by intracellular uptake of BP into osteoclast by endocytosis. Since other cells are not able to acidify the bone surface to release mineral-bound BPs osteoclasts appear to be the only cell type capable of internalizing substantial amount of BPs *in vivo* (Rogers et al, 2011; Sato et al, 1991). *In vitro* studies have shown that BPs can decrease osteoclasts' lactic acid production, proton secretion, lysosomal enzyme activity, and prostaglandin synthesis (Fleisch, 2000)

### *4.6 BP's Effect on OBs*

The inhibitory effect of BP has on OC has been well-documented. However, there is limited detail on the effect BP has on OB. BP has been shown to decrease expression of RANKL and increase expression of osteoprotegrin (OPG), which acts as a RANKL decoy receptor. (Viereck et al, 2001; Pan et al, 2004). RANKL is a protein expressed by OB and it binds to the RANK receptor on OC. This interaction increases bone resorption by inducing the differentiation of OC progenitor cells and promotes activity of osteoclasts. OB also secretes osteoprotegrin (OPG) which interferes with OC formation by blocking the interaction between RANKL and RANK.

Some studies have shown that BP enhances osteoblast proliferation,

differentiation, and bone mineralization (Tenenbaum et al, 1992; Giuliani et al, 1998; D'Aoust et al, 2000), while other studies showed contradictory effects (Tsuchimoto et al, 1994; Idris et al, 2008). At low concentrations ranging from $10^{-8}$M to $10^{-9}$M BP stimulated osteoblast proliferation whereas concentrations higher than $10^{-6}$M inhibited osteoblast proliferation and differentiation (Plotkin et al, 1999). ALN increased osteoblast proliferation at 5 μM but decreased osteoblast proliferation at concentration higher than 20 μM (Kruger et al, 2016).

## *4.7 BP's Effect on Bone Mineral*

BP binds strongly to bone matrix and inhibits bone resorption by inhibiting the dissolution of the hydroxyapatite crystals. BP has a high affinity for the $Ca_{2+}$ cation in hydroxyapatite crystals on the bone surface. They are in in high concentration at sites of osteoclast-mediated bone resorption or areas of active bone turnover. During bone formation BP becomes embedded in the bone matrix and becomes inactive. But during bone resorption the acidic pH in the resorption lacuna causes BP to be dissociated from the bone mineral surface and become active.

## *4.8 Pharmacokinetics*

### *4.8.1 Intestinal Absorption*

The bioavailability of BP through an oral dose is low ranging between 1 to 10%, most likely due to its low lipophilicity and high negative charge which prevent paracellular transport. Absorption of BP in the GI tract can occur in the

stomach as well as in the small intestine through passive diffusion. The absorption is significantly diminished when BP is taken with a meal; especially in the presence of calcium and iron. The decrease may be due to conversion of BP into a nonabsorbable form.

### *4.8.2 Distribution*

Twenty to eighty percent of absorbed BP is taken up by bone and the remainder is rapidly excreted in urine. The amount of deposition is proportional to amount of BP administered. When large amounts of BP are given through rapid intravenous injection formation of insoluble complexes or aggregates may happen that can impair kidney function.

The half-life of circulating BP is between 0.5-2 hours. After uptake by bone BP is deposited in areas of both bone formation and bone resorption. Once deposited in bone BP can be buried under new layer of bone, and is only released under the condition of bone resorption. Therefore the half-life of BP deposited in bone depends on the rate of bone turnover and can be as long as 10 years.

### *4.8.3 Renal Clearance*

BP has high renal clearance and is actively secreted through the urinary system. Decrease in urinary secretion has been noted in cases of renal failure and it is poorly removed through peritoneal dialysis. Therefore the use of BP should be very cautious in patients with chronic kidney disease.

### *4.9 Side Effects*

Some of the common side effects associated with BP administration include GI tract discomfort, renal toxicity, hypocalcaemia, secondary hyperparathyroidism, BP-related osteonecrosis of the jaw (BRONJ), and atypical fractures of femoral diaphysis. Due to the long half-life BP can have in the human body these side effects can persist after completion of treatment.

Oral administration of BP can be accompanied by irritation of esophagus and GI tract which can result in nausea, dyspepsia, vomiting, diarrhea, and sometimes even esophageal erosion. These side effects might be due to the inhibitory effect of NBP on the mevalonate pathway which can inhibit keratinocyte growth. In order to reduce the side effects it has been recommended for patients to sit upright for 30 minutes after ingestion, take the medication with water, or to discontinue the medication in the presence of symptoms (de Groen et al, 1996)

When BP is administered through intravenous injection, caution must be taken to avoid administration of large amount of BP in a short period of time. Rapid injection of BP can lead to renal failure due to formation of insoluble aggregate with metal ions which cannot be filtered and are held back in the kidney. (Fleisch, 2000).

Hypocalcaemia may be observed within the first few weeks of BP administration due to its inhibitory effect on osteoclasts. This is usually without clinical consequence but prolonged hypocalcaemia can lead to cardiac arrhythmia, seizure, or parathesia of the lips, mouth and limbs. Secondary hyperparathyroidism can sometimes be noticed as the body tries to compensate

for the deficiency in calcium. Hyperplasia of the parathyroid glands may occur, and the excessive production of PTH would stimulate OC bone resorption, increase release of calcium into bloodstream, and increase tubular reabsorption of calcium.

BRONJ can be defined as “an area of exposed bone in the maxillofacial region that does not heal within 8 weeks after identification in a patient who received BPT and had not received radiation therapy to the craniofacial region.” (Vescovi et al, 2012) The etiology of BRONJ remains unknown but it was proposed that BRONJ might be caused by BP’s suppression of bone turnover which can inhibit bone’s ability to repair microdamages (Allen & Burr, 2009). The most common sites for BRONJ to occur are the mylohyoid ridge and the maxillary alveolar ridge. The development of BRONJ can be affected by the type of BP, length of treatment, concomitant therapy (such as chemotherapy, radiation treatment of the head and neck area), and systemic conditions (i.e. anemia, diabetes, hypercalcemia, and coagulation disorder). Invasive dental procedures such as teeth extraction, dental implant placement, and dentoalveolar surgery can increase the risk of developing BRONJ; therefore dentists need to be cautious when considering such treatments for patients with history of BPT.

Symptoms of BRONJ include non-healing area of exposed bone, fistulization, purulent discharge, pain, nerve paresthesia, teeth mobility, maxillary sinus involvement and mandibular fracture. BRONJ can be diagnosed using orthopantomography, computed tomography (CT) scans, and magnetic

resonance imaging (MRI). Histologic characteristics of BRONJ include non-vital bone, empty lacunae, and lack of bone remodeling. (Vescovi et al, 2012).

Treatment options for BRONJ can be diverse including discontinuation of BP, surgical therapy, oxygen hyperbaric therapy, ozone application, and laser surgery (Vescovi et al, 2012).

## 5. Aim and Goals

The current study evaluated and determined the interplay between Alendronate (Fosamax), a clinically used nitrogen-containing bisphosphonate (NBP), squamous cell carcinoma cells, and osteocytes/osteoblasts/osteoclasts using an ex-vivo three-dimensional live cancer-bone interactive model. The experimental approaches were designed to determine the effect of NBP on osteoclastic bone resorption and osteoblastic bone formation, with or without the presence of oral cancer cells, using live neonatal mouse calvarial bone.

Two model systems were used:

(i) The resorption model used oral cancer cells-induced osteoclast formation and bone resorption. (ii) The formation model used ascorbic acid-induced osteoblast differentiation and bone formation. Quantitative analysis for media calcium changes, tartrate-resistant acid phosphatase (TRAP) enzyme activity (which reflects osteoclast activity), and alkaline phosphatase (ALP) enzyme activity (which reflect osteoblast activity) and qualitative analysis by Neutral Red staining, histological observation and two-photon confocal-microscopy were performed

# 6. MATERIALS AND METHODS

## *6.1 Effect of ALN on SCC2-dsRED cells*

Oral cancer cells (SCC2-dsRED) (Dr. David Sherr's laboratory) were grown with DMEM in the presence of 10% Fetal Calf Serum (FCS, Sigma-Aldrich, Co) at 37°C until confluent using 10cm culture dishes and media changes every 2 days. At the start of the experiment, the cancer cells were rinsed with PBS and harvested using Trypsin in 10 ml of DMEM followed by centrifugal pelleting. The collected cancer cells were re-suspended in 10 ml of DMEM and re-pelleted. The cancer cells were then suspended in DMEM and total number of cells was estimated by microscopy. 2 ml of DMEM spiked with (3 X $10^5$) cancer cells were added to each well of a 6-well cell culture plate. One control group (0 μM ALN in media) and four experimental groups (1 μM ALN, 5 μM ALN, 15 μM ALN, 30 μM ALN in media) were included in the study. In addition, the effects of FCS vs. bovine serum albumin (BSA) in cell-culture media, ascorbic acid (ASC) (150 μg/ml), different timing of ALN addition (seeding vs. confluence) on oral squamous carcinoma cells were investigated. See Fig. 13 for experimental design. The experiment was carried out for 10 days and the cell-culture media was changed every 2 days. At time of each media change, number of detached cancer cells suspended in cell culture media was counted using microscopic approach. At the end of the experiment, each well was treated with Trypsin in 2 ml of DMEM, and the number of cancer cells attached to the well was counted by microscopy.

| Experiment | FCS in Media | BSA in Media | Ascorbic Acid (150 µg/ml ) in Media | Timing of ALN Addition | ALN (0 µM) | ALN (1 µM) | ALN (5 µM) | ALN (15 µM) | ALN (30 µM) |
|---|---|---|---|---|---|---|---|---|---|
| 1A | X | | | Confluence | X | X | X | X | X |
| 1B | X | | X | Confluence | X | X | X | X | X |
| 2A | X | | | Seeding | X | X | X | X | X |
| 2B | X | | X | Seeding | X | X | X | X | X |
| 3A | | X | | Confluence | X | X | X | X | X |
| 3B | | X | X | Confluence | X | X | X | X | X |
| 4A | | X | | Seeding | X | X | X | X | X |
| 4B | | X | X | Seeding | X | X | X | X | X |

**Figure 13. Summary of experimental design for 2D SCC2 .**

### *6.2 Live Mouse Calvaria Bone Organ Cultures*

Under sterile conditions, 5-8 day-old neonatal CD-1 mice calvaria (Charles River Laboratories, MA) were dissected and trimmed into a trapezoidal structure by partial removal of occipital lobe and two frontal lobes. After dissection each calvarium was placed free floating in a roller tube (15 cm X 16 cm, Bellco, Inc., NJ) containing 2.0 ml of bone culture media under normal oxygen condition with or without SCC2 cells (2.5 X $10^5$ cells per tube) in suspension, in the absence and presence of ALN (Sigma-Aldrich). The live bone organ culture medium preparation consisted of Dulbecco's Modified Eagle's Medium (DMEM) with bovine serum album (BSA) or fetal calf serum (FCS), 100 U/ml penicillin, and 250 ng/ml amphotericin B (Gibco, Grand Island, NY). In addition, ASC (150 μg/ml) and different concentration of ALN were supplemented to the medium depending on the experimental designs. Through this approach we were able to dissociate the process of bone resorption and bone formation involved in bone modeling.

#### *6.2.1 SCC2-dsRED Oral Squamous Carcinoma Cell Culture*

SCC2-dsRED oral squamous carcinoma cells (Dr. David Sherr's laboratory) were grown with DMEM, in the presence of 10% Fetal Calf Serum (FCS, Sigma-Aldrich, Co) at 37°C until confluent using 10cm culture dishes and media changes every 2 days. On the day of bone organ co-cultures with SCC2-dsRED cells, the cancer cells were rinsed with 10 ml of bone organ culture media, then harvested using trypsin in 10 ml of bone culture media, followed by centrifugal pelleting. The collected cancer ells were re-suspended in 10 ml of bone organ culture media and re-pelleted. The cancer cells were then

suspended in bone organ culture media and total number of cells was counted by microscopy. Bone culture media 2 ml with 2.5 X $10^5$ cancer cells were added to each roller tube to be co-cultured with a single full calvarial bone.

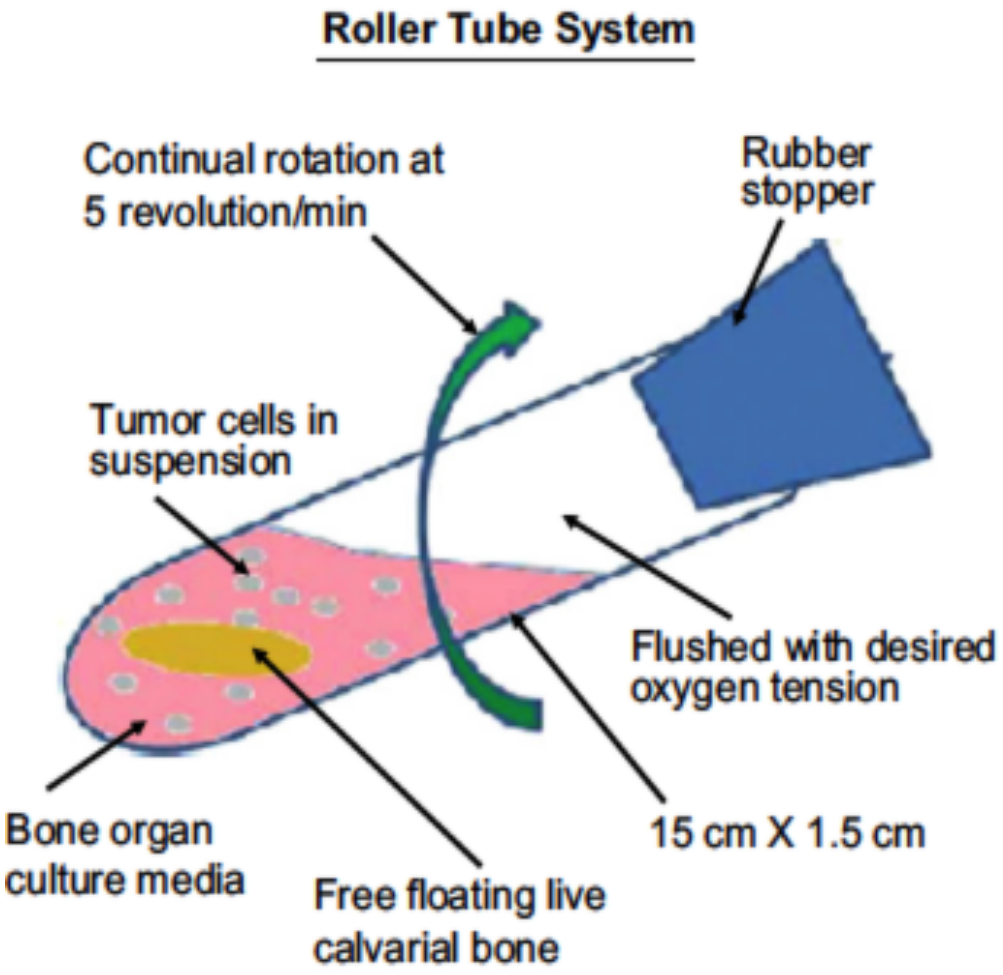


**Figure 14. The set up of the roller tube system.** In each roller tube one calvarial bone was cultured with SCC2-dsRED oral squamous carcinoma cells and 2 ml of culture media. Sterile stoppers were used to seal the tubes, and the tubes were then placed on a roller tube apparatus with a setting of 5 revolutions per minute in a 37°C incubator. Reproduced from (Curtin et al, 2012)

- Calvaria alone, SCC2 cells alone, or calvaria with SCC2 cells were placed in each roller tube along with 2 ml of culture medium.
- Sterile stoppers were used to seal the tubes, and the tubes were placed on a roller tube apparatus with a setting of 5 revolutions per minute in a 37°C incubator.
- Media was changed every 2 days under sterile condition, for a total of 8 days.
- On the day of media changes, medium from each tube was collected and aliquoted into a labeled 2 ml eppendorf tube, and stored in 4°C refrigerator to be used for calcium, and tartrate-resistant phosphatase (TRAP) analysis.
- The cells suspended in medium were pelleted centrifugally, and then re-suspended in 200 µl of DMEM. The cells suspended in medium were then counted by microscopy.
- On the last day of the experiment each test tube was treated with 2 ml of Trypsin and the number of SCC2 cells attached to the wall of the roller tube was counted.
- At the conclusion of the experiment all of the calvaria were hemi-dissected in the mid sagittal suture:

1. Two half calvaria from each of the experimental groups were placed in 2 ml eppendorf tube with 1 ml of Trypsin, and placed in a 37°C incubator for 5 minutes. The cells were then centrifugally pelleted and re-suspended in 200 µl of DMEM. SCC2 cells that had been attached to the calvaria were then counted by microscopy.
2. Two half calvaria from each group were fixed in 10% formalin, paraffin sectioned, and stained with hematoxylin and eosin (H&E, Boston Medical Center, Department of Pathology) for histological analysis.
3. Two half calvaria from each group were stained with neutral red (NR, Sigma-CO) to visualize general OCs activity.
4. Two half calvaria from each group were prepared for two-photon confocal-microscopy, see section 6.7

**Table 1 - General Experimental Procedures for 3D Roller-Tube Co-Culture.**

General experimental procedures for 3D roller-tube co-culture are outlined. The procedures are applicable to both bone resorption and bone formation models.

### *6.2.2 Effect of ALN on Bone Resorption Model*

The effect of ALN on OC and bone resorption was studied utilizing live mouse calvarial co-cultures with SCC2 cells. Six cultures were set up as follows: (a) calvaria negative control (culture medium only) (n = 7); (b) calvaria with 30 μM ALN (Sigma-Co) (n = 4); (c) SCC2 cells negative control (culture medium with FCS (Sigma-Co)) (n = 7); (d) SCC2 cells negative control (culture medium with BSA (Sigma-Co)) (n = 3); experimental treatment of (e) calvaria + SCC2 cells (culture medium only) (n = 7); and (f) calvaria + SCC2 cells + 30 μM ALN (Sigma-Co) (n = 4), Figure 15. See Table 1 for general experimental procedures.

#### *6.2.2.1 Effect of ALN Concentration on Bone Resorption Model*

To further evaluate the effect of different ALN concentrations on OC and bone resorption, a total of three cultures were set up as follows: (a) calvaria + SCC2 cells + 0.5 μM ALN (single dosage) (n = 4); (b) calvaria + SCC2 cells + 0.5 μM ALN for 8 days (Sigma-Co) (n = 4), (c) calvaria + SCC2 cells + 1.5 μM ALN for 8 days (Sigma-Co) (n = 4); Figure 15. See Table 1 for general experimental procedures.

### *6.2.3 Effect of ALN on ASC Stimulated Bone Formation Model*

The effect of ALN on OB and bone formation was studied by utilizing live mouse calvarial co-cultures with SCC2 cells. Total of six cultures were set up as follows: (a) calvaria control with 150 μg/ml ASC (n = 3); (b) calvaria with 150 μg/ml ASC + 30 μM ALN (Sigma-Co) (n = 4); (c) SCC2 cells control (culture medium with FCS + 150 μg/ml ASC) (Sigma-Co)) (n = 7); (d) SCC2 cells control

(culture medium with BSA + 150 µg/ml ASC) (Sigma-Co)) (n = 3); experimental treatment of (e) calvaria + SCC2 cells (culture medium + 150 µg/ml ASC) (n = 9); and (f) calvaria + SCC2 cells + 30 µM ALN + 150 µg/ml ASC (Sigma-Co) (n = 9), Figure 15. See Table 1 for general experimental procedures.

#### *6.2.3.1 Effect of ALN Concentration on ASC Stimulated Bone Formation Model*

To further evaluate the effect of different ALN concentrations on OB and bone formation, a total of three cultures were set up as follows: (a) calvaria + SCC2 cells + 0.5 µM ALN (single dosage) + 150 µg/ml ASC for 8 days (n = 4); (b) calvaria + SCC2 cells + 0.5 µM ALN + 150 µg/ml ASC for 8 days (Sigma-Co) (n = 4), (c) calvaria + SCC2 cells + 1.5 µM ALN + 150 µg/ ml ASC for 8 days (Sigma-Co) (n = 4); Figure 15. See Table 1 for general experimental procedures.

### *6.2.4 Effect of Calvarial Cells Viability on Bone Resorption Model*

To evaluate the effect of calvarial cells viability on OC and bone resorption, two groups of cultures were set up as followed: (a) calvaria (freeze & thaw) + SCC2 cells (n = 3); (b) calvaria (treated with 10% formaldehyde) + SCC2 cells (n = 3); Figure 15. Calvaria in group A were placed in -4°C freezer overnight the night before the start of experiment. On the day of experiment, the eppendorf tube was taken out of freezer and thawed at room temperature for 30 minutes. For group b, calvaria were treated with 10% formaldehyde prior to start of experiment. See Table 1 for general experimental procedures.

### *6.2.5 Effect of Calvarial Cells Viability on ASC Stimulated Bone Formation Model*

To evaluate the effect of calvarial cells viability on OB and bone formation, two groups of cultures were set up as followed: (a) calvaria (freeze & thaw) + SCC2 cells + 150 µg/ml ASC (n = 3); (b) calvaria (treated with 10% formaldehyde) + SCC2 cells + 150 µg/ml ASC (n = 3); Figure 15. Calvaria in group A were placed in -4°C freezer overnight the night before the start of experiment. On the day of experiment, the eppendorf tube was taken out of freezer and thawed at room temperature for 30 minutes. For group b, calvaria were treated with 10% formaldehyde prior to start of experiment. See Table 1 for general experimental procedures.

| Experimental Control (Calvaria) |
| --- |
| Media only for 8 days (n = 7) |
| Ascorbic Acid (150 µg/ ml) for 8 days (n= 3) |
| ALN (30 µM) for 8 days (n = 4) |
| Ascorbic Acid (150 µg/ ml) & ALN (30 µM) for 8 days (n = 4) |

| Experimental Control (SCC2 Cells) |
| --- |
| Media (FCS) only for 8 days (n = 7) |
| Media (BSA) only for 8 days (n = 3) |
| Media (FCS) & Ascorbic Acid (150 µg/ ml) for 8 days (n = 7) |
| Media (BSA) & Ascorbic Acid (150 µg/ ml) for 8 days (n = 3) |

| Resorption Model (SCC2 Cells + Calvaria) |
| --- |
| Media only for 8 days (n = 7) |
| ALN (30 µM) for 8 days (n = 4) |
| ALN (0.5 µM, 1 dosage) for 8 days (n = 4) |
| ALN (0.5 µM) for 8 days (n = 4) |
| ALN (1.5 µM) for 8 days (n = 4) |
| Calvaria (Freeze/Thaw), Media only for 8 days, (n = 3) |
| Calvaria (10% Formaldehyde), Media only for 8 days, (n = 3) |

| Formation Model (SCC2 Cells + Calvaria) |
| --- |
| Ascorbic Acid (150 µg/ ml) for 8 days (n = 9) |
| Ascorbic Acid (150 µg/ ml) & ALN (30 µM) for 8 days (n = 9) |
| Ascorbic Acid (150 µg/ ml) & ALN (0.5 µM, 1 dosage) for 8 days (n = 4) |
| Ascorbic Acid (150 µg/ ml) & ALN (0.5 µM) for 8 days (n = 4) |
| Ascorbic Acid (150 µg/ ml) & ALN (1.5 µM) for 8 days (n = 4) |
| Calvaria (Freeze/Thaw), Ascorbic Acid (150 µg/ ml) for 8 days (n = 3) |

Calvaria (10% Formaldehyde), Ascorbic Acid (150 µg/ ml) for 8 days (n = 3)

**Figure 15 - Summary of experimental treatment groups.** Categorized by control groups, resorption model and formation model.

### 6.3 *Observation of Global OC Activity by Neutral Red*

Neutral red has been known to be rapidly absorbed by OC cells, therefore neutral red staining can provide quantitative estimation of OC activity due to the multinucleated nature of OC cells (Curtin et al, 2012). At the end of each experiment, the bisected half calvaria were stained with 70 µg/ ml NR (Sigma-Co) then incubated under 37°C for 45 minutes. The calvaria were then observed under microscope and digital images were taken. The calvaria were then washed with phosphate buffered saline (PBS) before fixing in 10% formalin overnight.

### *6.4 Assessment of Media Calcium Release and Uptake in Bone Resorption and Formation Model*

In both the bone resorption and formation models for the calvaria cultures, calcium release and uptake were reflected in the media respectively. Calcium assays are based on the chemical reaction between calcium chelating chromorphoric reagent and calcium ion available in the media (Dorogi, 1984). The reaction forms an intense purple complex, which is reflected by the absorbance that is directly proportional to the calcium concentration of the media.

#### *6.4.1 Determination of Standard Curve for Calcium Assay*

The determination of media calcium concentration was calculated by using a standard curve. Stock calcium chloride solution was made by weighing 1.8 mg O-Cresolphthalein complex one (Sigma-Aldrich Co.) reagent, and dissolved in 10 ml sodium bicarbonate buffer, pH 10.8 (concentration = 50 mM). Calcium

chloride ($CaCl_2$) standards with concentrations ranging from 0-70 nmol/10µl were prepared. 10 µl $CaCl_2$ standards and 190 µl O-Cresolphthalein complex one regent solution were loaded into 96 well plate, and absorbance value was obtained using Berthold Tristar LB 941 plate reader (Berthold Technologies GmbJ & Co. KG.) at wavelength of 590nm. Linearity of assay and correlation value greater than 0.98 were achieved, see Figure 16.

*6.4.2 O-Cresolphthalein Complex One Calcium Assay*

190 µl of calcium reagents were pipetted into a 96 well plate, followed by addition of 10 µl of each standard and sample into its respective well. The assay was carried out in duplicates. The absorbance values were obtained with Berthold Tristar LB 941 plate reader (Berthold Technologies GmbJ & Co. KG.) at wavelength of 590nm.

Average absorbance values were calculated for each standard and sample. Background reading was adjusted by subtracting averaged blank standard absorbance value from the averaged sample absorbance values. Average standard absorbance values were plotted as a function of final calcium concentration to obtain the standard curve equation of y = mx. Corrected sample absorbance values were plotted to calculate the final calcium concentration. Sample dilution factor was taken into account by multiplying the final calcium concentration with 0.1 to obtain units of µM/ ml. The data produced reflect calcium release or uptake at each collection time point. Using Microsoft Excel the date were plotted as a function of time and cumulative calcium release or uptake graphs.

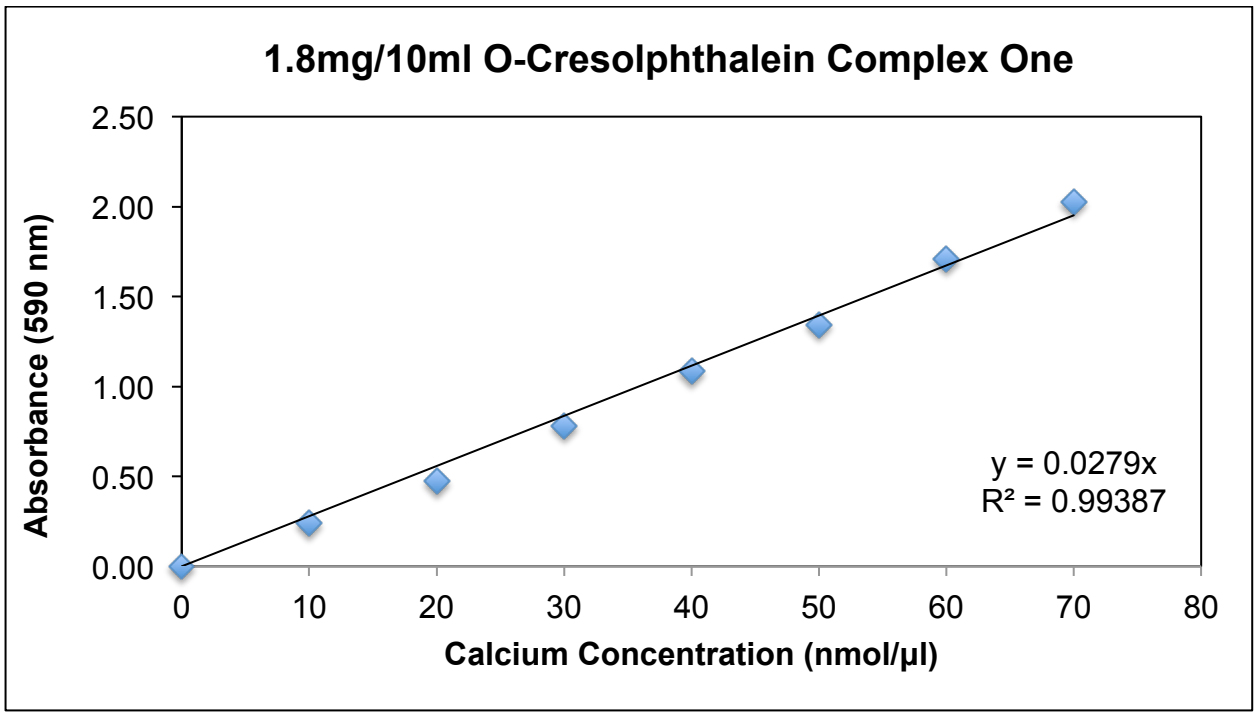


**Figure 16 – Example of Actual Standard Curve Used.** Experimental standard curve plotted after background correction to be used in the calculation of calcium concentration. The absorbance values were obtained with Berthold Tristar LB 941 plate reader (Berthold Technologies GmbJ & Co. KG.) at wavelength of 590nm.

### *6.5 Assessment of OC with TRAP Activity*

During bone resorption, TRAP is highly expressed by OC, therefore it is an ideal marker for OC activity level. The TRAP assay utilizes the inhibitory effect of tartrate on non-TRAP to isolate the TRAP activity, and the OC activity is determined utilizing p-nitrophenyphosphate (p-NPP) as a chromogenic substrate in the assay. TRAP dephosphorylates p-NPP producing p-nitrophenol (p-NP) which under alkaline condition deprotonates the phenolic (-OH) group producing a bright yellow color that can be measured by ultraviolet and visible light spectrophotometry.

The TRAP reagent buffer, pH 4.8, consisted of 0.1 M Sodium Acetate ($C_2H_3NaO_2$), 50 mM Tartaric Acid ($C_4H_6O_6$), 16 mM p-NPP (Sigma-Aldrich, Co.), 1 mM Zinc Chloride (ZnCl2). The assay was carried out in duplicate and TRAP activity was measured by incubating 50 µl medium of each sample with 250 µl of the TRAP reagent buffer in each well of a 96 well plate for 30 minutes at 37°C. At the end of the incubation time 10 µl of 1M NaOH was added to each well to stop the reaction, and absorbance measured at a wavelength of 410nm with Genius Detector as described in (Curtin et al, 2012).

### 6.6 Assessment of OB with ALP Activity

ALP was used as a marker for OB activity in the formation model. The ALP assay utilized p-NPP as a chromogenic agent. The ALP reagent buffer, pH 7.8, consisted of 0.15 M sodium chloride (NaCl), 30 mM sodium bicarbonate ($NaHCO_3$), 16 mM p-NPP. The assay was carried out in duplicate and ALP

activity was measured by incubating 50 µl medium of each sample with 250 µl of the ALP reagent buffer in each well of a 96 well plate for 30 minutes at 37°C. After incubating, absorbance was measured at a wavelength of 405nm with Genius detector as described in (Wang et al, 1998).

6.6.1 TRAP and ALP Calculation

The absorbance measurements for both TRAP and ALP assays were calculated by subtracting the average background absorbance. Concentration of p-NP was calculated with adjusted measured absorbance using Beer-Lambert law equation, $c = A\lambda / (\varepsilon\lambda X\ l)$. Using the molar absorptivity constant ($\varepsilon_{405}$) of 12,500 $(mol/L)^{-1}cm^{-1}$ and a path length (1) of 1cm. Incubation time of 30 minutes was used to calculate the rate of substrate hydrolysis in units of mol/L*min. The final enzyme activity is expressed in unit of µMol/L*min.

### *6.7 Histology Preparations*

Histological observations were obtained from 2 bisected half calvaria of each treatment group. All digital images of H & E stained sections were captured under 10X magnification with a`compound microscope (Nikon), by Retiga 1300 digital camera (Qimaging, Canada).

### *6.8 High-Resolution Two-Photon Confocal-Microscopy*

High-resolution two-photon confocal miscopy was performed on two bisected half calvaria co-cultured with SCC2 cancer cells under both bone resorption and formation conditions in the absence and presence of 30 µM ALN

doses. The calvaria were washed twice with 1 ml of 50 mM Tris buffer, pH7.5 and incubated in 0.5 ml of 50 mM Tris buffer, pH7.4 containing 0.5% Triton-100 for 2 hour over ice. The calvaria were then washed three times with 1 ml of 50 mM Tris buffer, pH7.4 and suspended in 0.5 ml of the 50 mM Tris buffer containing 5% BSA and a primary human cytokeratin 7 antibody (mouse monoclonal [OV-TL 12/30], Abcam, Co) overnight at 4°C. The next day, the primary antibody was removed and the calvaria were washed three times with 1 ml of 50 mM Tris buffer followed by incubation with 5 µg of green-fluorescent-tagged secondary antibody raised against mouse IgG in goat (Alexa Fluor® 488 green dye, emission = 519nm, absorption = 495nm, Life Technology, Inc) in 0.5 ml Tris buffer overnight at 4°C. The calvaria were removed from the secondary fluorescent antibody buffer, washed three times with Tris buffer and left in 0.5 ml of Tris buffer. To prepare for two-photon confocal microscopy, the calvaria were labeled with blue-fluorescent DAPI (4',6-diamidino-2-phenylindole dihydrochloride, emission = 455nm, absorbance = 345nm, Sigma-Aldrich, Co) at dilution of 1:1000 and 0.4 nmol of red-fluorescent bisphosphonate (OsteoSense 680EX, Perkin-Elmer, Inc.) for 1 hour at room temperature. The calvaria were mounted on confocal microscope dishes with Vectashield mounting medium for Fluorescence (Vector Laboratories, Inc. Burlingame, CA 94010) and three fluorescent emissions (green, blue, and red) were acquired at 200X magnification and 5 µM intervals with total coverage of 100 µM distance for vertical scanning observations, and up to 180 µM distance for horizontal scanning observations using high resolution two-photon confocal microscope LSM 710 model. The

acquired images were analyzed using Image J software program for generating merged fluorescent spatial orientation of the SCC2 cells relative to bone cells and the mineralized bone matrix. The merged images were viewed in 3D orientation and recorded as an AVI movie to provide continuous visualization of the cellular characteristics as a function of different planes relative to the mineralized bone matrix.

### *6.9 Statistical Analysis*

Chemical and biochemical data are presented as mean ± S.D. The statistical significance of the difference between controls and different treatment groups were evaluated using two-tailed, paired *t* test with equal variance. The differences between groups were considered statistically significant for $p < 0.05$.

## 7. Results

### *7.1. Effect of ALN Concentration on SCC2-dsRED Cells*

The data analysis of 2D-cells co-culture of SCC2 cells with different concentrations of ALN in the absence or presence of ASC at time of seeding or confluence are presented in Figures 17-24. In the 2D-cell culture of SCC2 cells in FCS media, with ALN added at time of confluence (Figure 17), ALN increased SCC2 detachment and decreased SCC2 attachment in a concentration-dependent manner while there was no significant change in SCC2 cell viability. In the 2D-cell culture of SCC2 cells in FCS media with ASC with ALN added at time of confluence (Figure 18), ALN decreased total cell number and increased SCC2 cell detachment in a concentration-dependent manner while increasing the percentage of dead SCC2 cells. In the 2D-cell culture of SCC2 cells in FCS media with ALN added at seeding (Figure 19), there was no significant change in total cell number or SCC2 cell attachment, except in the groups treated with 15 μM ALN and 30 μM ALN ($p<0.05$). ALN did not affect viability of overall or attached SCC2 cells. However, when compared with the same experimental condition at time of confluence all of the groups showed higher percentage of dead SCC2 cells overall and lower percentage of live attached SCC2 cells. In 2D-cell culture of SCC2 cells in FCS media with ASC with ALN added at seeding (Figure 20), ALN decreased total cell number and the number of attached SCC2 cells in a concentration-dependent manner while increasing SCC2 cell detachment and decreasing SCC2 cell attachment for groups treated with 15 μM

ALN and 30 μM ALN. In addition, ALN significantly decreased the SCC2 viability except in the group treated with 1 μM ALN ($p$<0.05).

The effect of ASC & ALN in 2D-cells co-culture of SCC2 cells in media containing BSA instead of FCS, with ALN added in the presence or absence of ASC at time of seeding or confluence is show Figure 21-24. When ALN is added to the cell culture at time of confluence, as shown by Figure 21, ALN significantly increased SCC2 cells detachment in the groups treated with 15 μM ALN and 30 μM ALN ($p$<0.05). ALN also significantly decreased the SCC2 cell viability in the groups treated with 15 μM ALN and 30 μM ALN while had no significant effect on the viability of attached SCC2 cells. Figure 22 shows data for 2D-cell cultures of SCC2 cells in BSA media with ASC, with ALN added at time of confluence. ALN increased SCC2 cell detachment and decreased SCC2 cell attachment in a concentration-dependent manner. ALN also significantly decreased the SCC2 cell viability in the groups treated with 15 μM ALN and 30 μM ALN. Figure 23-24 showed 2D-cells co-culture of SCC2 cells in BSA media, with ALN added in the presence or absence of ASC at time of seeding. Both figures showed that SCC2 cells do not survive well in this condition, but ALN did not affect SCC2 cells detachment or SCC2 cell viability.

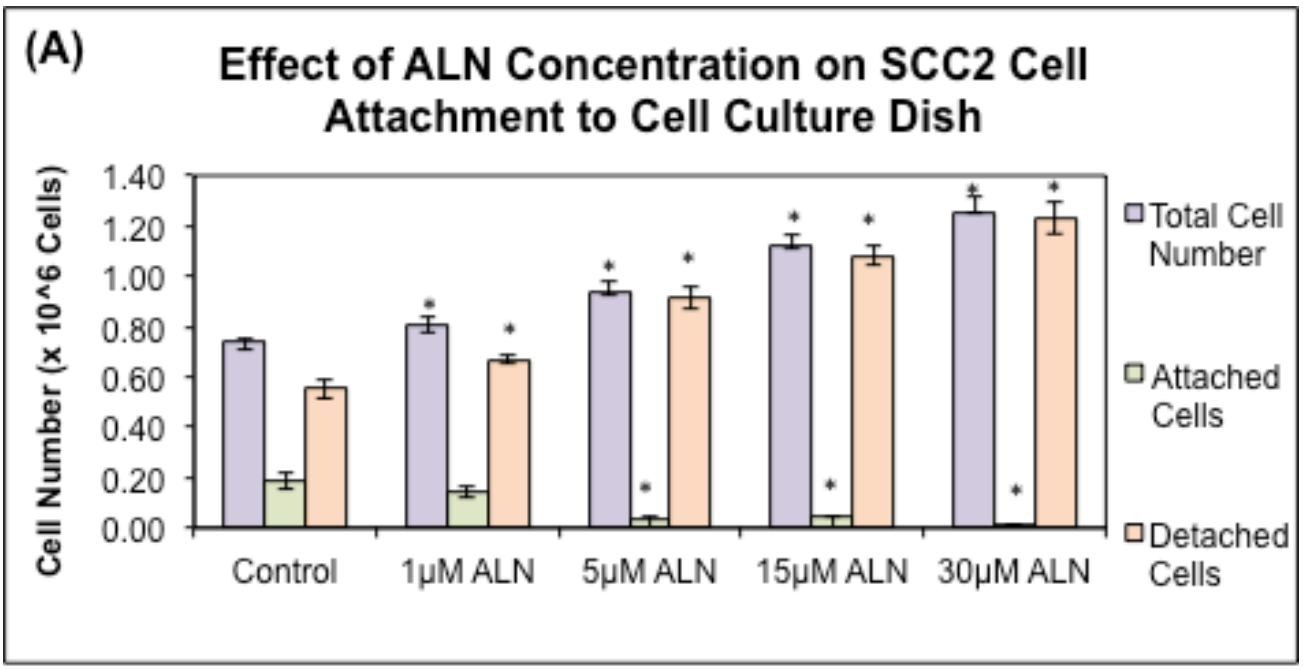
(A)
Effect of ALN Concentration on SCC2 Cell Attachment to Cell Culture Dish
Cell Number (x 10^6 Cells)
1.40
1.20
1.00
0.80
0.60
0.40
0.20
0.00
Control
1μM ALN
5μM ALN
15μM ALN
30μM ALN
Total Cell Number
Attached Cells
Detached Cells

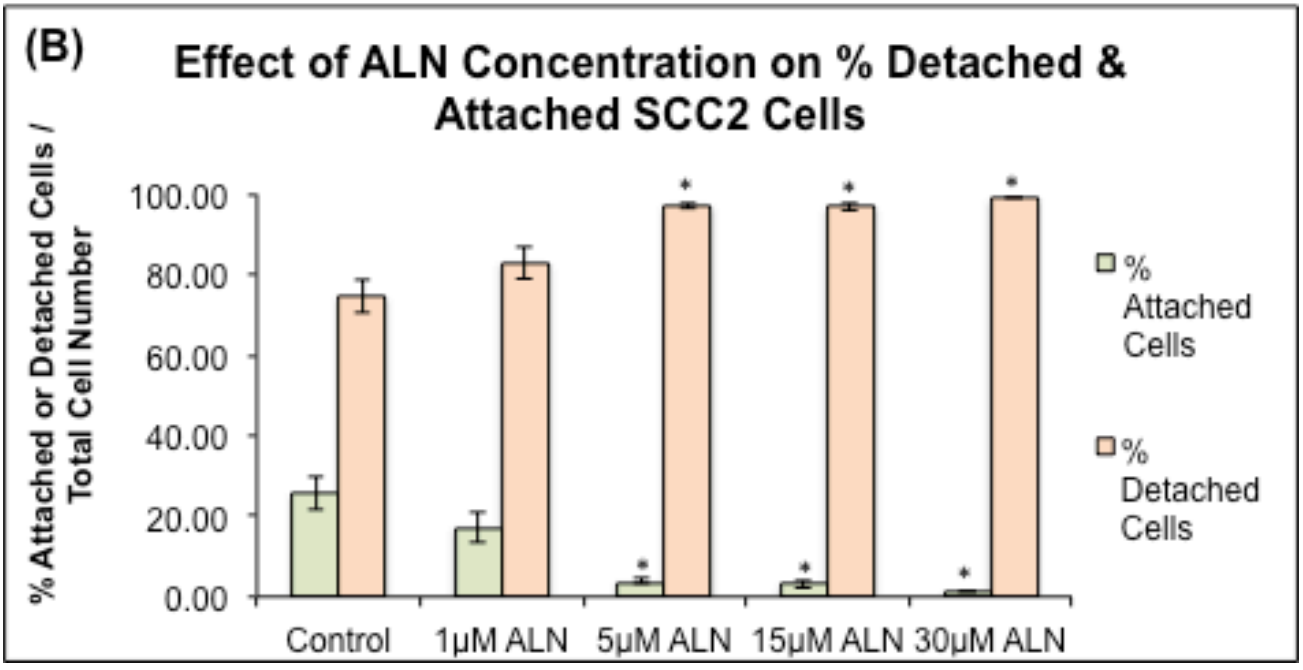
(B)
Effect of ALN Concentration on % Detached & Attached SCC2 Cells
% Attached or Detached Cells / Total Cell Number
100.00
80.00
60.00
40.00
20.00
0.00
Control
1μM ALN
5μM ALN
15μM ALN
30μM ALN
% Attached Cells
% Detached Cells

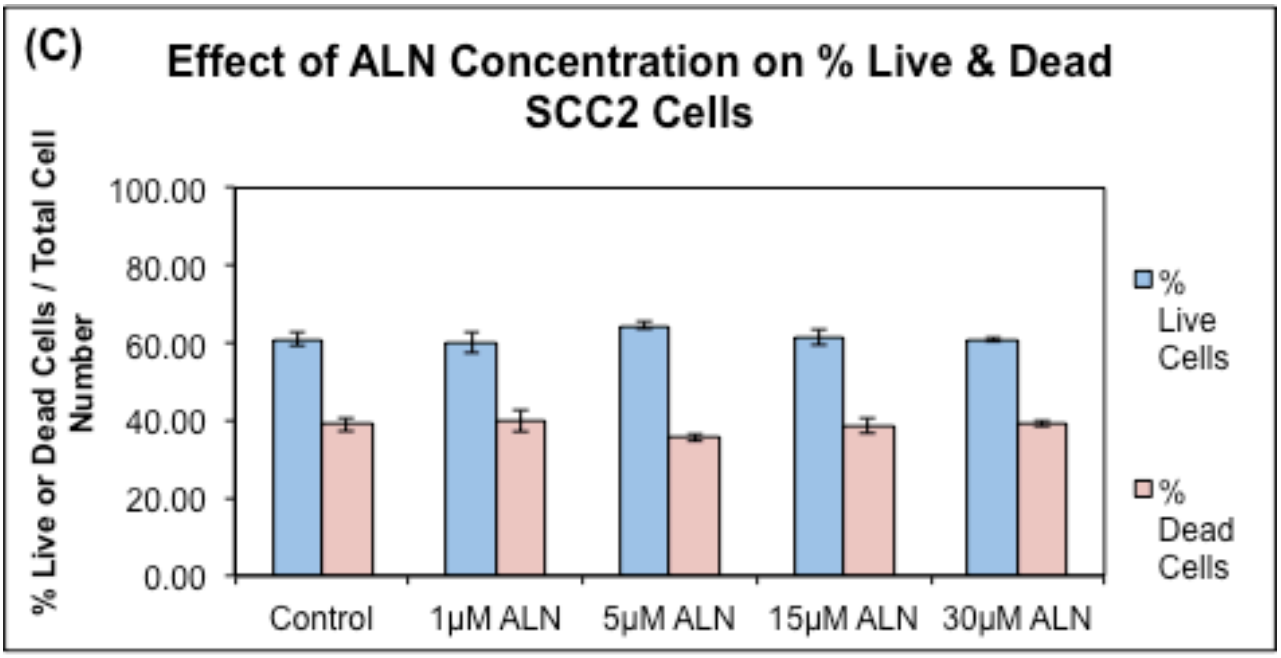
(C)
Effect of ALN Concentration on % Live & Dead SCC2 Cells
% Live or Dead Cells / Total Cell Number
100.00
80.00
60.00
40.00
20.00
0.00
Control
1μM ALN
5μM ALN
15μM ALN
30μM ALN
% Live Cells
% Dead Cells

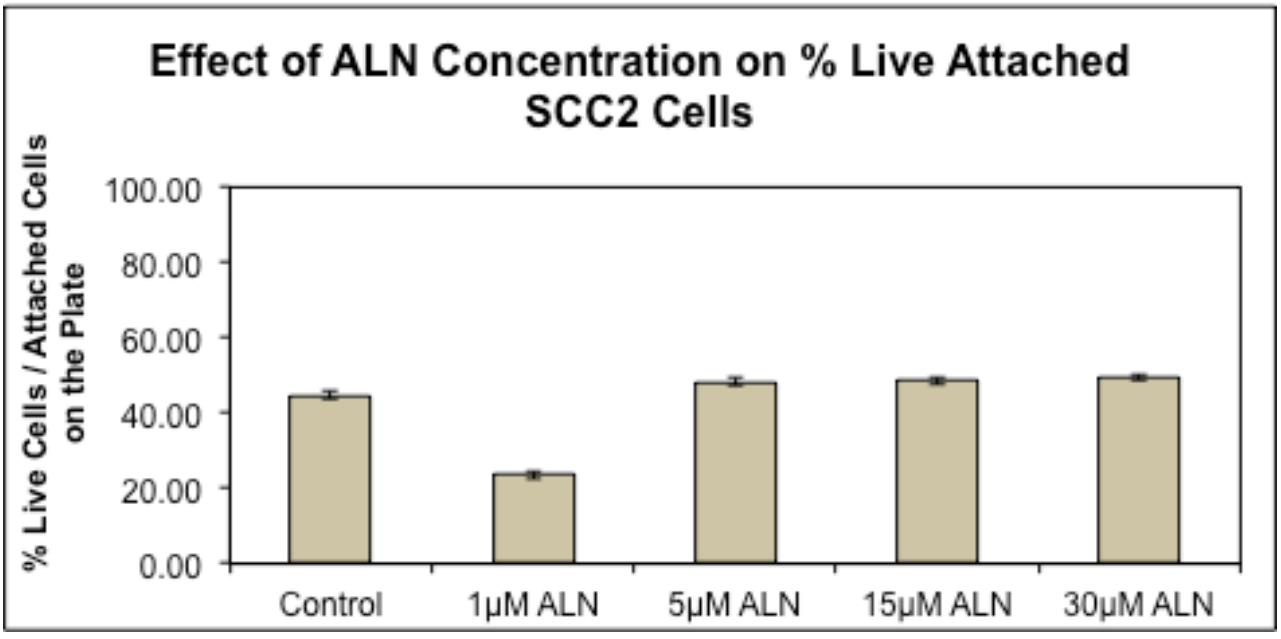
Effect of ALN Concentration on % Live Attached SCC2 Cells
% Live Cells / Attached Cells on the Plate
100.00
80.00
60.00
40.00
20.00
0.00
Control
1μM ALN
5μM ALN
15μM ALN
30μM ALN

**Figure 17 – SCC2 2D-Cell Culture in FCS Media with ALN at Confluence.**

2D-cell cultures of SCC2 cells in FCS media in the presence or absence of ALN added at tim cell confluence: (A) and (B) ALN increased total cell number and decreased SCC2 attachment in a concentration-dependent manner. Results are expressed as a mean ± S.D. (n=3) (*, $P<0.05$, **, $P<0.001$, Two-tailed t test with equal variance compared with Control); (C) and (D) ALN did not affect viability of overall or attached SCC2 cells.

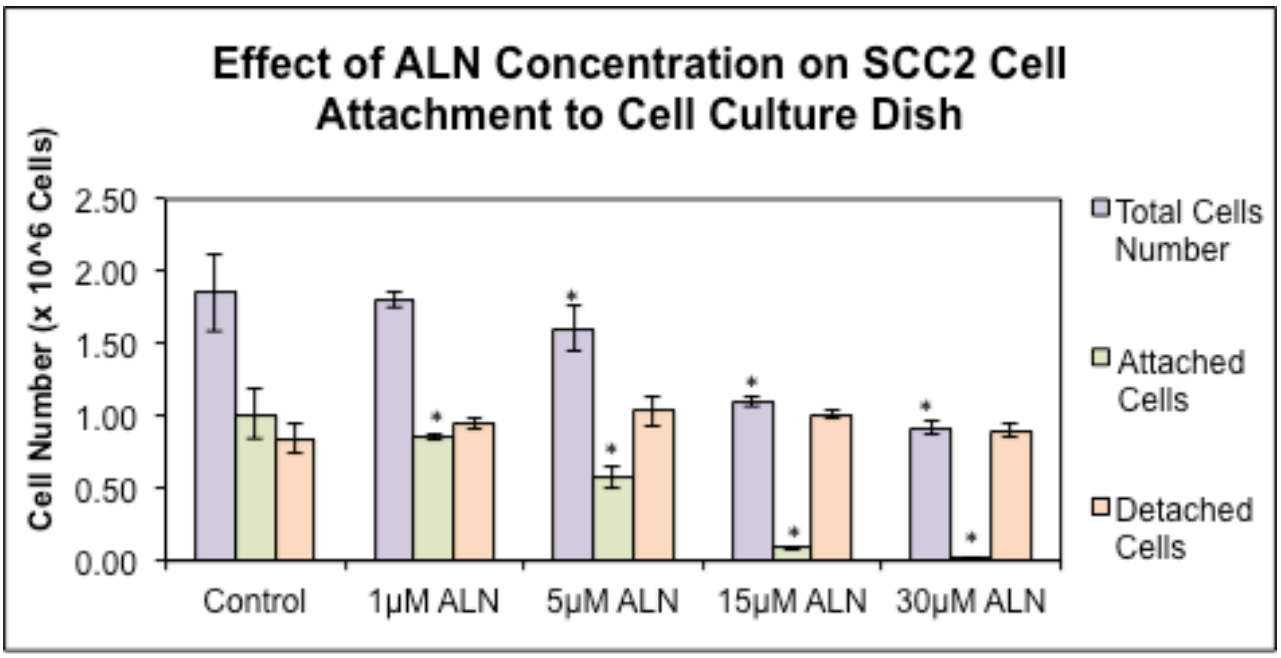
Effect of ALN Concentration on SCC2 Cell Attachment to Cell Culture Dish
Cell Number (x 10^6 Cells)
2.50
2.00
1.50
1.00
0.50
0.00
Control
1μM ALN
5μM ALN
15μM ALN
30μM ALN
Total Cells Number
Attached Cells
Detached Cells

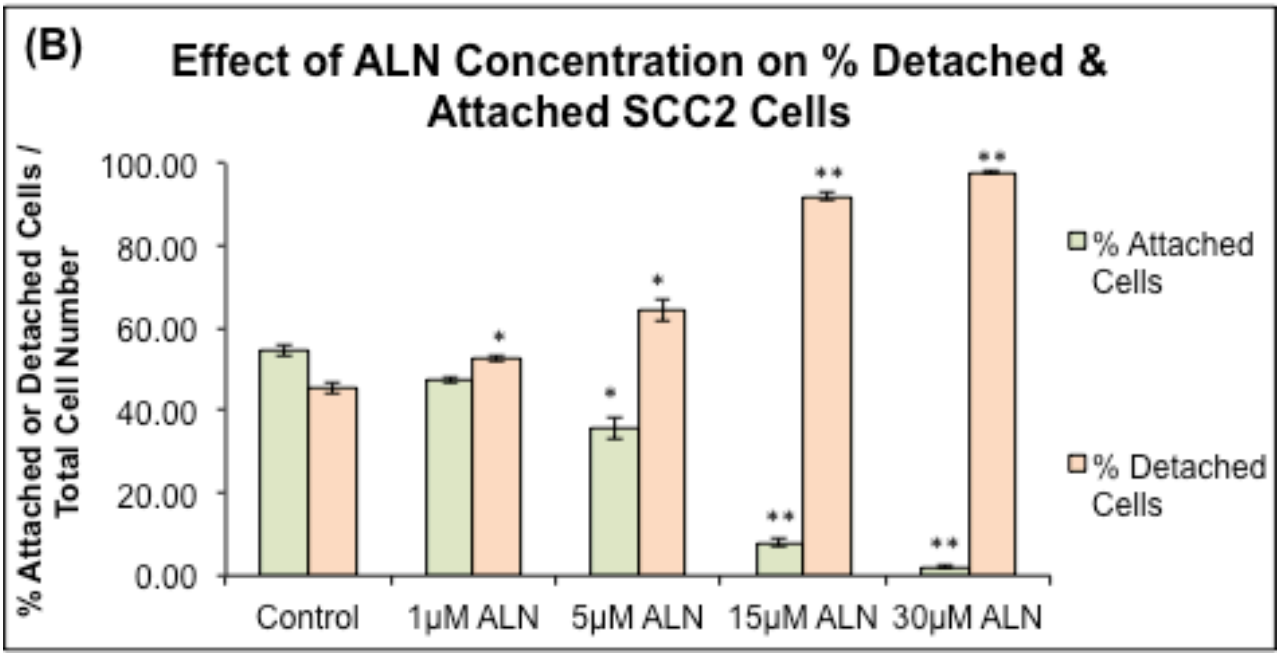
(B)
Effect of ALN Concentration on % Detached & Attached SCC2 Cells
% Attached or Detached Cells / Total Cell Number
100.00
80.00
60.00
40.00
20.00
0.00
Control
1μM ALN
5μM ALN
15μM ALN
30μM ALN
% Attached Cells
% Detached Cells

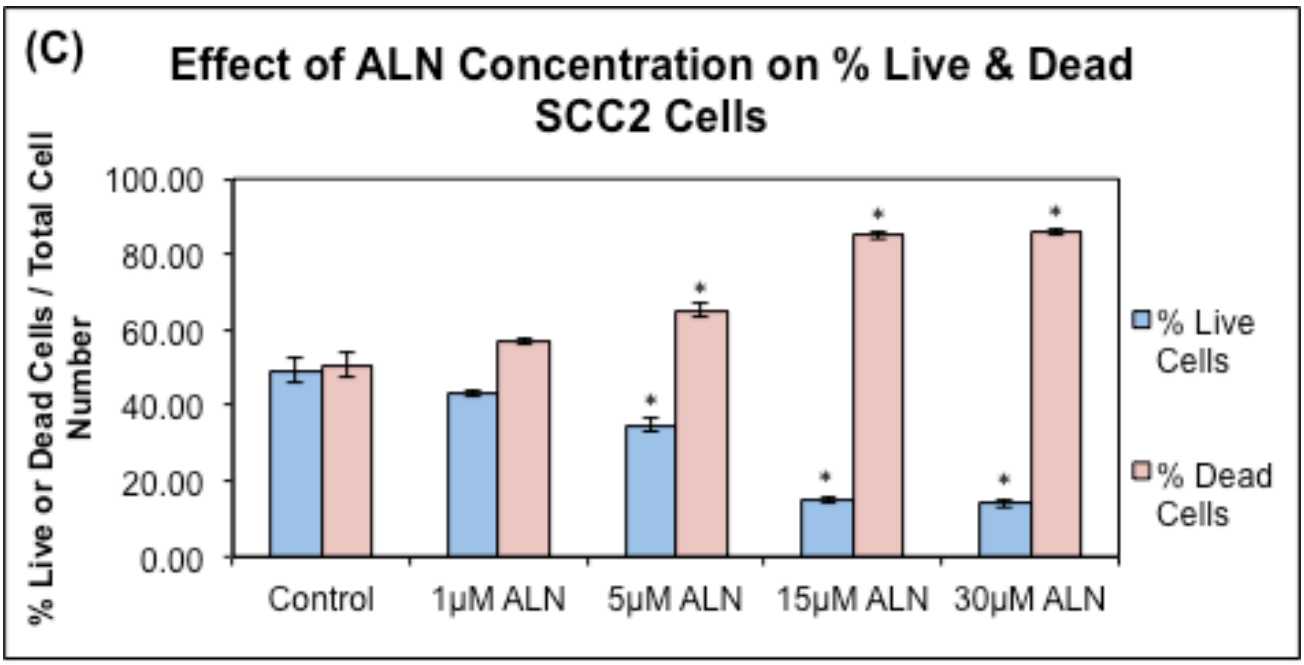
(C)
Effect of ALN Concentration on % Live & Dead SCC2 Cells
% Live or Dead Cells / Total Cell Number
100.00
80.00
60.00
40.00
20.00
0.00
Control
1μM ALN
5μM ALN
15μM ALN
30μM ALN
% Live Cells
% Dead Cells

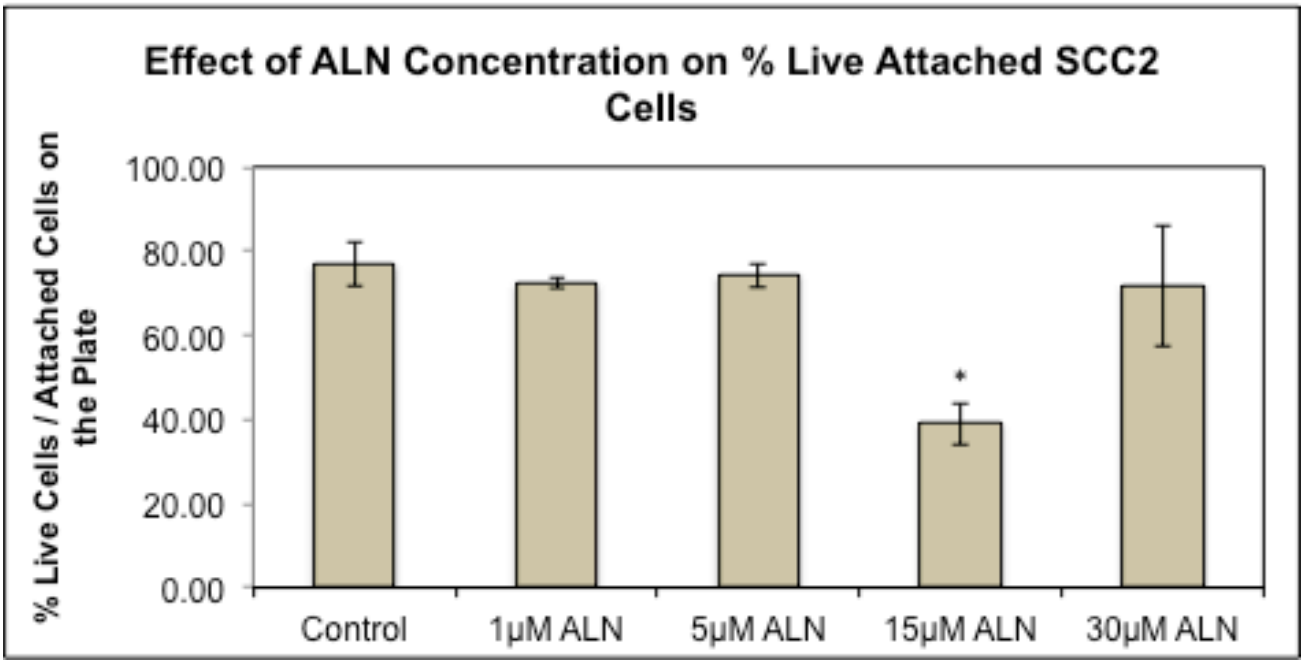
Effect of ALN Concentration on % Live Attached SCC2 Cells
% Live Cells / Attached Cells on the Plate
100.00
80.00
60.00
40.00
20.00
0.00
Control
1μM ALN
5μM ALN
15μM ALN
30μM ALN

**Figure 18 – SCC2 2D-Cell Culture in FCS Media with ALN and ASC at Confluence.** 2D-cell cultures of SCC2 cells in FCS media wit ASC in the presence or absence of ALN added at time of cell confluence: (A) and (B) ALN decreased total cell number and increased percentage of SCC2 cells detachment in a concentration-dependent manner, except in the experimental group treated with 1 μM ALN. Results are expressed as a mean ± S.D. (n=3) (*, $P<0.05$, **, $P<0.001$, Two-tailed t test with equal variance compared with Control); (C) ALN significantly increased percentage of dead SCC2 cells in a concentration-dependent manner except in the group treated with 1 μM ALN. Results are expressed as a mean ± S.D. (n=3) (*, $P<0.05$, **, $P<0.001$, Two-tailed t test with equal variance compared to Control); (D) ALN significantly decreased percentage of live cells in the experimental group treated with 1 μM ALN. Results are expressed as a mean ± S.D. (n=3) (*, $P<0.05$, **, $P<0.001$, Two-tailed t test with equal variance compared to Control).

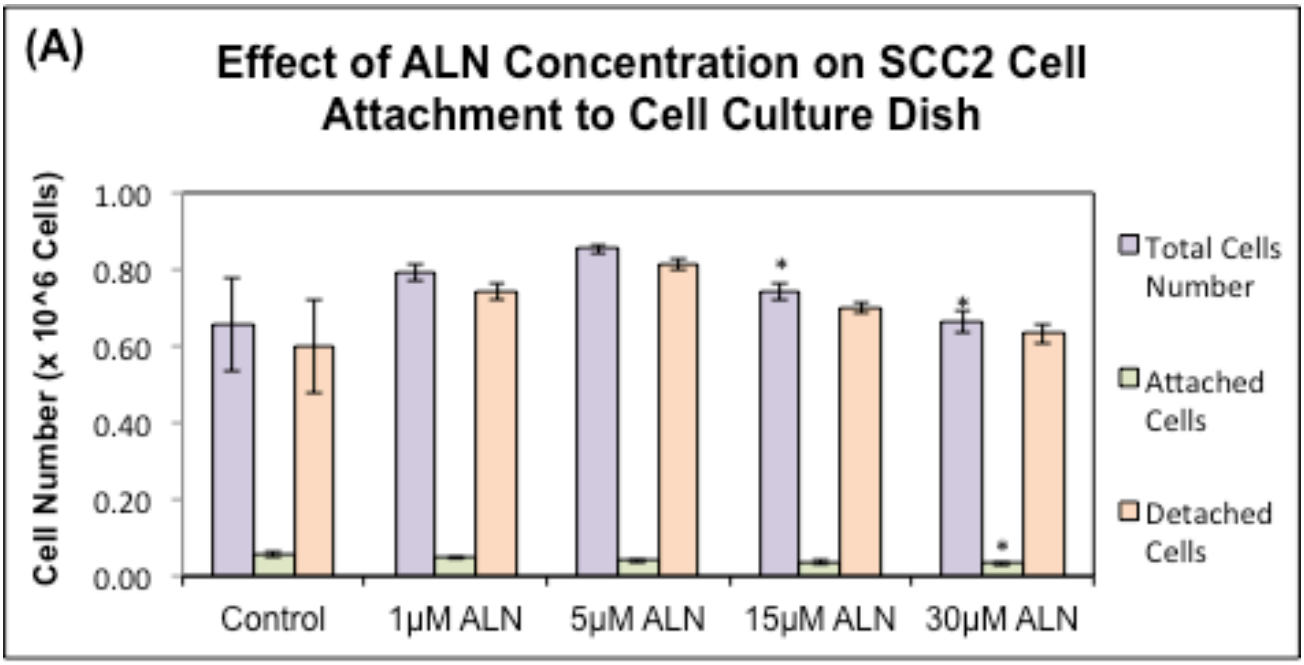
(A)
Effect of ALN Concentration on SCC2 Cell Attachment to Cell Culture Dish
Cell Number (x 10^6 Cells)
1.00
0.80
0.60
0.40
0.20
0.00
Control
1μM ALN
5μM ALN
15μM ALN
30μM ALN
Total Cells Number
Attached Cells
Detached Cells

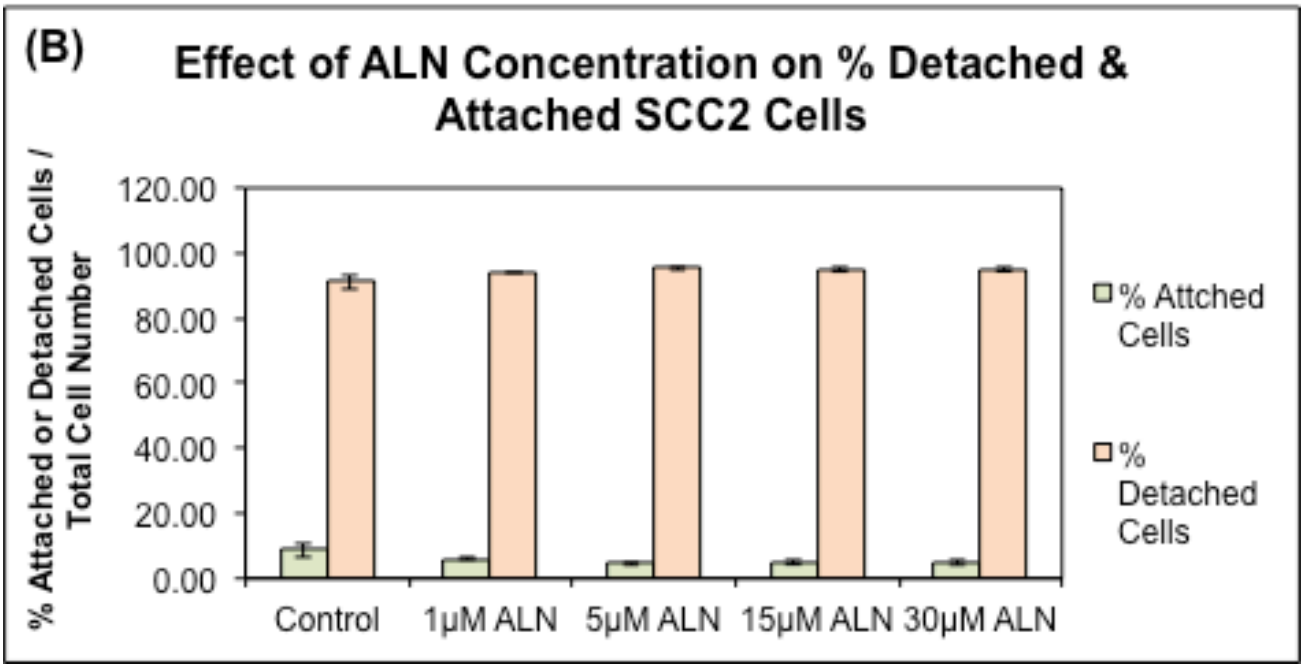
(B)
Effect of ALN Concentration on % Detached & Attached SCC2 Cells
% Attached or Detached Cells / Total Cell Number
120.00
100.00
80.00
60.00
40.00
20.00
0.00
Control
1μM ALN
5μM ALN
15μM ALN
30μM ALN
% Attched Cells
% Detached Cells

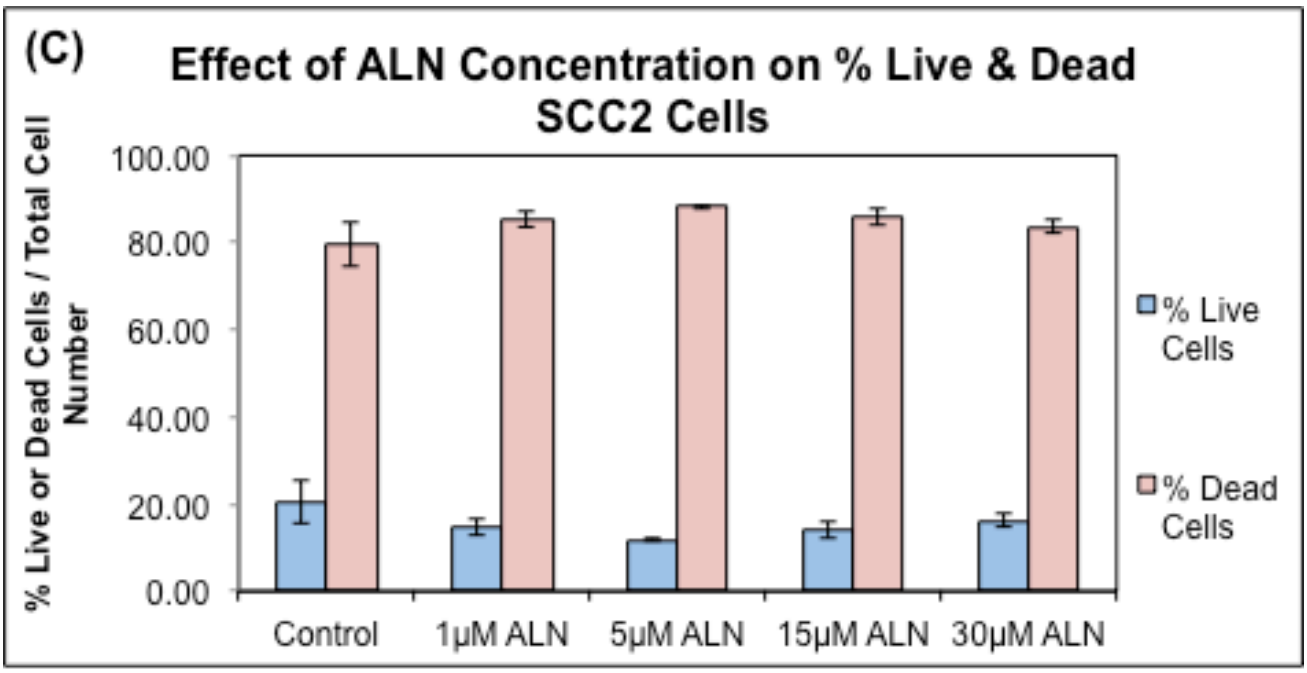
(C)
Effect of ALN Concentration on % Live & Dead SCC2 Cells
% Live or Dead Cells / Total Cell Number
100.00
80.00
60.00
40.00
20.00
0.00
Control
1μM ALN
5μM ALN
15μM ALN
30μM ALN
% Live Cells
% Dead Cells

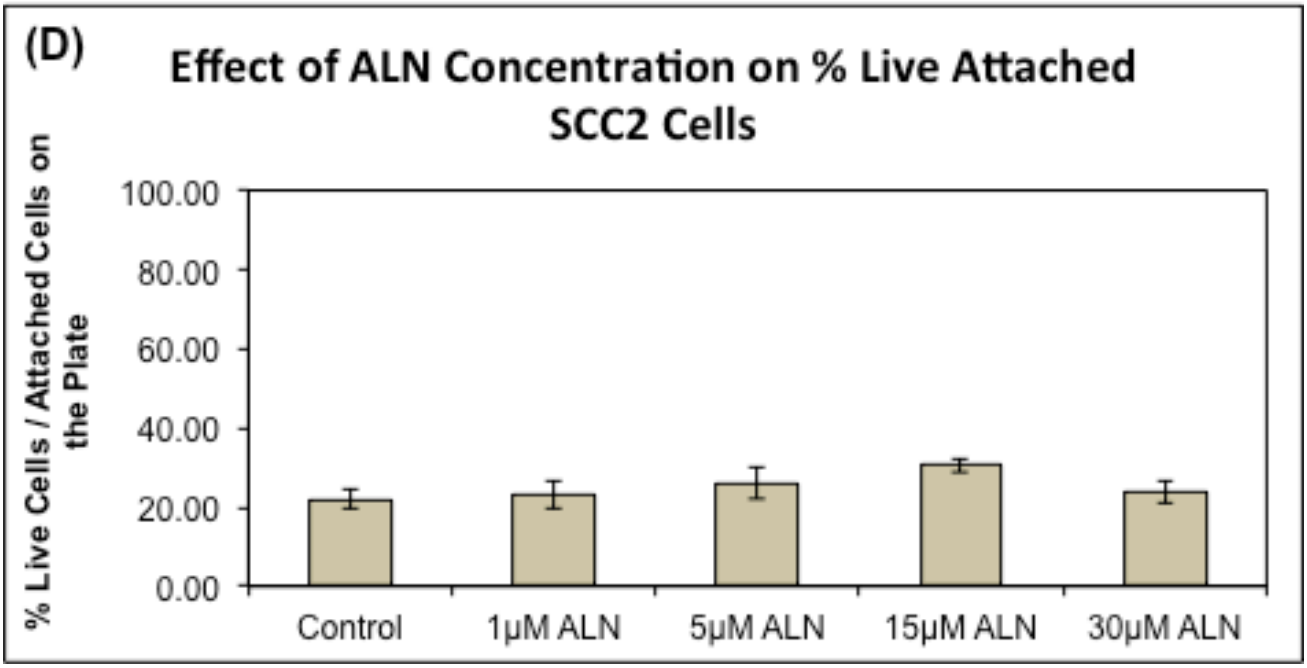
(D)
Effect of ALN Concentration on % Live Attached SCC2 Cells
% Live Cells / Attached Cells on the Plate
100.00
80.00
60.00
40.00
20.00
0.00
Control
1μM ALN
5μM ALN
15μM ALN
30μM ALN

**Figure 19 – SCC2 2D-Cell Culture in FCS Media with ALN at Seeding.** 2D-cell cultures of SCC2 cells in FCS media in the presence or absence of ALN added at seeding: (A) and (B) There was no significant change in total cell number or SCC2 cell attachment, except in the groups treated with 15 μM ALN and 30 μM ALN. Results are expressed as a mean ± S.D. (n=3) (*, $P<0.05$, **, $P<0.001$, Two-tailed t test with equal variance compared to Control); (C) and (D) ALN did not affect viability of overall or attached SCC2 cells. However, when compared to the same experimental groups at confluence, all of the groups showed higher percentage of dead SCC2 cells and lower percentage of attached SCC2 cells.

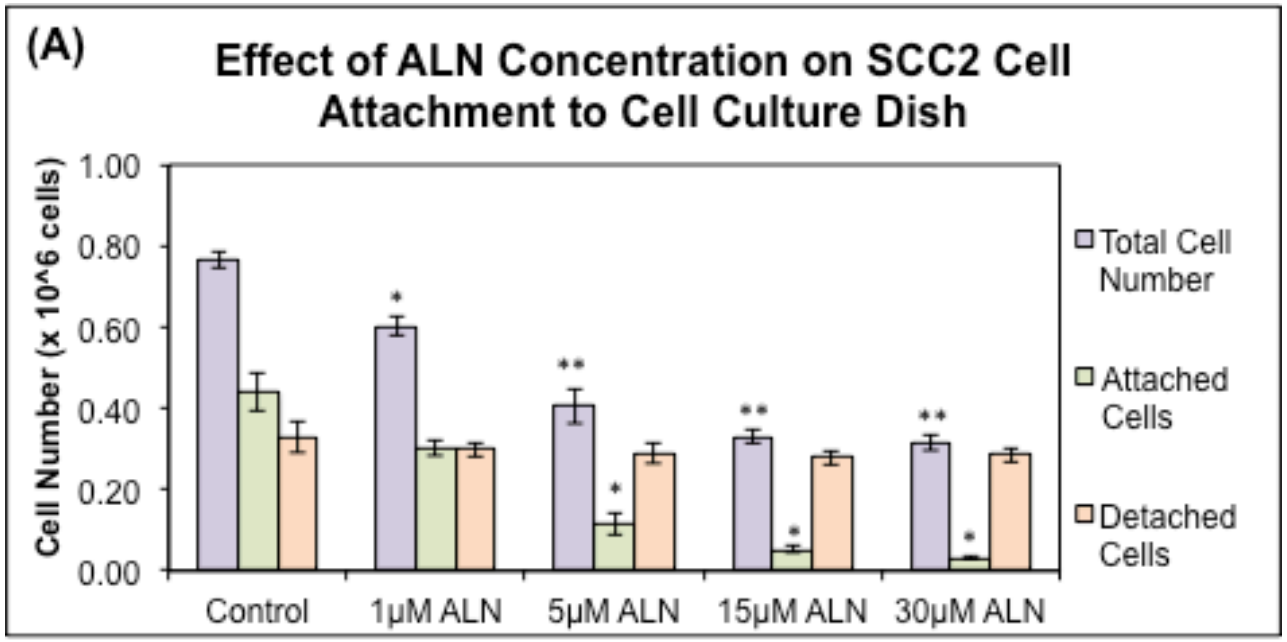
(A)
Effect of ALN Concentration on SCC2 Cell Attachment to Cell Culture Dish
Cell Number (x 10^6 cells)
1.00
0.80
0.60
0.40
0.20
0.00
Control
1μM ALN
5μM ALN
15μM ALN
30μM ALN
Total Cell Number
Attached Cells
Detached Cells

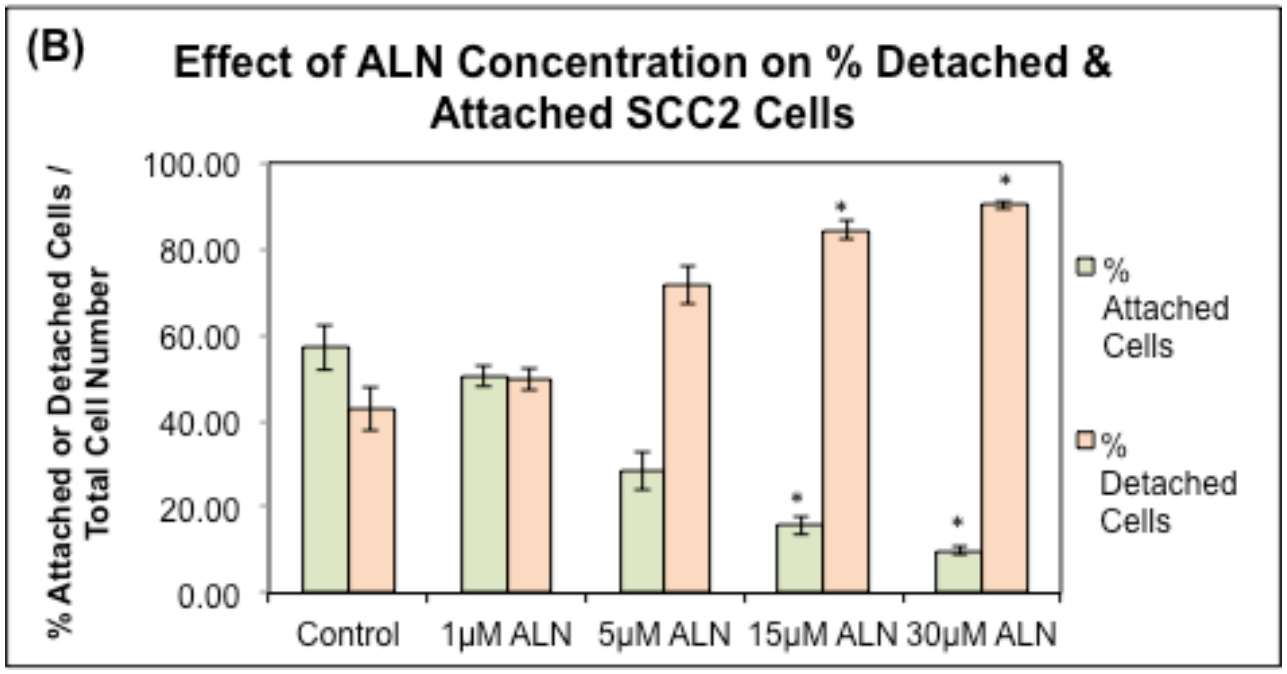
(B)
Effect of ALN Concentration on % Detached & Attached SCC2 Cells
% Attached or Detached Cells / Total Cell Number
100.00
80.00
60.00
40.00
20.00
0.00
Control
1μM ALN
5μM ALN
15μM ALN
30μM ALN
% Attached Cells
% Detached Cells

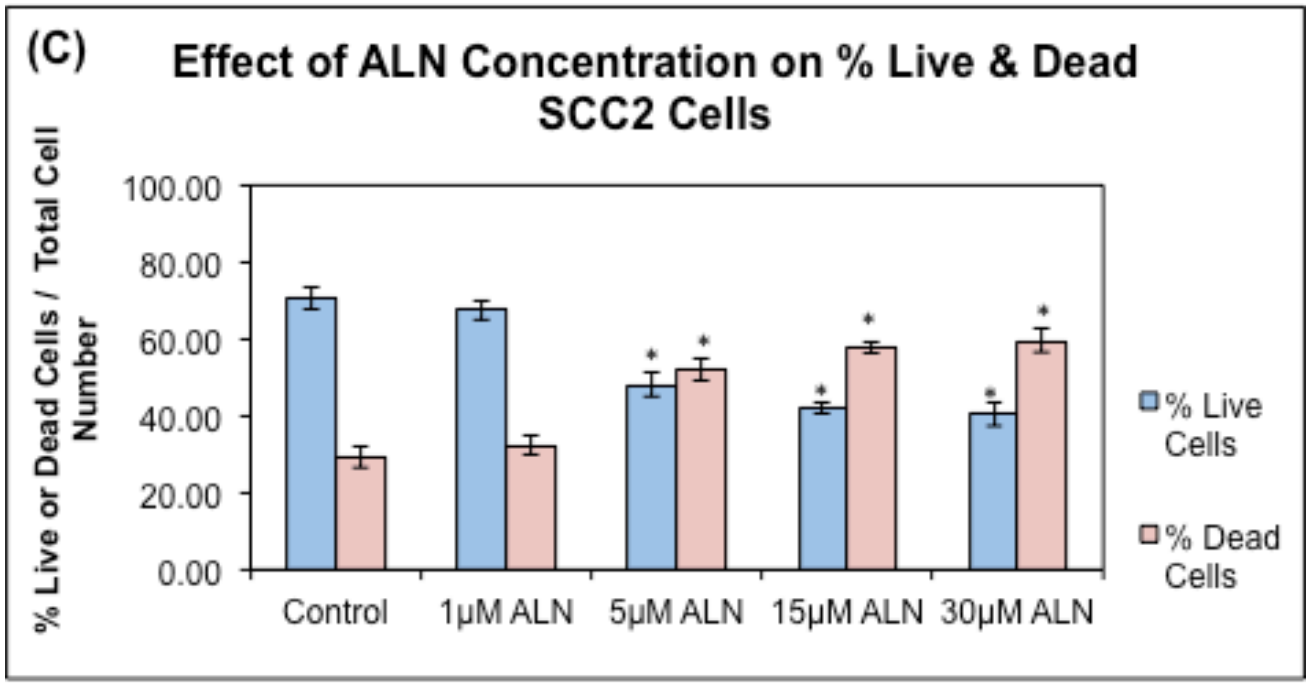
(C)
Effect of ALN Concentration on % Live & Dead SCC2 Cells
% Live or Dead Cells / Total Cell Number
100.00
80.00
60.00
40.00
20.00
0.00
Control
1μM ALN
5μM ALN
15μM ALN
30μM ALN
% Live Cells
% Dead Cells

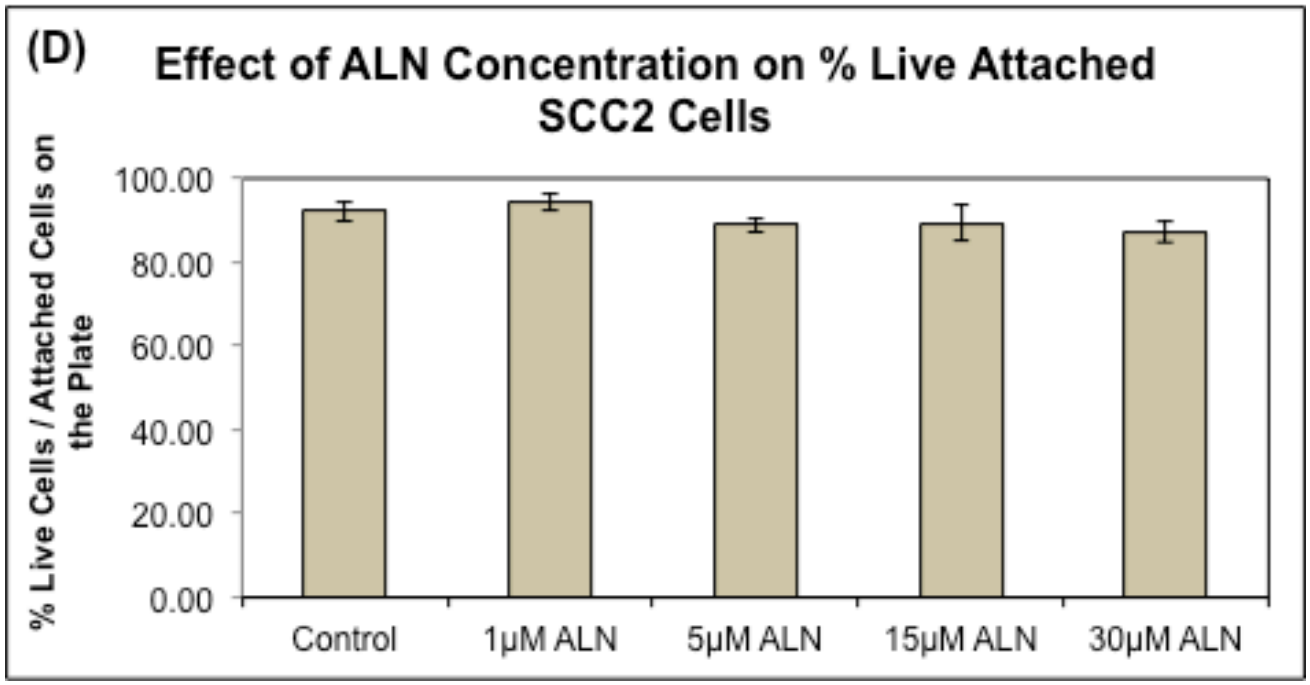
(D)
Effect of ALN Concentration on % Live Attached SCC2 Cells
% Live Cells / Attached Cells on the Plate
100.00
80.00
60.00
40.00
20.00
0.00
Control
1μM ALN
5μM ALN
15μM ALN
30μM ALN

**Figure 20 – SCC2 2D-Cell Culture in FCS Media with ALN and ASC at Seeding.** 2D-cell cultures of SCC2 cells in FCS media wit ASC in the presence and absence of ALN added at seeding: (A) ALN decreased total cell number and number of attached SCC2 cells in a concentration-dependent manner. Results are expressed as a mean ± S.D. (n=3) (*, $P<0.05$, **, $P<0.001$, Two-tailed t test with equal variance compared to Control); (B) ALN increased SCC2 cells detachment and decreased SCC2 cells attachment for groups treated with 15 μM ALN and 30 μM ALN. Results are expressed as a mean ± S.D. (n=3) (*, $P<0.05$, **, $P<0.001$, Two-tailed t test with equal variance compared to Control); (C) ALN significantly decreased the SCC2 viability except in the group treated with 1 μM ALN. Results are expressed as a mean ± S.D. (n=3) (*, $P<0.05$, **, $P<0.001$, Two-tailed t test with equal variance compared to Control); (D) ALN did not affect the viability of attached SCC2 cells.

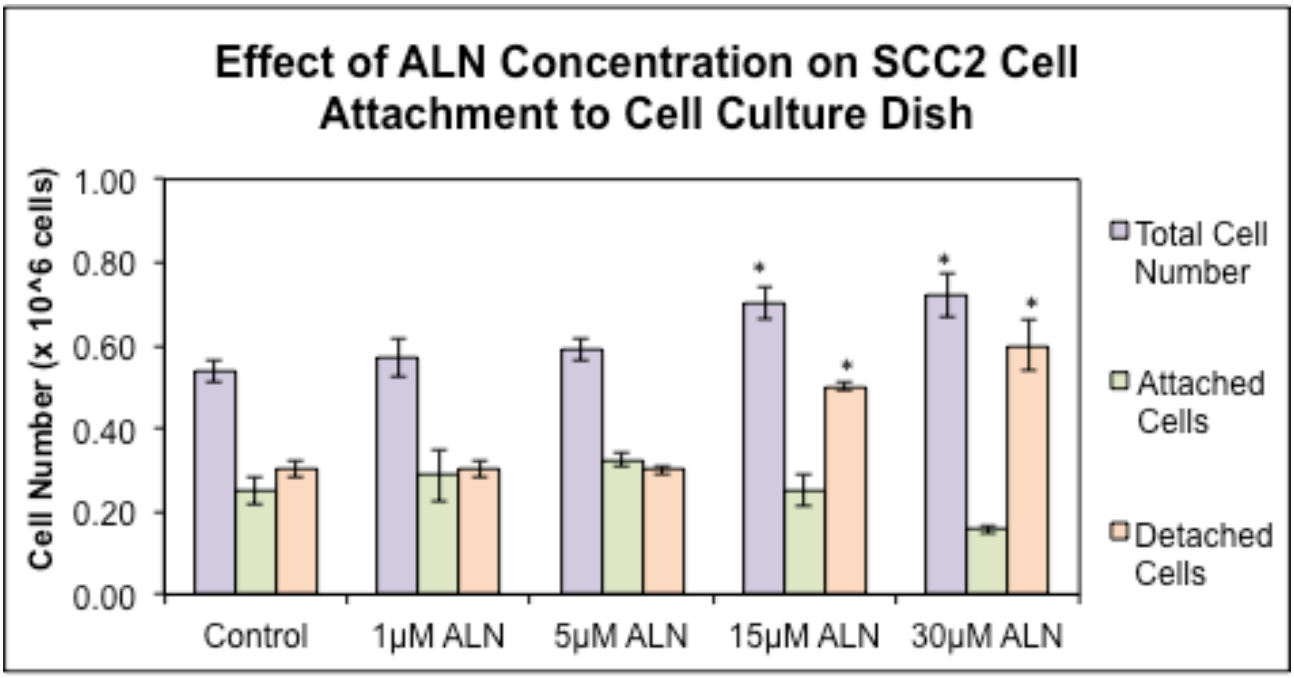
Effect of ALN Concentration on SCC2 Cell Attachment to Cell Culture Dish
Cell Number (x 10^6 cells)
1.00
0.80
0.60
0.40
0.20
0.00
Control
1μM ALN
5μM ALN
15μM ALN
30μM ALN
Total Cell Number
Attached Cells
Detached Cells

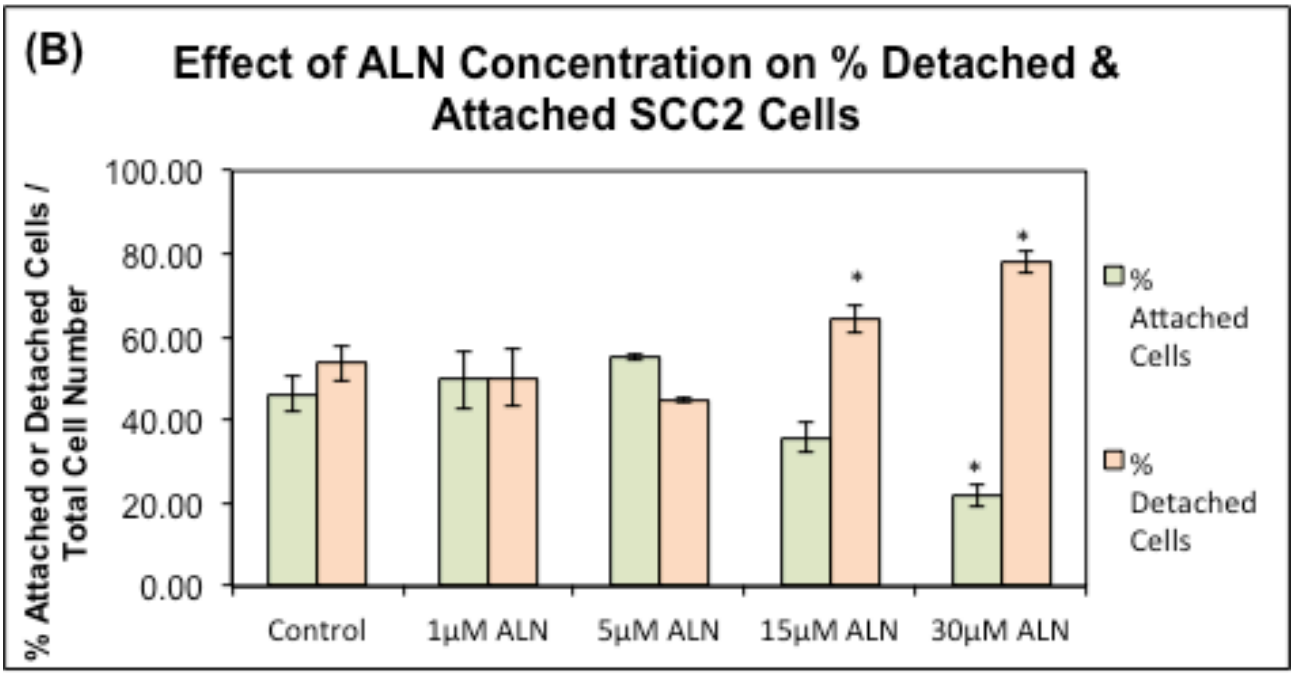
(B)
Effect of ALN Concentration on % Detached & Attached SCC2 Cells
% Attached or Detached Cells / Total Cell Number
100.00
80.00
60.00
40.00
20.00
0.00
Control
1μM ALN
5μM ALN
15μM ALN
30μM ALN
% Attached Cells
% Detached Cells

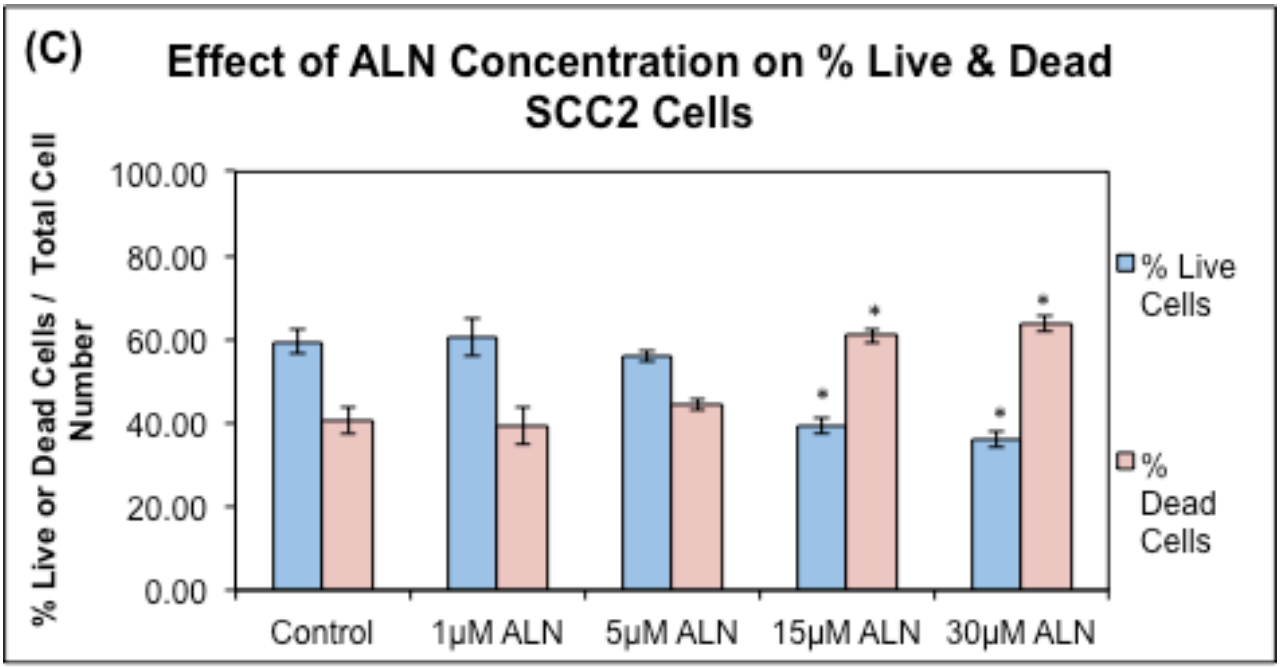
(C)
Effect of ALN Concentration on % Live & Dead SCC2 Cells
% Live or Dead Cells / Total Cell Number
100.00
80.00
60.00
40.00
20.00
0.00
Control
1μM ALN
5μM ALN
15μM ALN
30μM ALN
% Live Cells
% Dead Cells
*
*
*
*

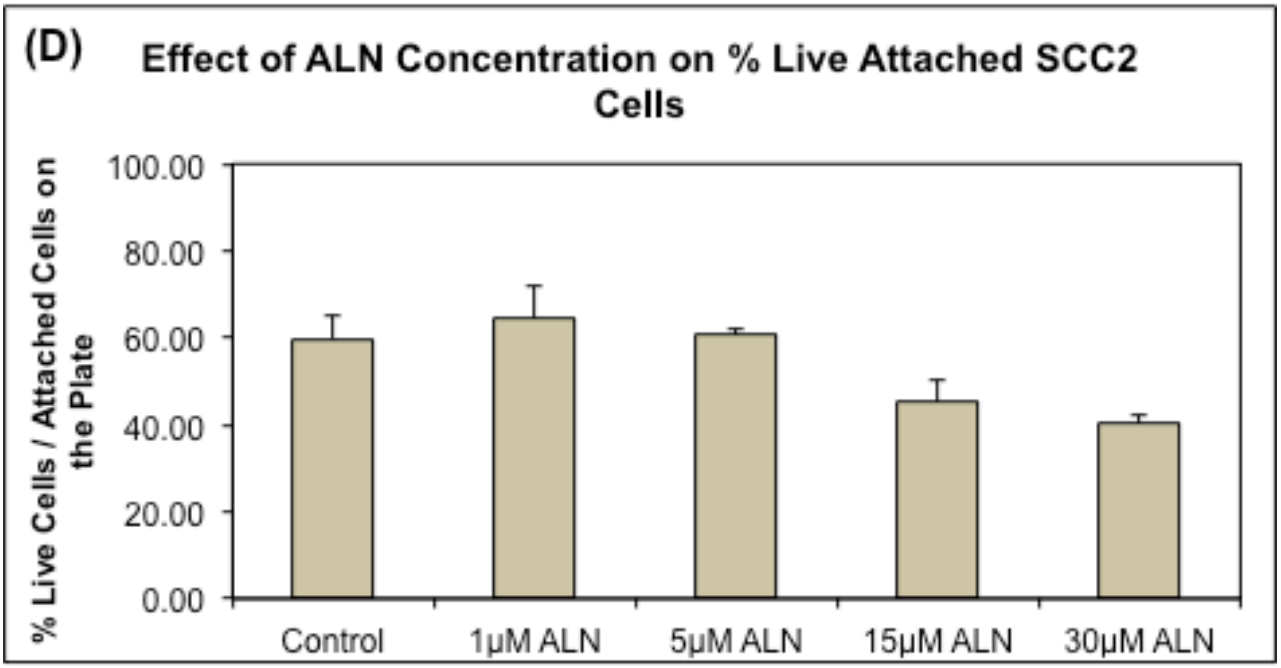
(D)
Effect of ALN Concentration on % Live Attached SCC2 Cells
% Live Cells / Attached Cells on the Plate
100.00
80.00
60.00
40.00
20.00
0.00
Control
1μM ALN
5μM ALN
15μM ALN
30μM ALN

**Figure 21 – SCC2 2D-Cell Culture in BSA Media with ALN at Confluence.** 2D-cell cultures of SCC2 cells in BSA media in the presence or absence of ALN added at cell confluence: (A) ALN increased total cell number and SCC2 cells detachment in the groups treated with 15 μM ALN and 30 μM ALN. Results are expressed as a mean ± S.D. (n=3) (*, $P<0.05$, **, $P<0.001$, Two-tailed t test with equal variance compared to Control); (C) and (D) ALN significantly decreased the SCC2 cell viability in the groups treated with 15 μM ALN and 30 μM ALN while had no significant effect on the viability of attached SCC2 cells. Results are expressed as a mean ± S.D. (n=3) (*, $P<0.05$, **, $P<0.001$, Two-tailed t test with equal variance compared to Control).

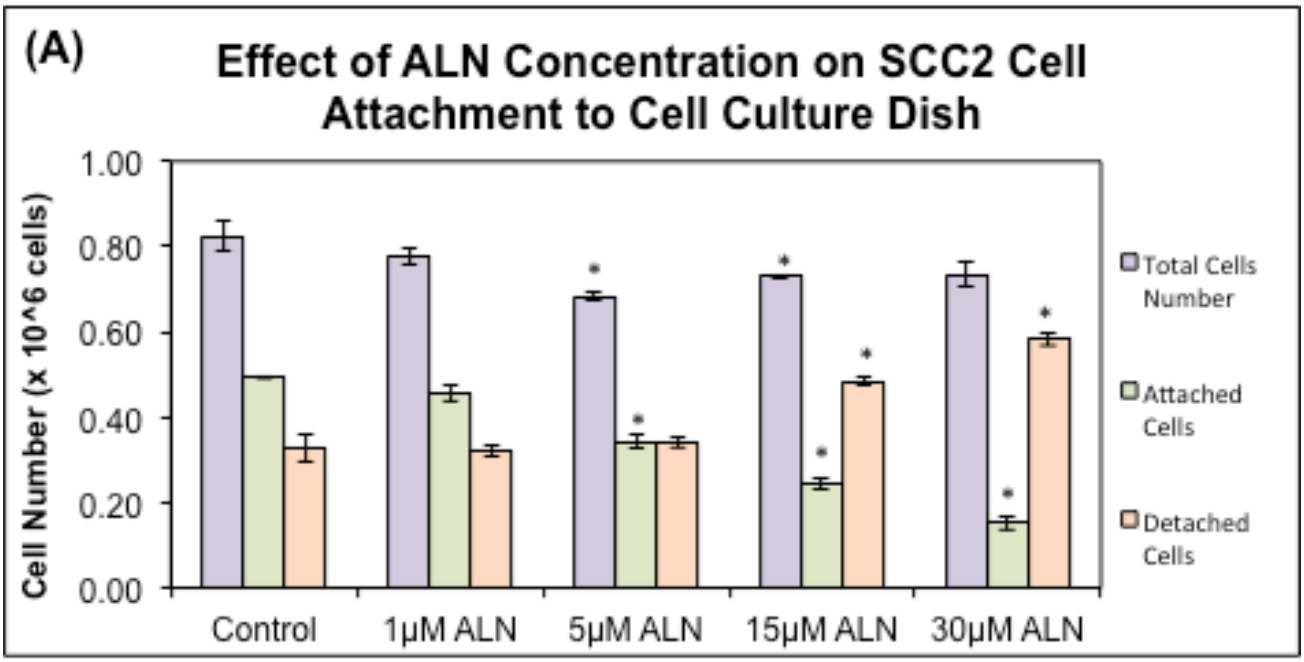
(A)
Effect of ALN Concentration on SCC2 Cell Attachment to Cell Culture Dish
Cell Number (x 10^6 cells)
1.00
0.80
0.60
0.40
0.20
0.00
Control
1μM ALN
5μM ALN
15μM ALN
30μM ALN
Total Cells Number
Attached Cells
Detached Cells

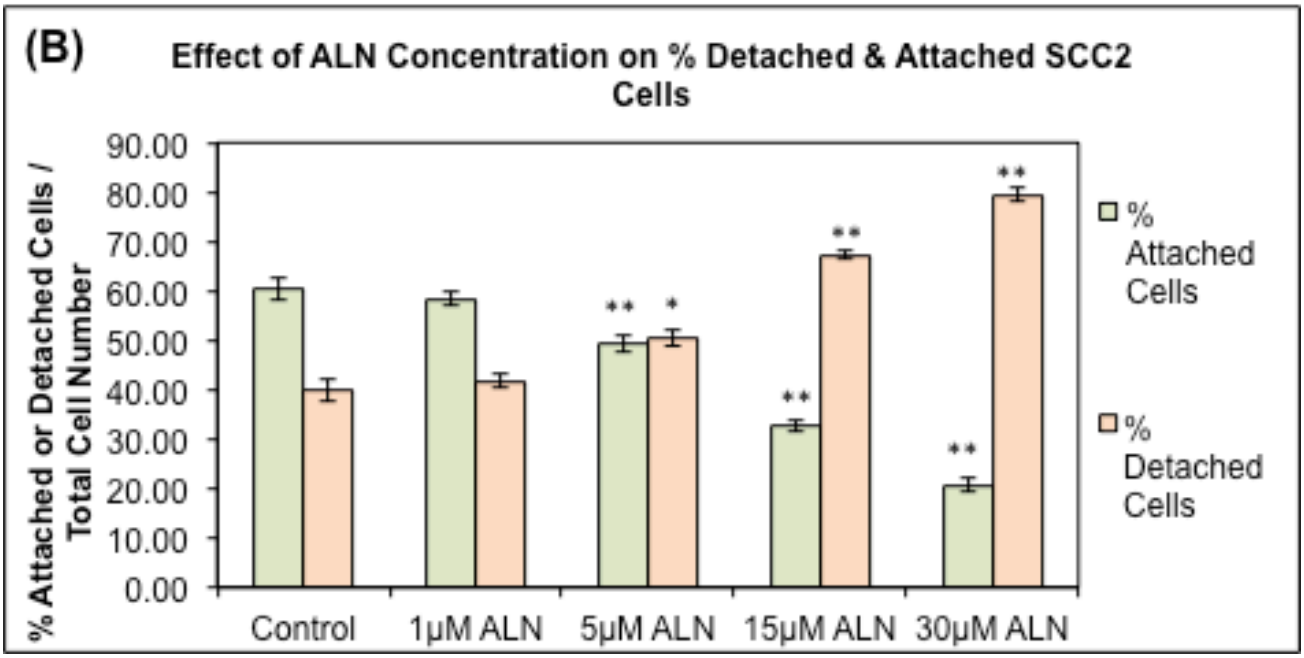
(B)
Effect of ALN Concentration on % Detached & Attached SCC2 Cells
% Attached or Detached Cells / Total Cell Number
90.00
80.00
70.00
60.00
50.00
40.00
30.00
20.00
10.00
0.00
Control
1μM ALN
5μM ALN
15μM ALN
30μM ALN
% Attached Cells
% Detached Cells

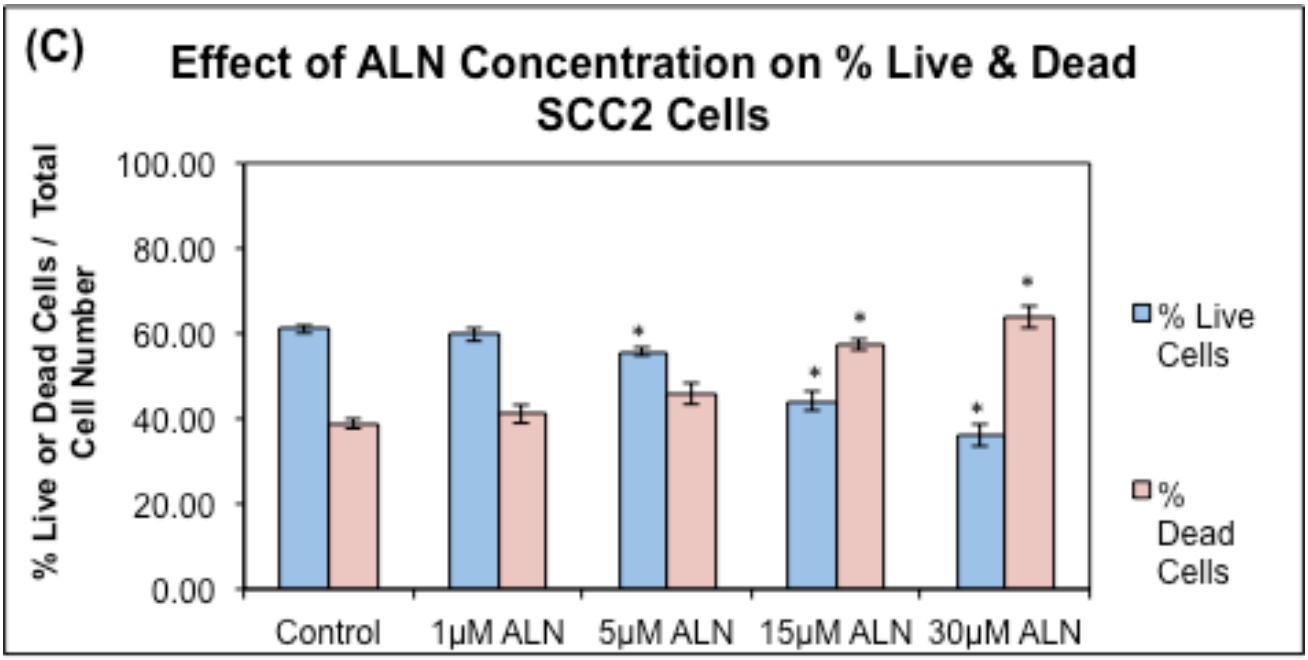
(C)
Effect of ALN Concentration on % Live & Dead SCC2 Cells
% Live or Dead Cells / Total Cell Number
100.00
80.00
60.00
40.00
20.00
0.00
Control
1μM ALN
5μM ALN
15μM ALN
30μM ALN
% Live Cells
% Dead Cells

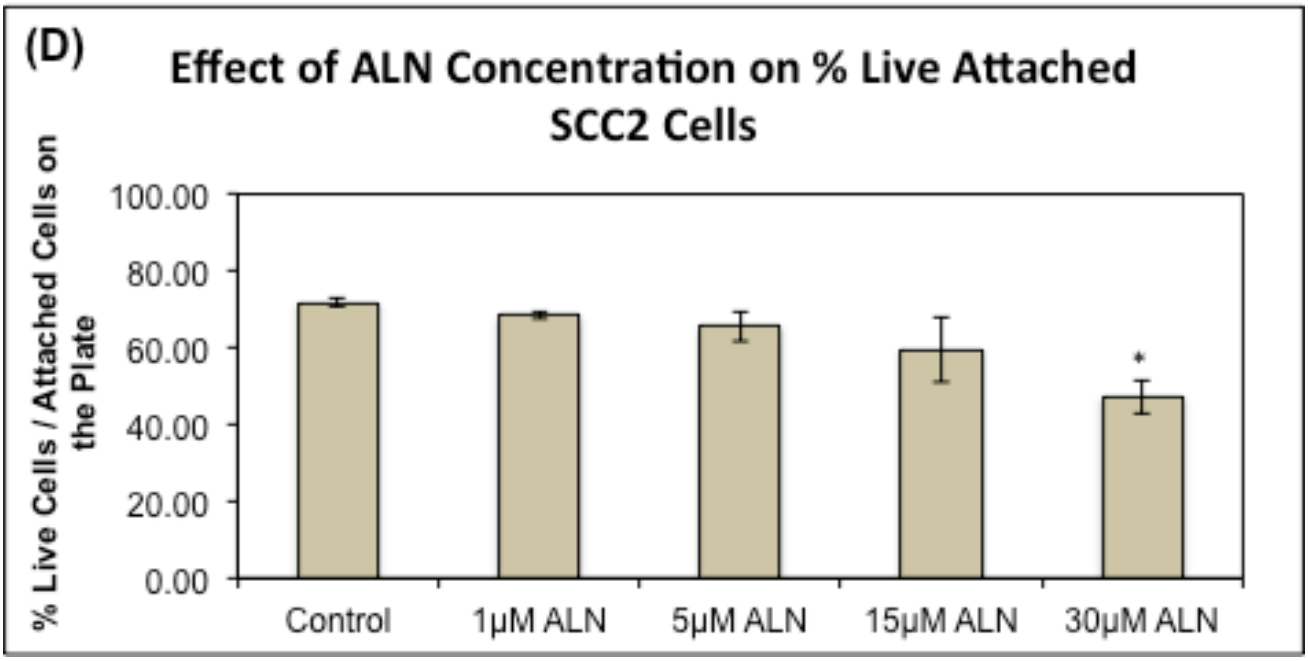
(D)
Effect of ALN Concentration on % Live Attached SCC2 Cells
% Live Cells / Attached Cells on the Plate
100.00
80.00
60.00
40.00
20.00
0.00
Control
1μM ALN
5μM ALN
15μM ALN
30μM ALN

**Figure 22 – SCC2 2D-Cell Culture in BSA Media with ALN and ASC at Confluence.** 2D-cell cultures of SCC2 cells in BSA media with ASC in the presence or absence of ALN added at time of cell confluence: (A) and (B) ALN increased SCC2 cell detachment and decreased SCC2 cell attachment in a concentration-dependent manner. Results are expressed as a mean ± S.D. (n=3) (*, $P<0.05$, **, $P<0.001$, Two-tailed t test with equal variance compared to Control); (C) and (D) ALN significantly decreased the overall SCC2 cell viability in the groups treated with 15 μM ALN and 30 μM ALN while decreasing viability of attached SCC2 cells treated with 30 μM ALN. Results are expressed as a mean ± S.D. (n=3) (*, $P<0.05$, **, $P<0.001$, Two-tailed t test with equal variance compared to Control).

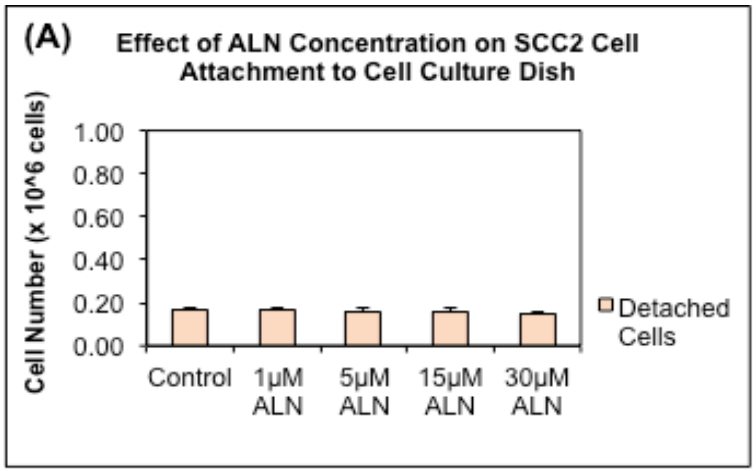


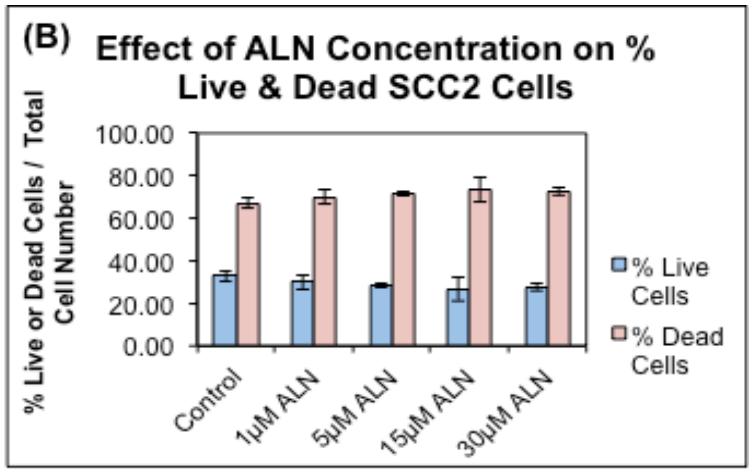


## (C) At Conclusion of Experiment

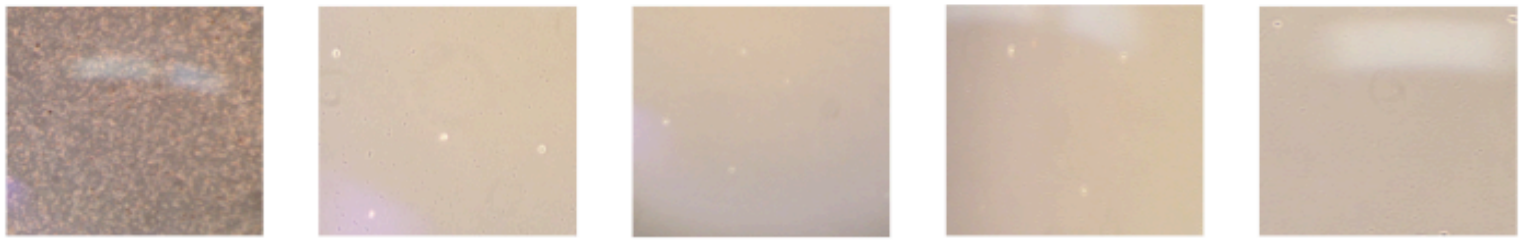

Control | 1 μM ALN | 5 μM ALN | 15 μM ALN | 30 μM ALN

**Figure 23 – SCC2 2D-Cell Culture in BSA Media with ALN at Seeding.** 2D-cell cultures of SCC2 cells in BSA media in the presence or absence of ALN added at seeding: (A) and (B) ALN did not affect SCC2 cells detachment or SCC2 cell viability among the experimental groups. (C) Photomicrographs of control and each experimental group were taken at last day of experiment (20X magnification). SCC2 cells do not survive well with BSA media and ALN.

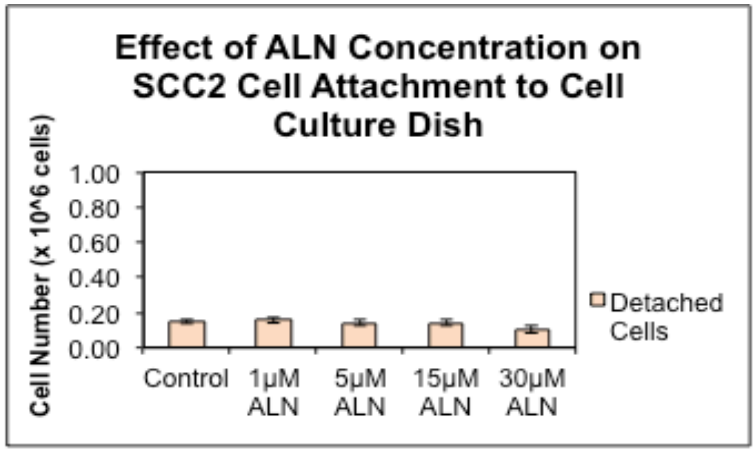


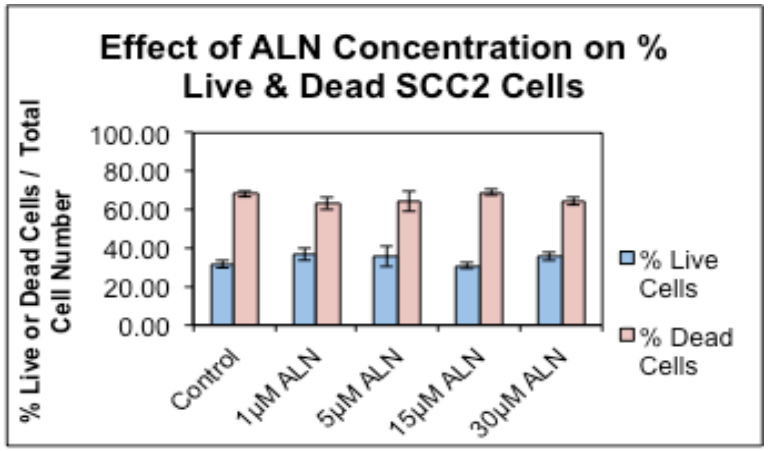


## (C) At Conclusion of Experiment

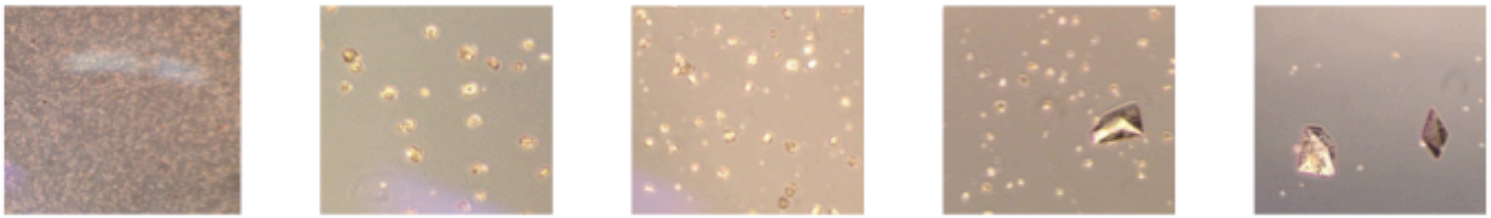

Control | 1 μM ALN | 5 μM ALN | 15 μM ALN | 30 μM ALN

**Figure 24 – SCC2 2D-Cell Culture in BSA Media with ALN and ASC at Seeding.** 2D-cell cultures of SCC2 cells in BSA media with ASC in the presence or absence of ALN added at seeding: (A) and (B) ALN did not affect SCC2 cells detachment or SCC2 cell viability. (C) Photomicrographs of control and each experimental group were taken at last day of experiment (20X magnification). SCC2 cells do not survive well with BSA media and ALN.

### *7.2. Histologic Observations and Visualization of Osteoclastic Activity by Neutral Red Staining: Effect of ALN and Calvarial Cells Viability on OCs Formation and Bone Resorption in Bone Resorptive Model.*

The H&E stained sections of calvaria bones in the bone resorptive models are illustrated in Figures 25-27. Figure 25 (A) and (E) showed no OCs formation and bone resorption for calvaria control in both H&E section and NR staining. H&E section and NR staining for calvaria treated with 30 μM ALN, showing no OCs formation and bone resorption (Figure 25 (B) and (F)). Calvaria co-cultured with SCC2 cells, H&E staining showed tumor cell colonization on the endosteal side of calvaria with areas of osteoclastic bone resorption (Figure 25 (C)) while NR staining of calvaria showed the presence of multinucleated OCs (MNOCs) (Figure 25 (G)). H&E section of parietal bone and NR staining for calvaria co-cultured with SCC2 cells and 30 μM ALN showed SCC2 cells colonization on the endosteal surface with inhibition of bone resorption and no presence of MNOC (Figure 25 (D) and (H)). These observations were expected since ALN inhibits OC proliferation and differentiation which reduces bone resorption.

H&E sections and NR stained calvaria for calvaria co-cultured with SCC2 cells and ALN (Figure 26). Calvaria co-cultured with single dosage of 0.5 μM ALN, H&E section of parietal bone showed SCC2 cells colonization and areas of osteoclastic bone resorption (Figure 26 (A)), and NR stained calvaria demonstrated presence of numerous MNOCs (Figure 25 (D)). Calvaria co-cultured with 0.5 μM ALN and 1.5 μM ALN, Figure 26 (B) & (C) and (E) & (F) showed similar observation for H&E sections and NR stained calvaria as the

calvaria co-cultured with SCC2 cells and single dose of 0.5 μM ALN.

H&E section for calvaria for calvaria that have been frozen and thawed prior to the co-culture with SCC2 cells showed reduced number of periosteal and endosteal cells while there was no sign of SCC2 cells colonization or osteoclastic bone resorption (Figure 27 (A)) and NR staining showed no presence of MNOC (Figure 27 (C)). For calvaria treated with 10% formaldehyde prior to co-culture with SCC2 cells, H&E section illustrated fixed calvarial bone cells with no tumor cell colonization (Figure 27 (B)), and no presence of MNOC on the NR stained calvaria (Figure 27 (D)).

**Figure 25 – Microscopic Observation for Bone Resorption Model: Control, Calvaria Co-culture with SCC2 Cells in the Absence and Presence of ALN.**

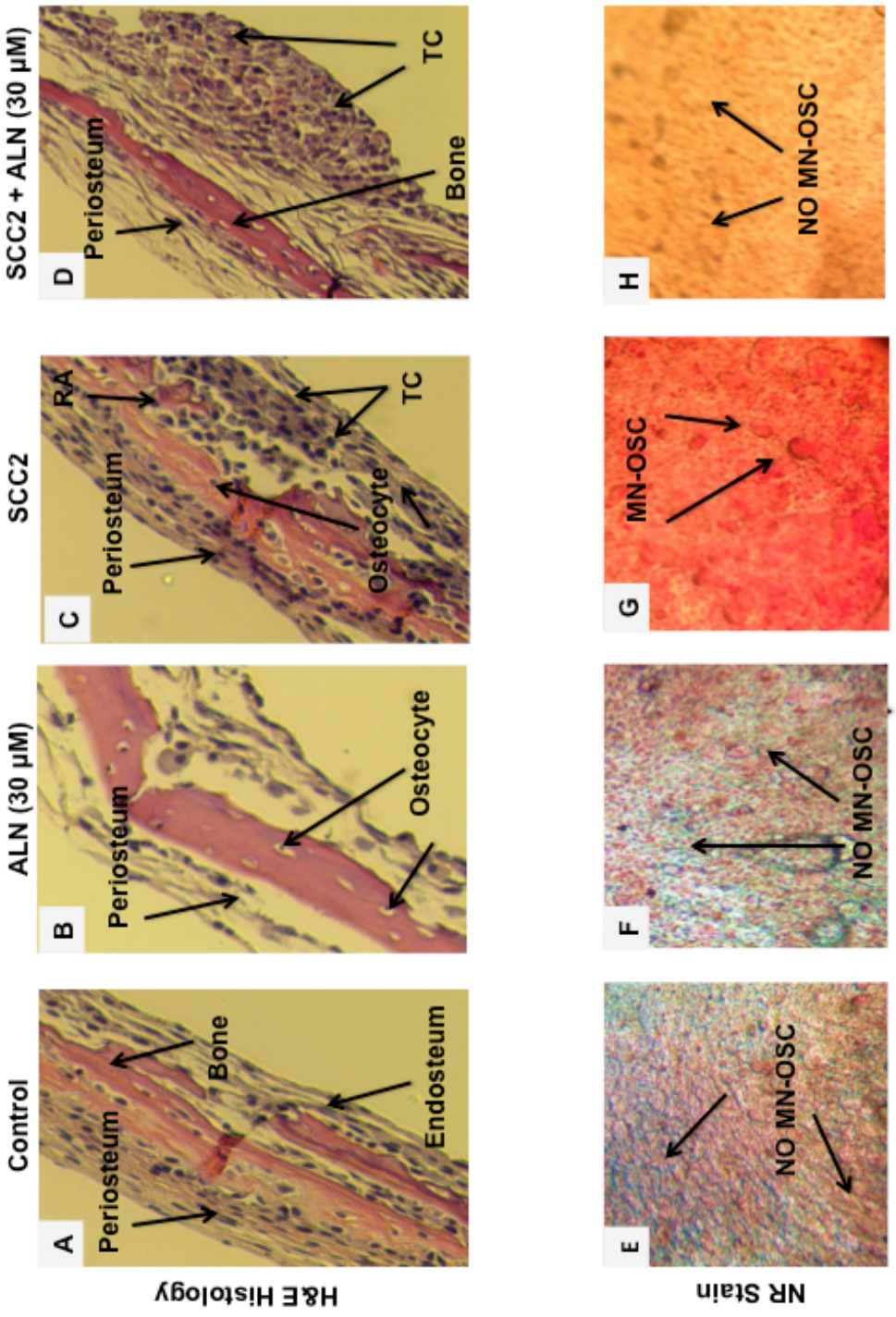

**Figure 26 – Microscopic Observation for Bone Resorption Model: Calvaria Co-culture with SCC2 Cells and Different ALN Concentrations**

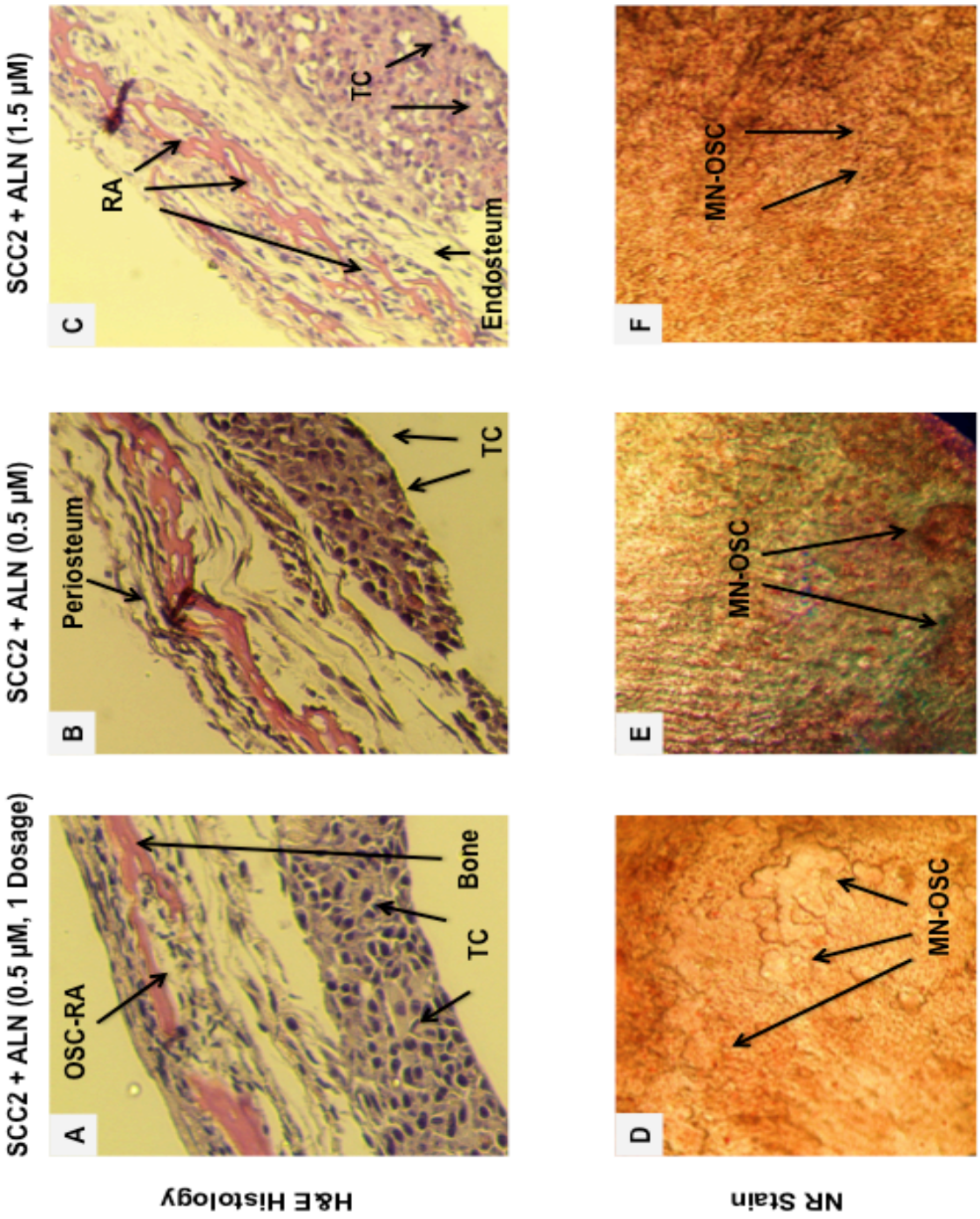

**Figure 27 – Microscopic Observation for Bone Resorption Model: Calvaria of Reduced Viability Co-culture with SCC2 Cells**

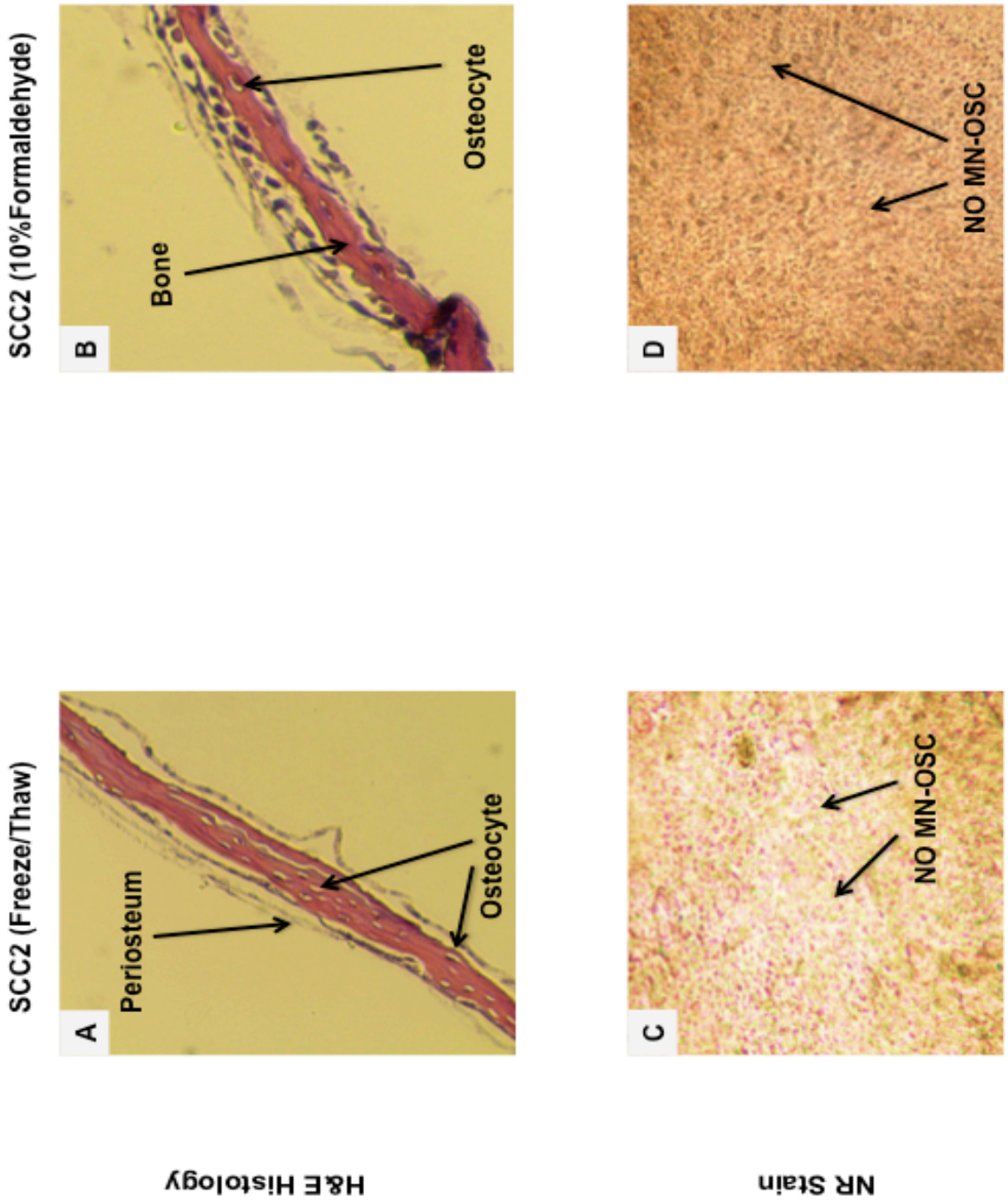

**Figures 25-27: Histology Observation and NR Staining in the Bone Resorption Model: Effect of ALN on OCs Formation and Bone Resorption.** The untreated media control, Figure 25 (A) calvaria showed no osteoclastic resorption, and (E) NR stained calvaria showed no resorption. For calvaria treated with 30 μM ALN, Figure 25 (B) H&E section showed no osteoclastic resorption, (F) NR stained calvaria showed no resorption. For calvaria co-cultured with SCC2 cells, calvaria showed osteoclastic bone resorption (Figure 25 (C)), with numerous multinucleated osteoclasts (MNOC) (Figure 25 (G)). Calvaria co-cultured with SCC2 cells and 30 μM ALN, calvaria showed partial osteoclastic bone resorption with most of the bone intact (Figure 25 (D)), with no MNOC (Figure 25 (H)). Calvaria co-cultured with SCC2 cells and single dosage of 0.5 μM ALN, Figure 26 (A) showed osteoclastic bone resorption with MNOC (Figure 26 (D)). Calvaria co-cultured with SCC2 cells and 0.5 μM ALN, Figure 26 (B) showed osteoclastic bone resorption with MNOC (Figure 26 (E)). Calvaria co-cultured with SCC2 cells and 1.5 μM ALN, Figure 26 (C) showed osteoclastic bone resorption with MNOC (Figure 26 (F)). Calvaria that have been frozen/thawed co-cultured with SCC2 cells, Figure 27 (A) showed no noticeable tumor cell colonization and no osteoclastic bone resorption with no MNOC (Figure 27 (C)). Calvaria treated with 10% formaldehyde co-cultured with SCC2 cells, Figure 27 (B) showed no tumor cells colonization and no bone resorption with no MNOC (Figure 27 (D)). Magnifications: H&E x10, NR x10.

### *7.3. Quantitative Evaluation of the Tumor Colony on Calvarial Bones and Cancer Cell Viability for Bone Resorptive Model*

Quantitative analysis measured for total cell number, cells suspended in media, cells attached to the roller tube and cells on calvarial bone, Figures 28-30. There was a significant increase in total cell number, cells suspended in media and cells on calvarial bones for calvaria co-cultured with SCC2 cells in the presence and absence of ALN (Figure 28 (A)). There was no significant difference for SCC2 cells cultured in FCS media and BSA media. Figure 28 (B) demonstrated that there is no significant difference in cell viability between the control groups and calvaria co-cultured with SCC2 cells and ALN.

A significant decrease in total cell number and cells suspended in media occurred in calvaria co-cultured with 0.5 μM ALN and 1.5 μM ALN (Figure 29 (A)). Figure 29 (B) illustrated no significant difference in cell viability between calvaria co-cultured with SCC2 cells and calvaria co-cultured with SCC2 cells and ALN.

Figure 30 demonstrated the analysis for co-cultures of calvaria that have either been frozen/thawed or treated with 10% formaldehyde prior to start of experiment with SCC2 cells. Figure 30 (A) demonstrated a significant decrease in total cell number and cells in media for both experimental groups, while Figure 30 (B) showed no significant difference in cell viability between calvaria co-cultured with SCC2 cells and the experimental groups.

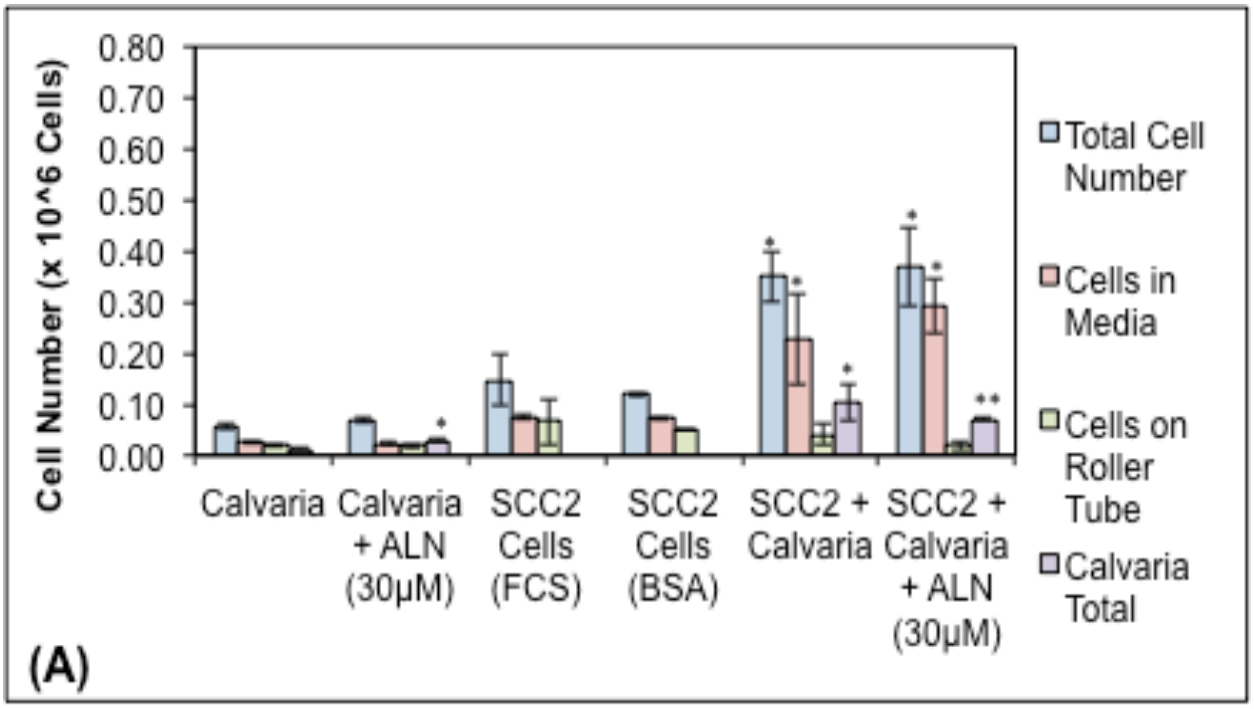
Cell Number (x 10^6 Cells)
0.80
0.70
0.60
0.50
0.40
0.30
0.20
0.10
0.00
Calvaria
Calvaria + ALN (30μM)
SCC2 Cells (FCS)
SCC2 Cells (BSA)
SCC2 + Calvaria
SCC2 + Calvaria + ALN (30μM)
Total Cell Number
Cells in Media
Cells on Roller Tube
Calvaria Total
(A)

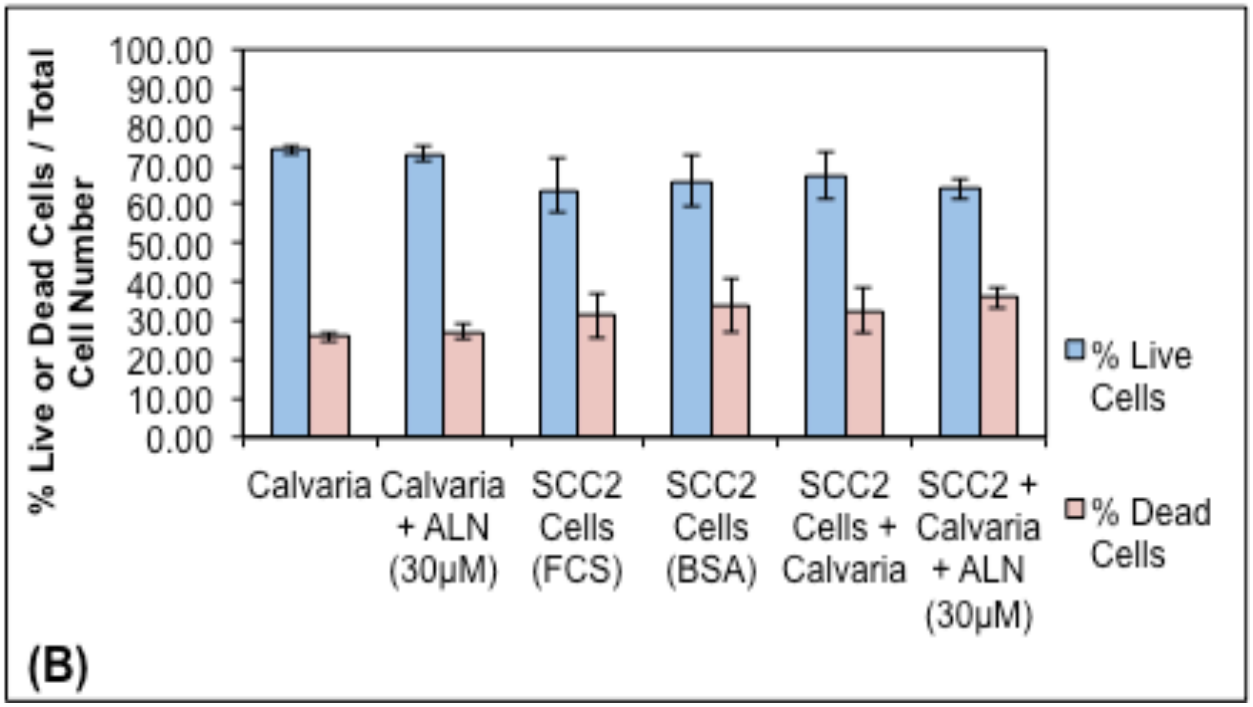
% Live or Dead Cells / Total Cell Number
100.00
90.00
80.00
70.00
60.00
50.00
40.00
30.00
20.00
10.00
0.00
Calvaria
Calvaria + ALN (30μM)
SCC2 Cells (FCS)
SCC2 Cells (BSA)
SCC2 Cells + Calvaria
SCC2 + Calvaria + ALN (30μM)
% Live Cells
% Dead Cells
(B)

**Figure 28 – Quantitative Evaluation of the Tumor Colony and Cancer Cell Viability for Bone Resorption Model: Control Groups, Calvaria Co-culture with SCC2 Cells in the Absence and Presence of ALN.** Quantitative analysis of total cell number, cells in the media, on the roller tube and calvarial bone, and overall cell viability. (A) There was no significant difference between SCC2 cells in FCS media and BSA media. There was a significant increase in the total cell number, cells suspended in media and number of cells on calvarial bone for calvaria co-cultured with SCC2 cells in the absence and presence of ALN. Results are expressed as a mean ± S.D. (*, $P<0.05$, **, $P<0.001$, Two-tailed t test with equal variance, compared with Calvaria); (B) There was no significant difference in cell viability between SCC2 cells in FCS media and BSA media, and in the presence and absence of ALN.

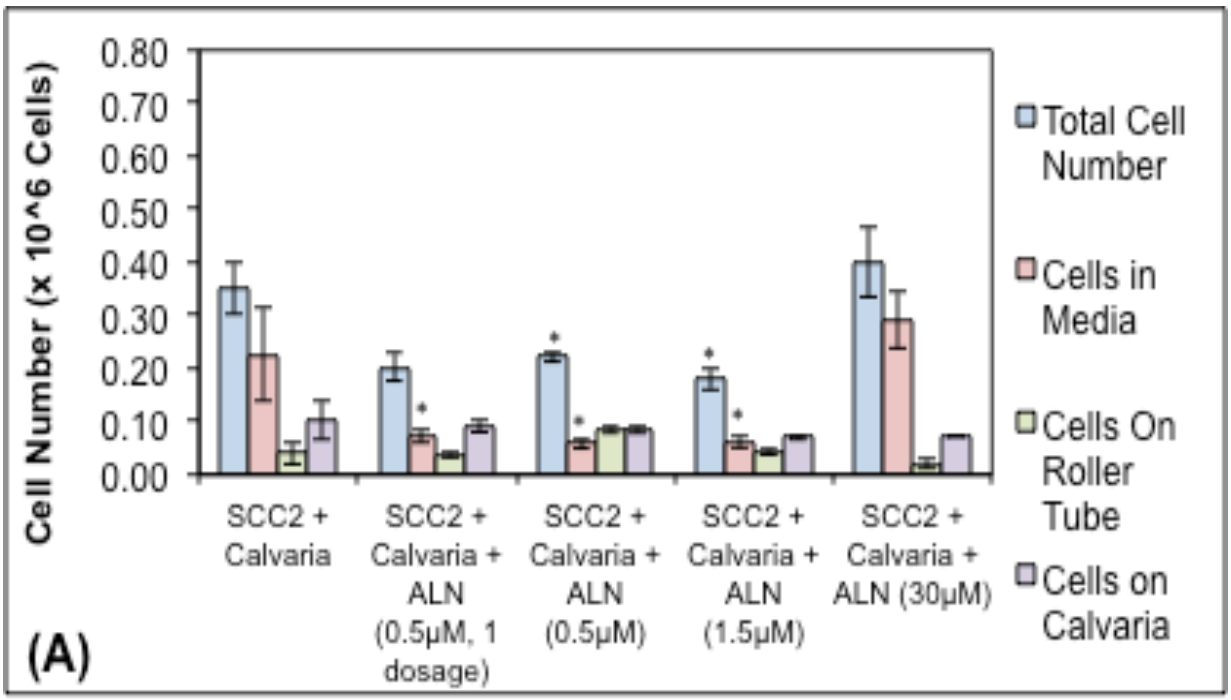
Cell Number (x 10^6 Cells)
0.80
0.70
0.60
0.50
0.40
0.30
0.20
0.10
0.00
SCC2 + Calvaria
SCC2 + Calvaria + ALN (0.5μM, 1 dosage)
SCC2 + Calvaria + ALN (0.5μM)
SCC2 + Calvaria + ALN (1.5μM)
SCC2 + Calvaria + ALN (30μM)
Total Cell Number
Cells in Media
Cells On Roller Tube
Cells on Calvaria
(A)

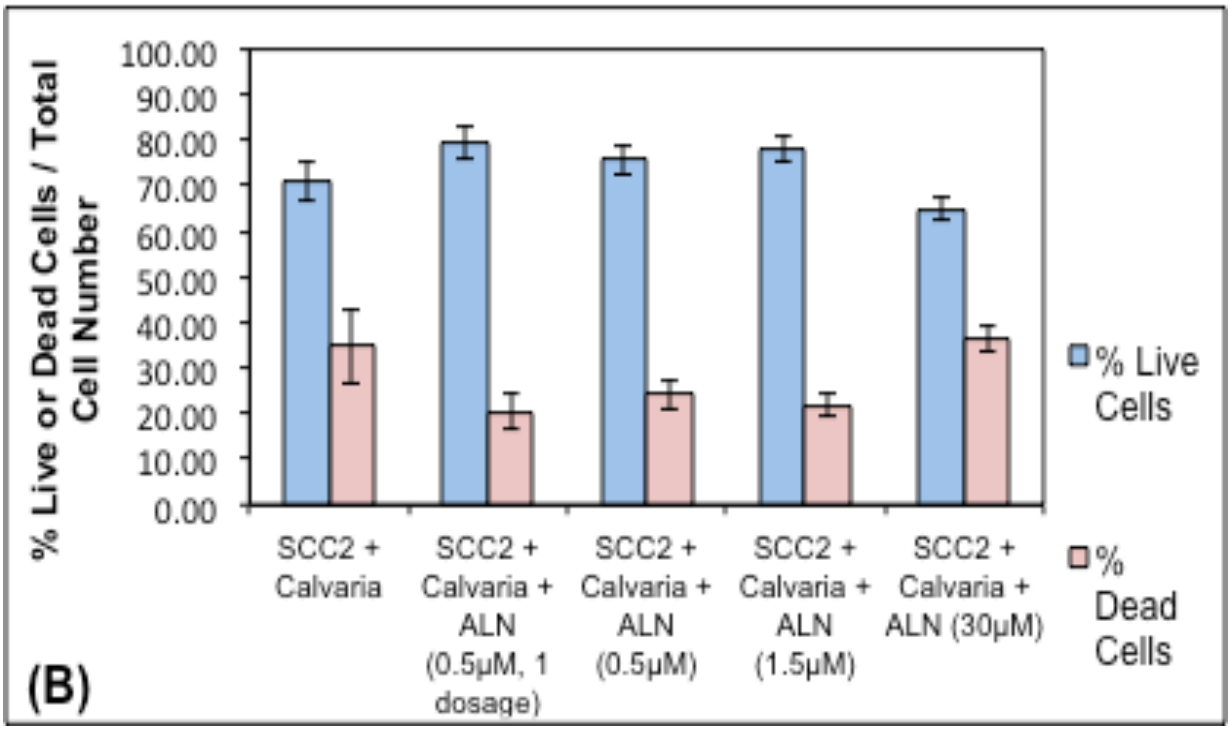
% Live or Dead Cells / Total Cell Number
100.00
90.00
80.00
70.00
60.00
50.00
40.00
30.00
20.00
10.00
0.00
SCC2 + Calvaria
SCC2 + Calvaria + ALN (0.5μM, 1 dosage)
SCC2 + Calvaria + ALN (0.5μM)
SCC2 + Calvaria + ALN (1.5μM)
SCC2 + Calvaria + ALN (30μM)
% Live Cells
% Dead Cells
(B)

**Figure 29 – Quantitative Evaluation of the Tumor Colony and Cancer Cell Viability for Bone Resorption Model: Calvaria Co-cultures with SCC2 Cells and Different ALN Concentrations.** Quantitative analysis of total cell number, cells in the media, on the roller tube and calvarial bone, and overall cell viability. (A) There was a significant decrease in the amount of cells suspended in media for calvaria co-cultured with 0.5 μM ALN and 1.5 μM ALN. Results are expressed as a mean ± S.D. (*, $P<0.05$, **, $P<0.001$, Two-tailed t test with equal variance, compared with calvarial co-cultured with SCC2 cells). (B) There was no significant difference in cell viability between calvaria co-cultured with SCC2 cells and calvaria co-cultured with SCC2 cells and ALN.

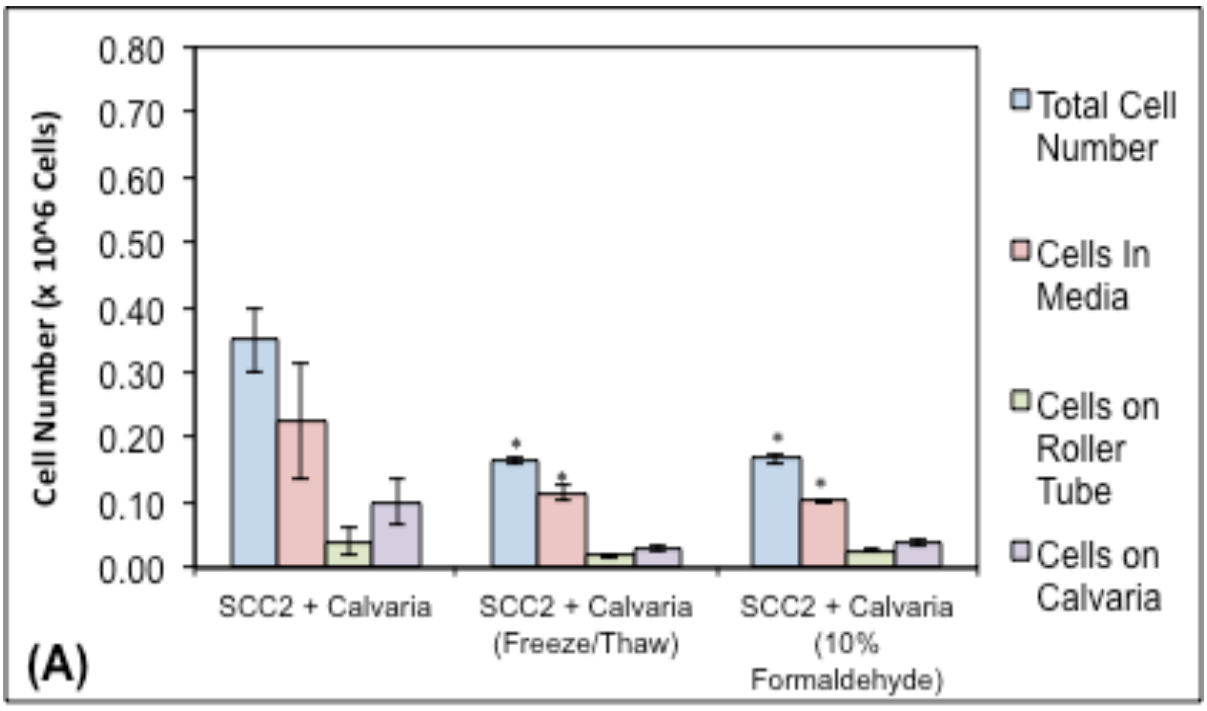
Cell Number (x 10^6 Cells)
0.80
0.70
0.60
0.50
0.40
0.30
0.20
0.10
0.00
SCC2 + Calvaria
SCC2 + Calvaria (Freeze/Thaw)
SCC2 + Calvaria (10% Formaldehyde)
Total Cell Number
Cells In Media
Cells on Roller Tube
Cells on Calvaria
(A)

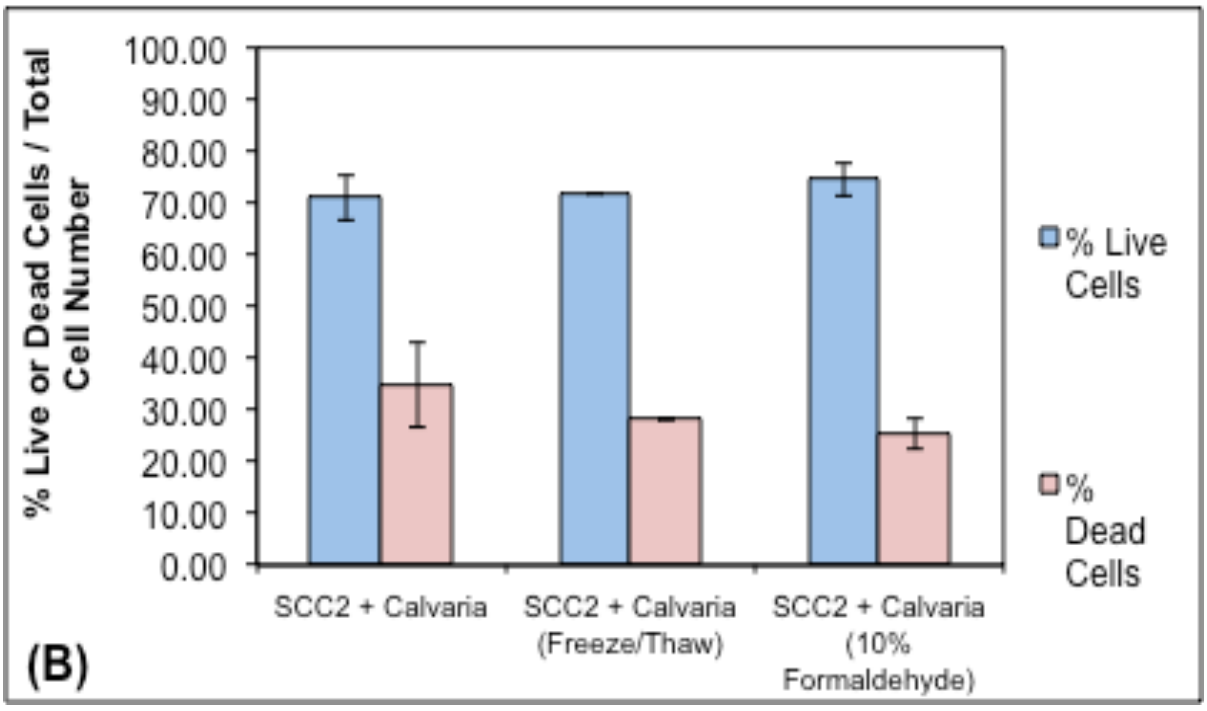
% Live or Dead Cells / Total Cell Number
100.00
90.00
80.00
70.00
60.00
50.00
40.00
30.00
20.00
10.00
0.00
SCC2 + Calvaria
SCC2 + Calvaria (Freeze/Thaw)
SCC2 + Calvaria (10% Formaldehyde)
% Live Cells
% Dead Cells
(B)

**Figure 30 – Quantitative Evaluation of the Tumor Colony and Cancer Cell Viability for Bone Resorption Model: Calvaria of Reduced Viability Co-cultured with SCC2 Cells.** Quantitative analysis of total cell number, cells in the media, on the roller tube and calvarial bone, and overall cell viability. (A) There was a significant decrease in the total cell number and amount of cells suspended in media for calvaria that have been frozen/thawed or treated with 10% formaldehyde. Results are expressed as a mean ± S.D. (*, $P<0.05$, **, $P<0.001$, Two-tailed t test with equal variance, compared with calvarial co-cultured with SCC2 cells). (B) There was no significant difference in cells viability between calvaria co-culture with SCC2 cells and the experimental groups.

## *7.4. Quantitative Analysis of Changes in Media Calcium Concentration and TRAP Activity: Effect of ALN and Calvarial Cells Viability on OCs Formation and Bone Resorption in Bone Resorptive Model.*

### *7.4.1 Calcium Release vs. Time*

Calcium release of each media collected over the 8-day culture period is demonstrated in Figure 31. The data represent net calcium release after correction with calcium concentration of media and reagent. Figure 31 (A) shows calcium concentration plotted as function of time for: calvaria control, calvaria + 30 μM ALN, calvaria co-cultured with SCC2 cells in the absence and presence of 30 μM ALN. Calvaria co-cultured with SCC2 cells showed substantial release of calcium with maximum release on day 4. Calvaria co-cultured with SCC2 cells and 30 μM ALN showed a decreased calcium release. Figure 31 (B) showed calcium concentration plotted as function of time for: calvaria control, calvaria co-cultured with SCC2 cells and different concentrations of ALN. Calvaria treated with single dosage of 0.5 μM ALN, 0.5 μM ALN, 1.5 μM ALN all demonstrated higher level of calcium release, compared to the calvaria control on day 4, with calvaria c-cultured with SCC2 cells + 1.5 μM ALN showing the highest level of calcium release. All 3 groups showed decreased calcium release on day 6 and day 8, and all 3 groups have similar calcium release level on day 8. Figure 31 (C), calvaria control, calvaria co-cultured with SCC2 cells, SCC2 Cells + calvaria (Freeze/Thaw, and SCC2 cells + calvaria treated with 10% formaldehyde. Both experimental groups showed lower calcium release than calvaria co-cultured with SCC2 cells, but calvaria (Freeze/Thaw) showed higher level of calcium release

than calvaria control on day 4. Both groups experienced peak of calcium release on day 6, with subsequent decrease on day 8.

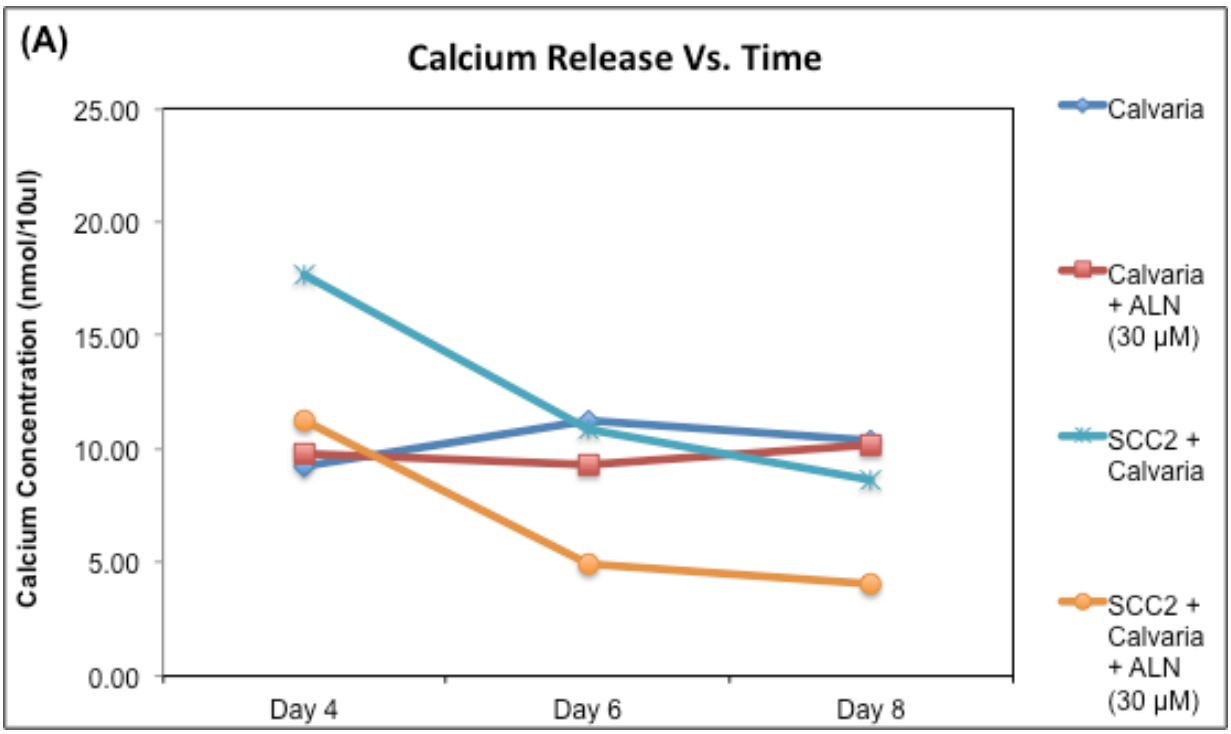
(A)
Calcium Release Vs. Time
Calcium Concentration (nmol/10ul)
25.00
20.00
15.00
10.00
5.00
0.00
Day 4
Day 6
Day 8
Calvaria
Calvaria + ALN (30 µM)
SCC2 + Calvaria
SCC2 + Calvaria + ALN (30 µM)

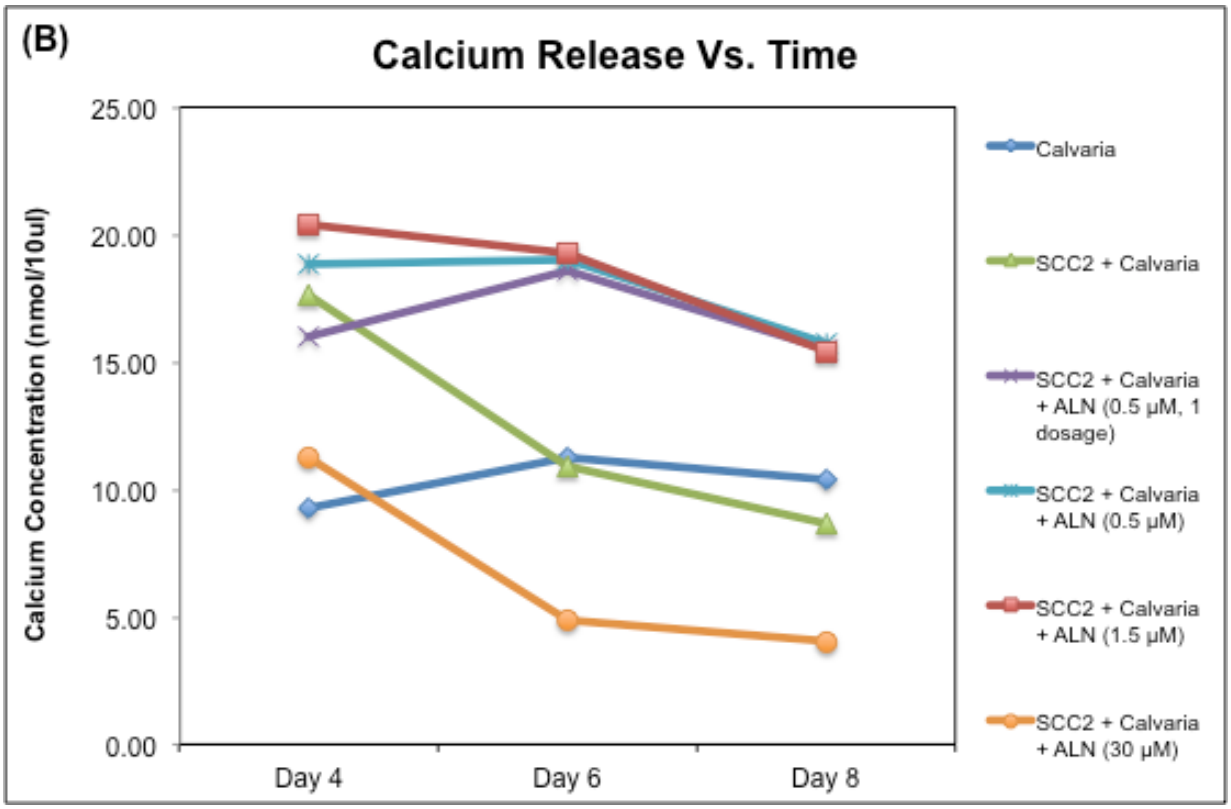
(B)
Calcium Release Vs. Time
Calcium Concentration (nmol/10ul)
25.00
20.00
15.00
10.00
5.00
0.00
Day 4
Day 6
Day 8
Calvaria
SCC2 + Calvaria
SCC2 + Calvaria + ALN (0.5 µM, 1 dosage)
SCC2 + Calvaria + ALN (0.5 µM)
SCC2 + Calvaria + ALN (1.5 µM)
SCC2 + Calvaria + ALN (30 µM)

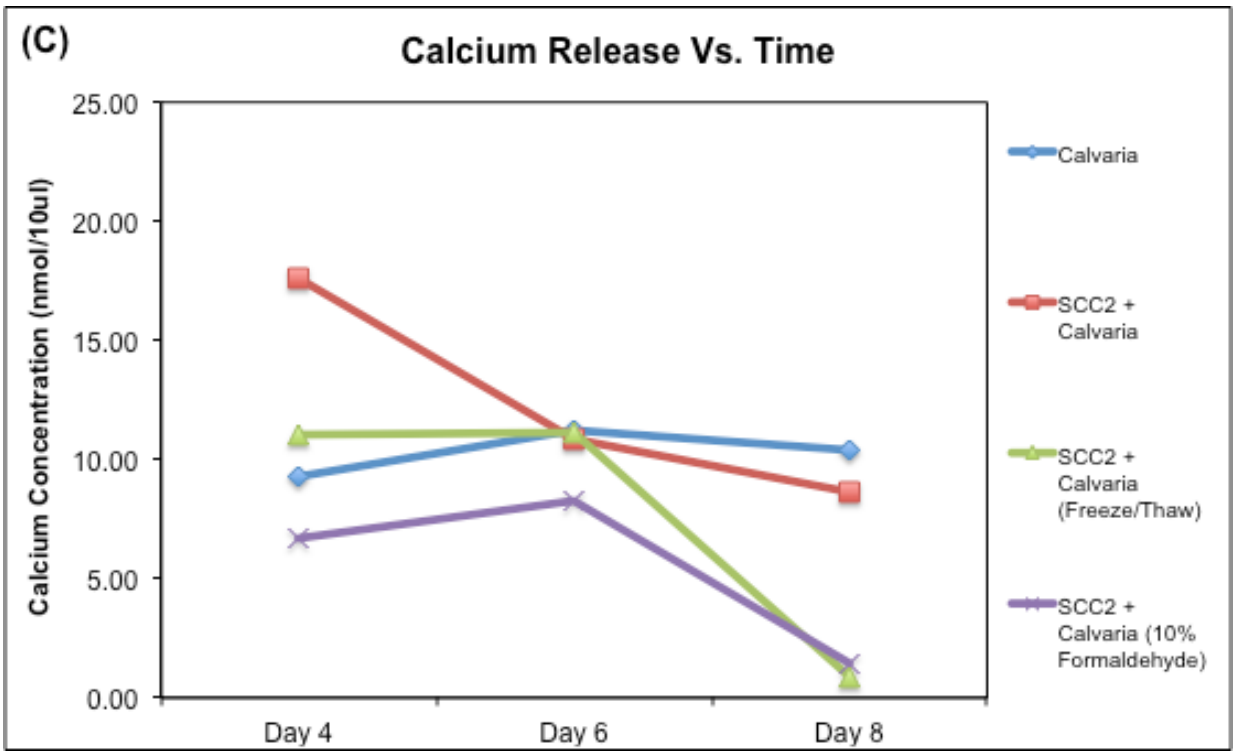
(C)
Calcium Release Vs. Time
Calcium Concentration (nmol/10ul)
25.00
20.00
15.00
10.00
5.00
0.00
Day 4
Day 6
Day 8
Calvaria
SCC2 + Calvaria
SCC2 + Calvaria (Freeze/Thaw)
SCC2 + Calvaria (10% Formaldehyde)

**Figure 31 – Bone Resorption Model: Calcium Release Vs. Time.** Calcium release from calvaria control, calvaria co-cultured with SCC2 cells in the presence and absence of 30 μM ALN (Figure 31 (A)). Calvaria co-cultured with SCC2 cells showed substantial release of calcium with maximum release on day 4 of experiment. Calvaria co-cultured with SCC2 cells and 30 μM ALN showed a decrease in calcium release. In addition, the peak release of calcium was no longer observed which reflects the inhibitory effect of ALN on osteoclasts. Calvaria treated with single dosage of 0.5 μM ALN, 0.5 μM ALN, 1.5 μM ALN all demonstrated higher level of calcium release compared to the calvaria control on day 4, with calvaria co-cultured with SCC2 cells + 1.5 μM ALN showing the highest release of calcium (Figure 31 (B)). All 3 groups showed decrease in calcium release on day 6 and day 8, and all 3 groups had similar calcium release level on day 8. Figure 31 (C), SCC2 cells + calvaria (Freeze/Thaw) and SCC2 cells + calvaria treated with 10% formaldehyde showed lower level of calcium release than calvaria co-cultured with SCC2 cells, but calvaria (Freeze/Thaw) showed higher level of calcium release than calvaria control on day 4. Both groups' calcium release peaked on day 6, with subsequent decrease on day 8.

### *7.4.2 Cumulative Calcium Release and TRAP Activity*

Total cumulative calcium release for each experimental group over the eight days culture period and TRAP activity are represented in Figures 32-34. Figure 32 (A) showed quantitative calcium analysis of media collected from calvaria control groups, calvaria co-cultured with SCC2 cells in the presence and absence of 30 μM ALN. Comparison between calvarial control and calvaria co-cultured with SCC2 cells showed significant increase in cumulative calcium release, reflecting extensive bone resorption. Comparison between calvaria co-culture and the inclusion of 30 μM ALN showed significant decrease in cumulative calcium release, reflecting reduction in bone resorption. The data for cumulative calcium release are correlated with Figure 32 (B) showing significant increase in TRAP activity when comparing calvaria control and calvaria-cultured with SCC2 cells. A significant decrease in TRAP activity occurred between calvaria co-cultured with SCC2 cells and calvaria-SCC2 cells co-cultured with 30 μM ALN, and between calvaria co-cultured in the absence and presence of 30 μM ALN. This reflected a substantial decrease in osteoclastic bone resorption with the presence of ALN. There was a significant increase in cumulative calcium release in calvaria co-cultured with single dosage of 0.5 μM ALN, 0.5 μM ALN and 1.5 μM ALN (Figure 33 (A)). The data are correlated with TRAP activity in Figure 33 (B), which showed a significant increase in TRAP activity for those 3 experimental groups. Figure 34 (A) demonstrated no significant difference in calcium release between calvaria control and SCC2 cells + calvaria (Freeze/Thaw) and SCC2 cells + calvaria treated with 10% formaldehyde.

However, there is a significant difference in calcium release between these 2 groups and calvaria co-cultured with SCC2 cells. Calvaria treated with 10% formaldehyde also showed significantly lower calcium release than calvaria (freeze/thaw). Figure 34 (B) illustrated significantly lower TRAP activity for SCC2 cells + calvaria (freeze/thaw) and SCC2 cells + calvaria with 10% formaldehyde when compared to that of calvaria control and calvaria-SCC2 cells co-culture.

**Figure 32 – Cumulative Calcium Release and TRAP Activity for Bone Resorption Model: Control Groups, Calvaria Co-culture with SCC2 Cells in the Absence and Presence of ALN**

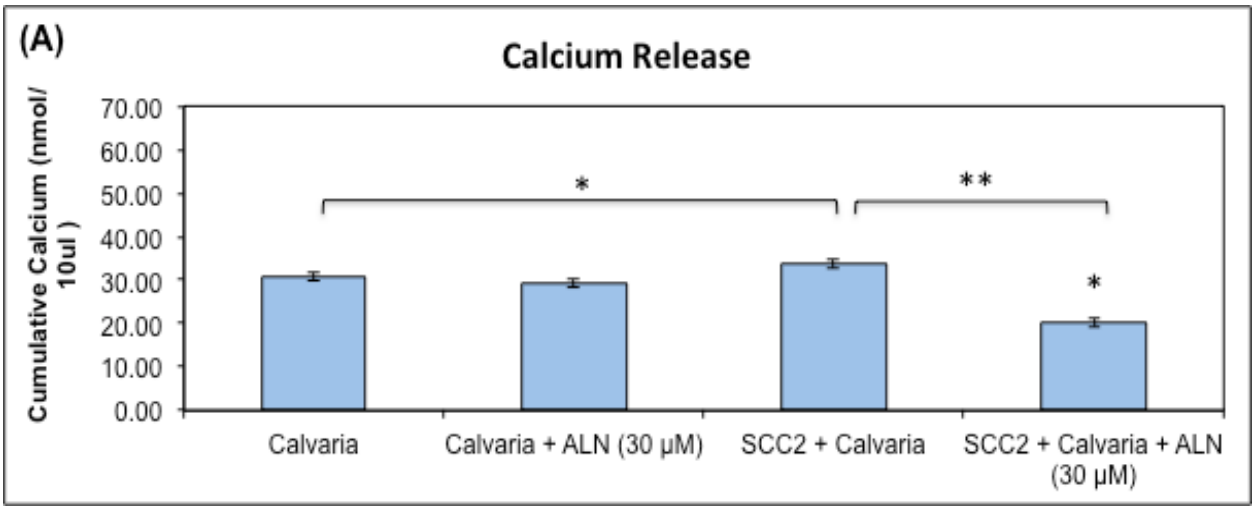


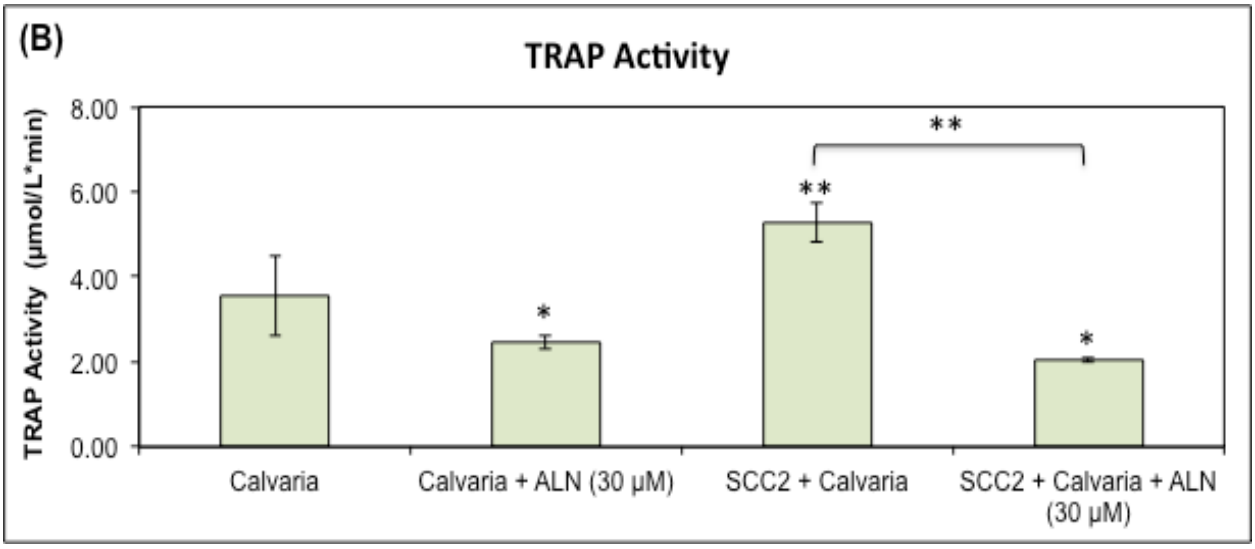

**Figure 33 – Cumulative Calcium Release and TRAP Activity for Bone Resorption Model: Calvaria Co-culture with SCC2 Cells and Different ALN Concentrations**

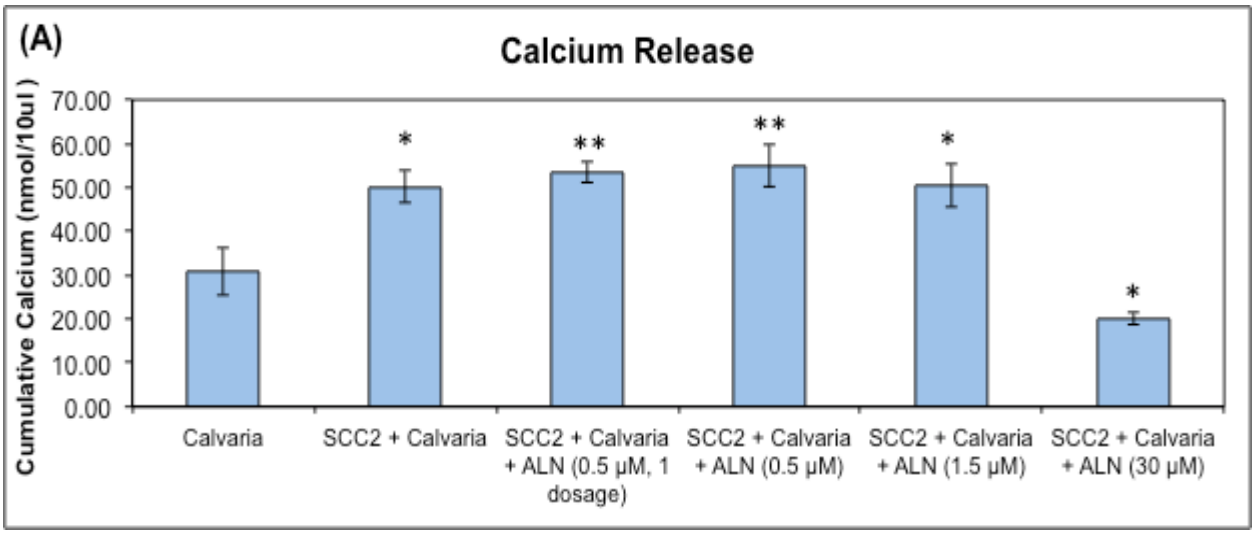


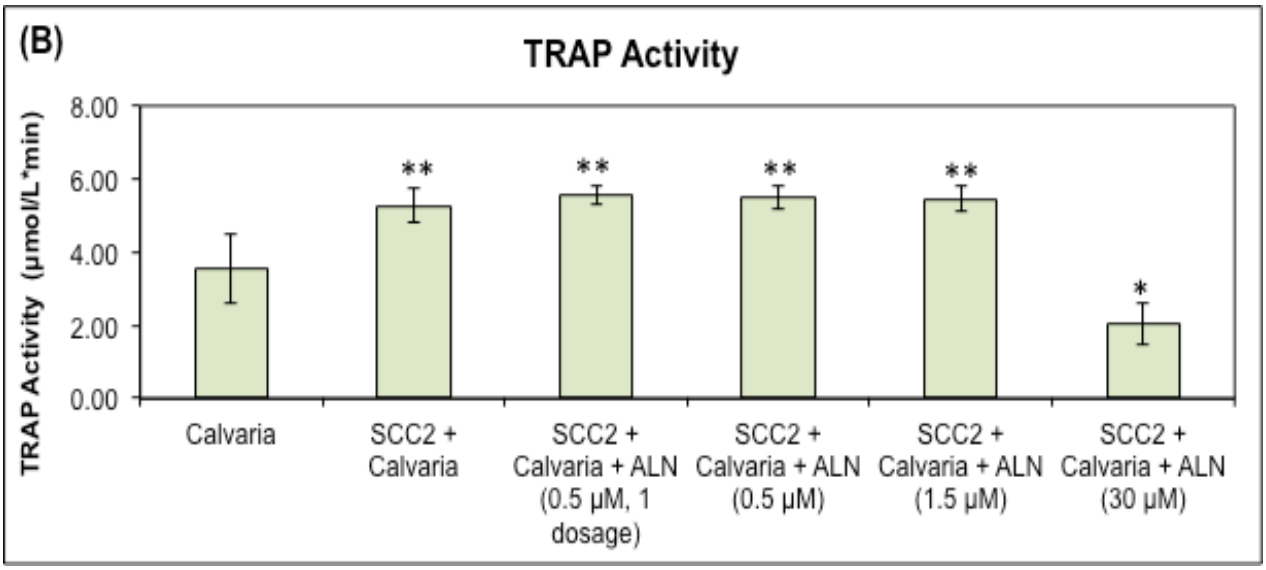

**Figure 34 – Cumulative Calcium Release and TRAP Activity for Bone Resorption Model: Calvaria of Reduced Viability Co-culture with SCC2 Cells**

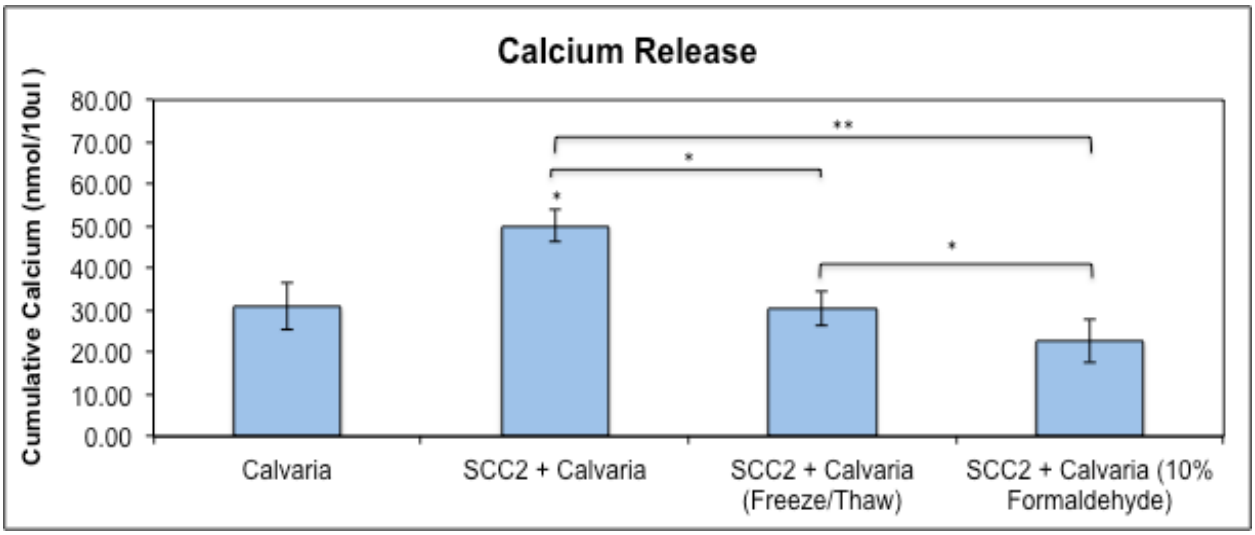


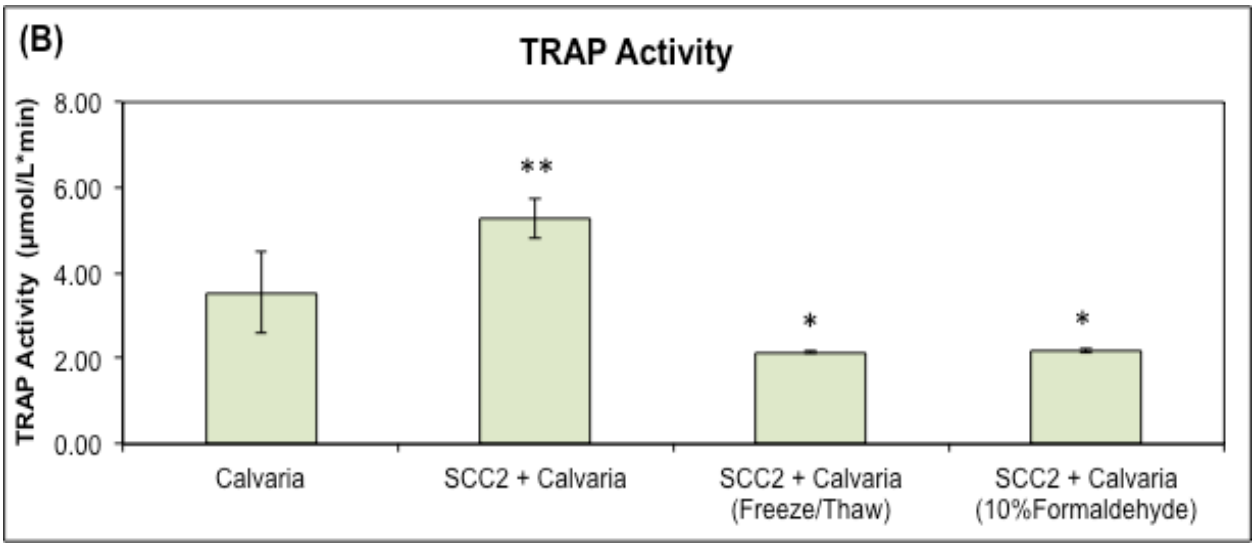

**Figures 32-34 – Quantitative Analysis of Cumulative Calcium Release and TRAP Activity for Bone Resorption Model.** Figure 32 (A), quantitative calcium analysis of media collected from calvaria control, calvaria + 30 μM ALN, calvaria co-cultured with SCC2 cells in the absence and presence of 30 μM ALN. Comparison between calvarial control and calvaria co-cultured with SCC2 cells showed significant increase in cumulative calcium release, reflecting extensive bone resorption. Comparison between calvaria-SCC2 cells co-culture and the calvaria co-culture with SCC2 cells + 30 μM ALN showed significant decrease in cumulative calcium release, reflecting reduction in bone resorption. Results are expressed as a mean ± S.D. (*, $P<0.05$, **, $P<0.001$, Two-tailed t test with equal variance compared with calvaria control). Figure 32 (B), quantitative TRAP activity of media collected from calvaria control groups, calvaria + 30 μM ALN, calvaria co-cultured with SCC2 cells in the absence and presence of 30 μM ALN. There is significant increase in TRAP activity when comparing data of calvaria control and that of calvaria-cultured with SCC2 cells. A significant decrease in TRAP activity occurred between calvaria co-cultured with SCC2 cells and calvaria-SCC2 cells co-culture with 30 μM ALN, and between calvaria in the absence and presence of 30 μM ALN. Results are expressed as a mean ± S.D. (*, $P<0.05$, **, $P<0.001$, Two-tailed t test with equal variance compared with calvaria control). This reflected substantial decrease in osteoclastic bone resorption with the presence of ALN. Figure 33 (A), cumulative calcium release for calvaria control, calvaria co-cultured with SCC2 cells and different ALN concentrations (single dosage of 0.5 μM ALN, 0.5 μM ALN, 1.5 μM ALN and 30

μM ALN). It illustrated significant increase in cumulative calcium release in calvaria co-cultured with single dosage of 0.5 μM ALN, 0.5 μM ALN and 1.5 μM ALN. Figure 33 (B), TRAP activity for calvaria control, calvaria co-cultured with SCC2 cells and different ALN concentrations (single dosage of 0.5 μM ALN, 0.5 μM ALN and 1.5 μM ALN), showing significant increase in TRAP activity for those 3 experimental groups. Results are expressed as a mean ± S.D. (*, $P<0.05$, **, $P<0.001$, Two-tailed t test with equal variance compared with calvarial control). Figure 34 (A) demonstrated no significant reduction in calcium release between calvaria control and SCC2 cells + calvaria (freeze/thaw) and SCC2 cells + calvaria treated with 10% formaldehyde. However, there is significant reduction in calcium release between calvaria co-cultured with SCC2 cells and SCC2 cells + calvaria (freeze/thaw) and SCC2 cells + calvaria treated with 10% formaldehyde. Calvaria treated with 10% formaldehyde co-culture with SCC2 cells also showed significantly lower calcium release than calvaria (freeze/thaw) co-culture with SCC2 cells. Results are expressed as a mean ± S.D. (*, $P<0.05$, **, $P<0.001$, Two-tailed t test with equal variance compared with calvaria control). Figure 34 (B) illustrated significantly lower TRAP activity for SCC2 cells + calvaria (freeze/thaw) and SCC2 cells + calvaria treated with 10% formaldehyde when compared to that of calvaria control. Results are expressed as a mean ± S.D. (*, $P<0.05$, **, $P<0.001$, Two-tailed t test with equal variance compared with calvaria control).

### *7.5. Histologic Observations: Effect of ALN and Calvarial Cells Viability on OBs Formation and Bone Formation in ASC-Stimulated Bone Formation Model.*

The histologic observations of H&E stained section of calvarial bones in the bone formation model are represented in Figures 35-37. Figure 35 (A) showed H&E section of calvaria ASC control with new osteoid formation while Figure 35 (B) showed H&E section of calvaria + ASC + 30 μM ALN with no sign of osteoblast differentiation or osteoid formation. Figure 35 (C) illustrated calvaria co-cultured with SCC2 cells + ASC, showing OB differentiation and new osteoid formation instead of bone resorption. H&E section of calvaria co-cultured with SCC2 cells + ASC + 30 μM ALN is displayed on Figure 35 (D), showing no sign of bone formation or resorption. The NR staining of all the above experimental groups, as displayed in Figure 35 (E)-(H) respectively, demonstrated absence of MNOC which confirmed with the histologic observations.

Figure 36 (A)–(C) showed H&E sections of calvaria cultured with SCC2 cells + ASC + different concentration of ALN. New osteoid formation is noted in calvaria treated with 0.5 μM ALN and 1.5 μM ALN, which is illustrated in Figure 36 (B) and (C). No presence of MNOC is noted in the NR staining of all three experimental groups, as shown in Figure 36 (D) – (F).

The H&E sections of calvaria that have been frozen/thawed co-cultured with ASC and SCC2 cells, and calvaria that were treated with 10% formaldehyde co-cultured with ASC and SCC2 cells are displayed in Figure 37 (A) and (B), respectively. No new osteoid formation is noted for both groups. Calvaria that

were frozen/thawed showed reduced number of periosteal and endosteal cells, and no nuclei were noted for the existing osteocytes. Calvaria that were treated with 10% formaldehyde showed fixed periosteal cells, endosteal cells and osteocytes. Figure 37 (C) and (D) demonstrated NR staining for both experimental groups respectively with absence of MNOC for both groups.

**Figure 35 – Microscopic Observation for ASC-Stimulated Bone Formation Model: Control, Calvaria Co-culture with SCC2 Cells in the Absence and Presence of ALN.**

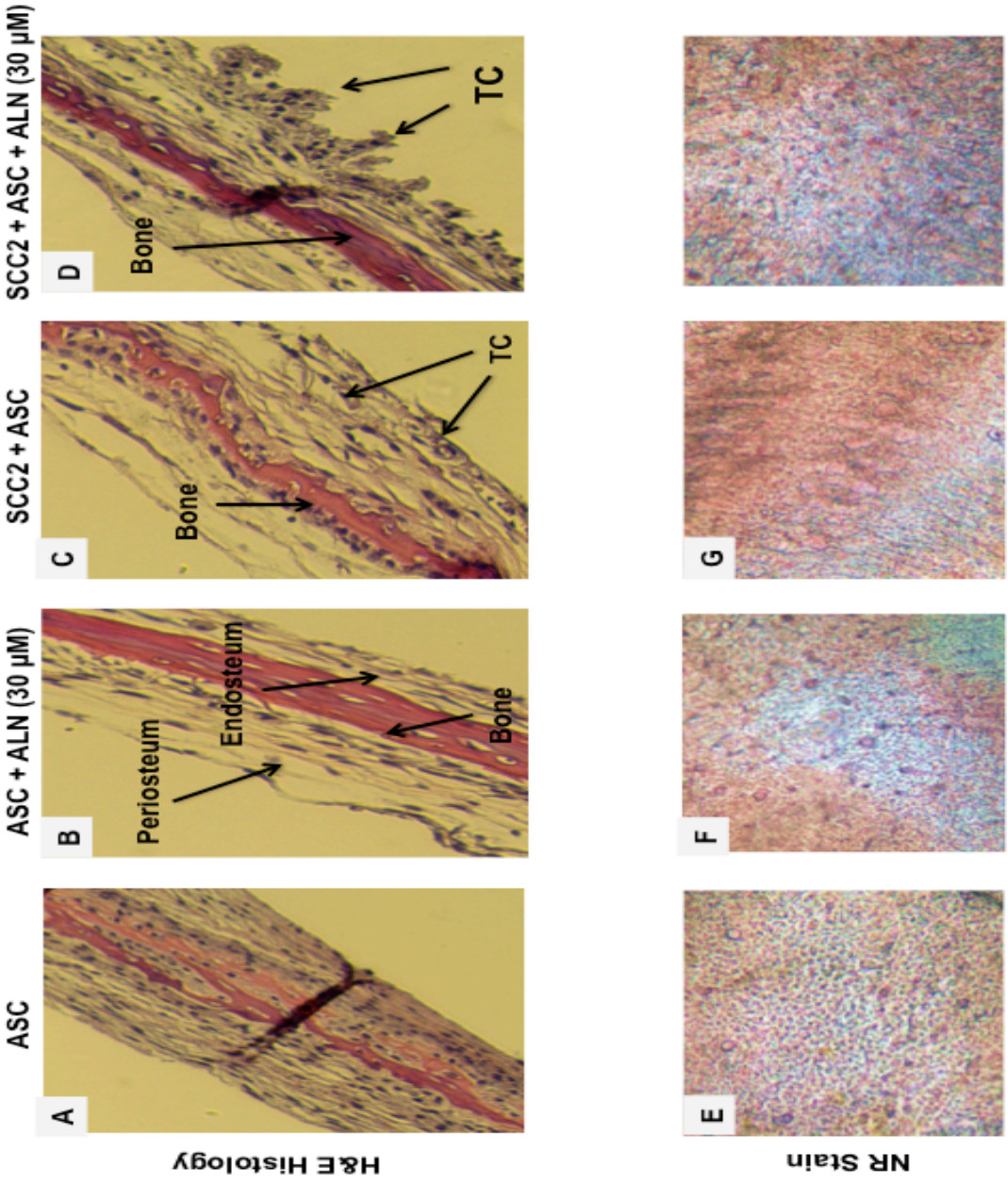

**Figure 36 – Microscopic Observation for ASC-Stimulated Bone Formation Model: Calvaria Co-culture with SCC2 Cells and Different ALN Concentrations**

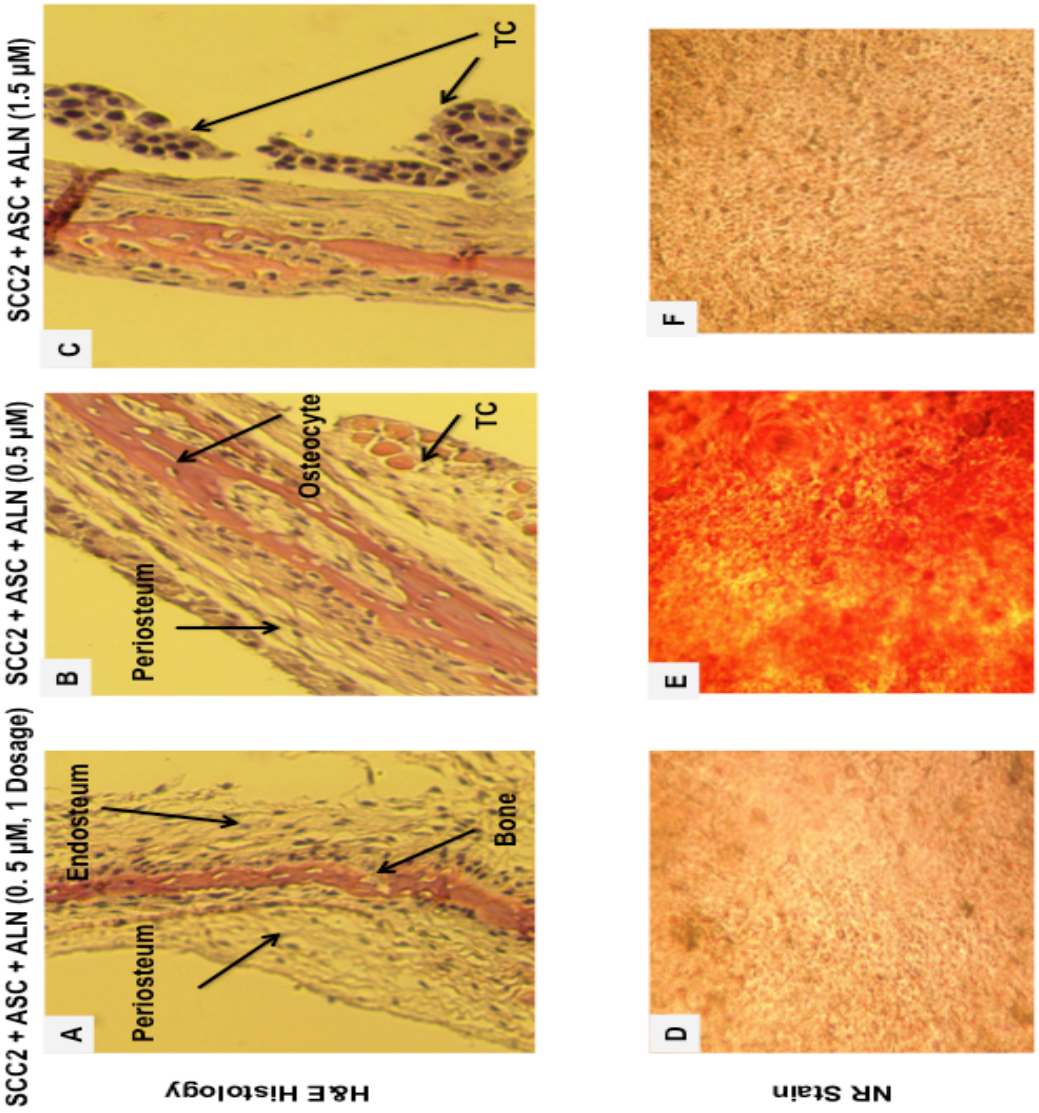

**Figure 37 –Microscopic Observation for ASC-Stimulated Bone Formation Model: Calvaria od Reduced Viability Co-culture with SCC2 Cells**

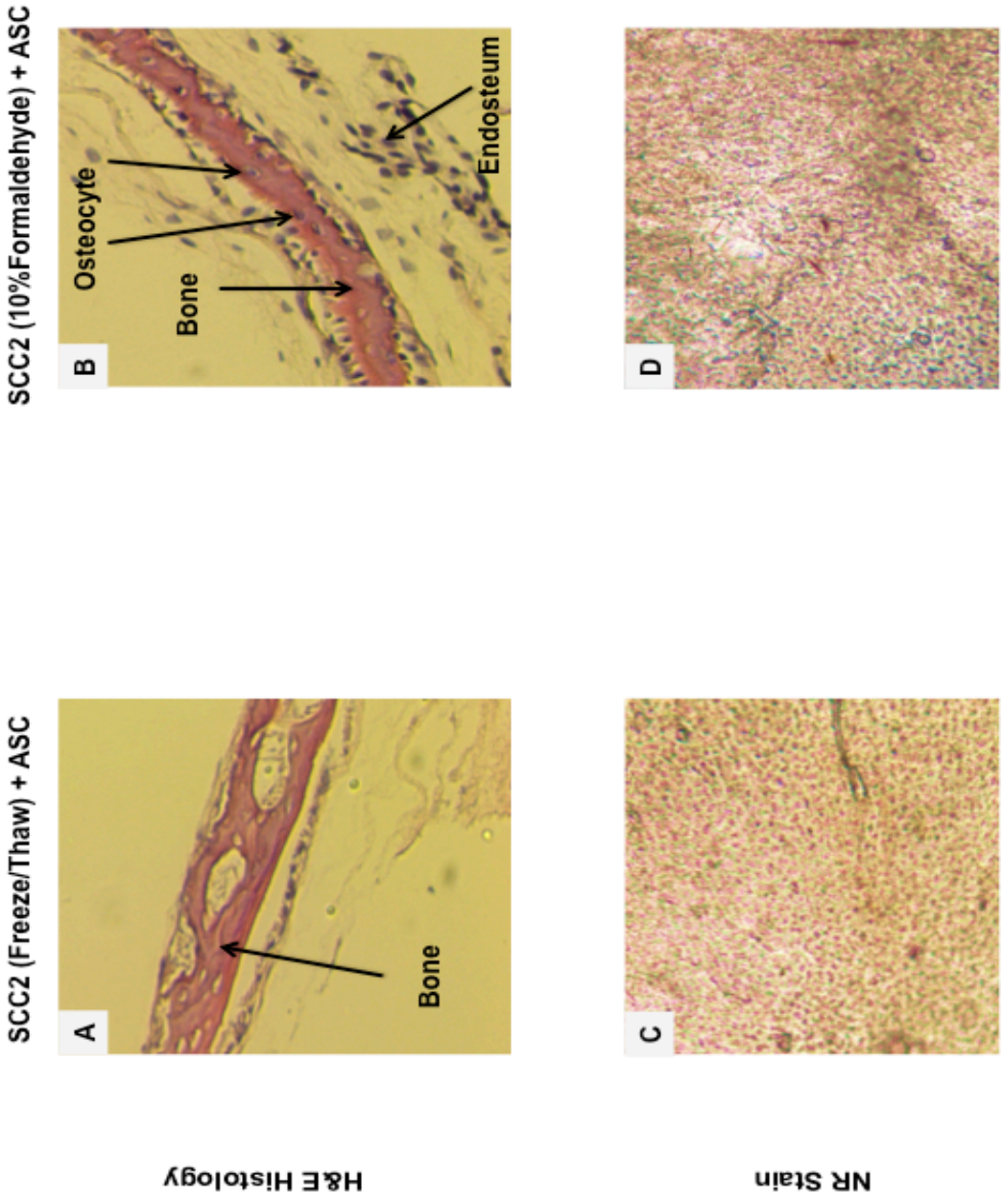

**Figures 35-37 – Histologic Observation, NR Staining in the ASC Stimulated Bone Formation Model.** ASC-stimulated control with new osteoid formation (Figure 35 (A)), while calvaria with ASC + 30 μM ALN showined no sign of bone formation or bone resorption (Figure 35 (B)). Calvaria co-cultured with SCC2 cells + ASC showed cancer cells colonization on the endosteal side of bone and new osteoid formation (Figure 35 (C)). Calvaria co-cultured with SCC2 + ASC + 30 μM ALN, showed tumor cells colonization and no sign of bone formation or bone resorption (Figure 35 (D)). NR stained calvaria of ASC control, calvaria with ASC + 30 μM ALN, calvaria co-cultured with SCC2 cells + ASC, and calvaria co-cultured with SCC2 cells + ASC + 30 μM ALN all showed absence of MNOC (Figure 35 (E)-(H)), confirming the observation made for the histologic sections. Calvaria co-cultured with SCC2 cells + ASC + one dosage 0.5 μM ALN showed no sign of bone resorption or formation (Figure 36 (A)). Calvaria co-cultured with SCC2 cells + ASC + 0.5 μM ALN showed tumor cells colonization on endosteal surface and no new osteoid formation (Figure 36 (B)). Calvaria co-cultured with SCC2 cells + ASC + 1.5 μM ALN showing tumor cells colonization on endosteal surface and no new osteoid formation (Figure 36 (C)). NR stained calvaria of calvaria co-culture with SCC2 cells + one dosage 0.5 μM ALN, calvaria co-cultured with SCC2 cells + ASC + 0.5 μM ALN, and calvaria co-cultured with SCC2 cells + ASC + 1.5 μM ALN all showed absence of MNOC (Figure 36 (D)-(F)), confirming observations made with histologic sections. Calvaria that have been frozen/thawed prior to start of experiment co-cultured with SCC2 cells showed no new osteoid formation (Figure 37 (A)). Calvaria treated with 10%

formaldehyde co-cultured with SCC2 cells showed no tumor cell colonization and no sign of bone formation (Figure 37 (B)). NR stained calvaria of the experimental groups mentioned above, respectively, illustrating absence of MNOC (Figure 37 (C) and (D)). Magnifications: H&E x10, NR x20.

### *7.6. Quantitative Evaluation of the Tumor Colony on Calvarial Bones and Cancer Cell Viability for ASC-Stimulated Bone Formation Model*

Quantitative analysis of total cell number, number of cells suspended in media, number of cells attached to roller tube, and number of colonized cells on calvaria along with quantitative analysis of cancer cell viability for the bone formation model are displayed in Figures 38-40. SCC2 cells in BSA media + ASC had significantly lower number of cells attached to roller tube ($p<0.05$) (Figure 38 (A)). When compared with calvaria ASC control, calvaria co-cultured with SCC2 cells + ASC + 30 μM ALN showed significant increase in total cell number ($p<0.001$), number of cells suspended in media ($p<0.05$), and cells colonized on calvaria ($p<0.001$) (Figure 38 (A)). No significant difference in cell viability was noted between calvaria control and the different experimental groups (Figure 38 (B)).

Figure 39 (A) illustrated no significant difference in the quantitative analysis of total cell number, number of cells suspended in media, number of cells attached to roller tube, and number of colonized cells on calvaria between calvaria control and the different experimental groups. Quantitative analysis of cell viability showed calvaria co-cultured with SCC2 cells + ASC + single dosage of 0.5 μM ALN and calvaria co-cultured with SCC2 cells + ASC + 1.5 μM ALN demonstrated higher percentage of live cells and lower percentage of dead cells ($p<0.05$ for single dosage of 0.5 μM ALN; $p<0.001$ for 1.5 μM ALN), as shown in Figure 39 (B).

Figure 40 (A) illustrated that when quantitative analysis for tumor colony

for calvaria co-cultured with ASC and SCC2 are compared with that of SCC2 cells + calvaria (freeze/thaw), and SCC2 cells + calvaria treated with 10% formaldehyde, both experimental groups showed significant decrease in amount of cells suspended in media and amount of colonized cells on calvaria ($p<0.05$). Figure 40 (B) showed that calvaria treated with 10% formaldehyde co-cultured with ASC and SCC2 cells demonstrated significant decrease in percentage of live cells and increase in percentage of dead cells ($p<0.05$ for live cells, $p<0.001$ for dead cells).

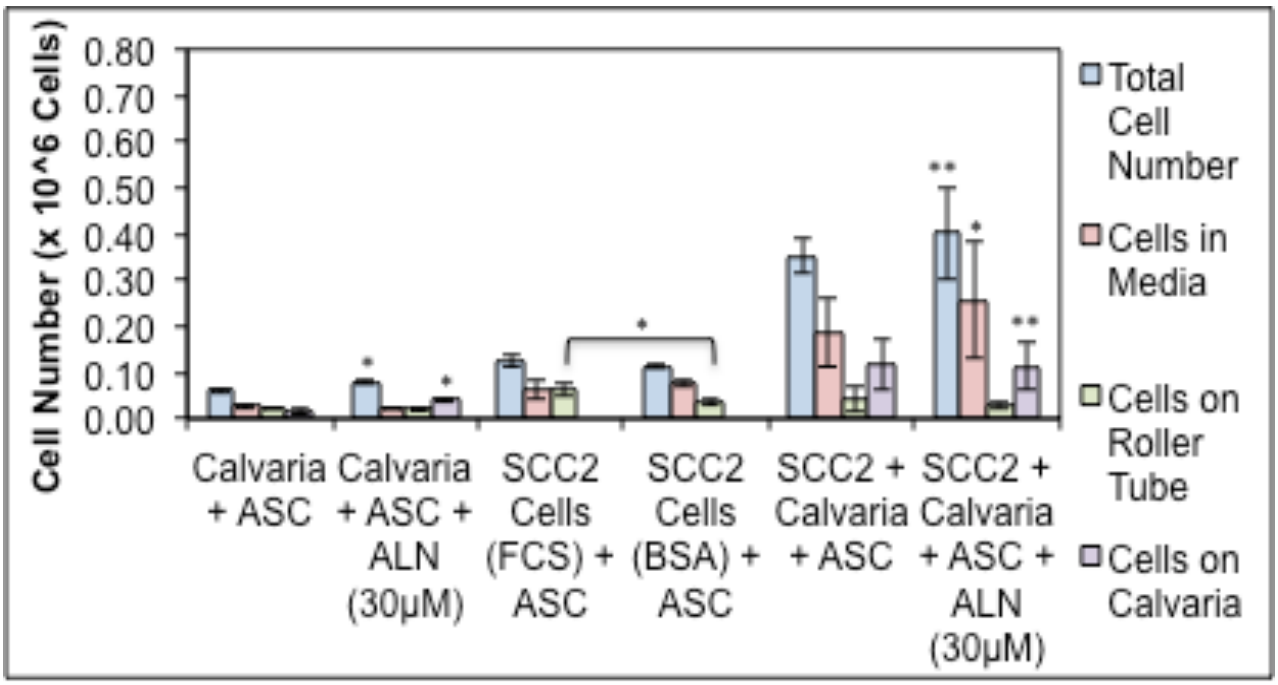
Cell Number (x 10^6 Cells)
0.80
0.70
0.60
0.50
0.40
0.30
0.20
0.10
0.00
Calvaria + ASC
Calvaria + ASC + ALN (30μM)
SCC2 Cells (FCS) + ASC
SCC2 Cells (BSA) + ASC
SCC2 + Calvaria + ASC
SCC2 + Calvaria + ASC + ALN (30μM)
Total Cell Number
Cells in Media
Cells on Roller Tube
Cells on Calvaria

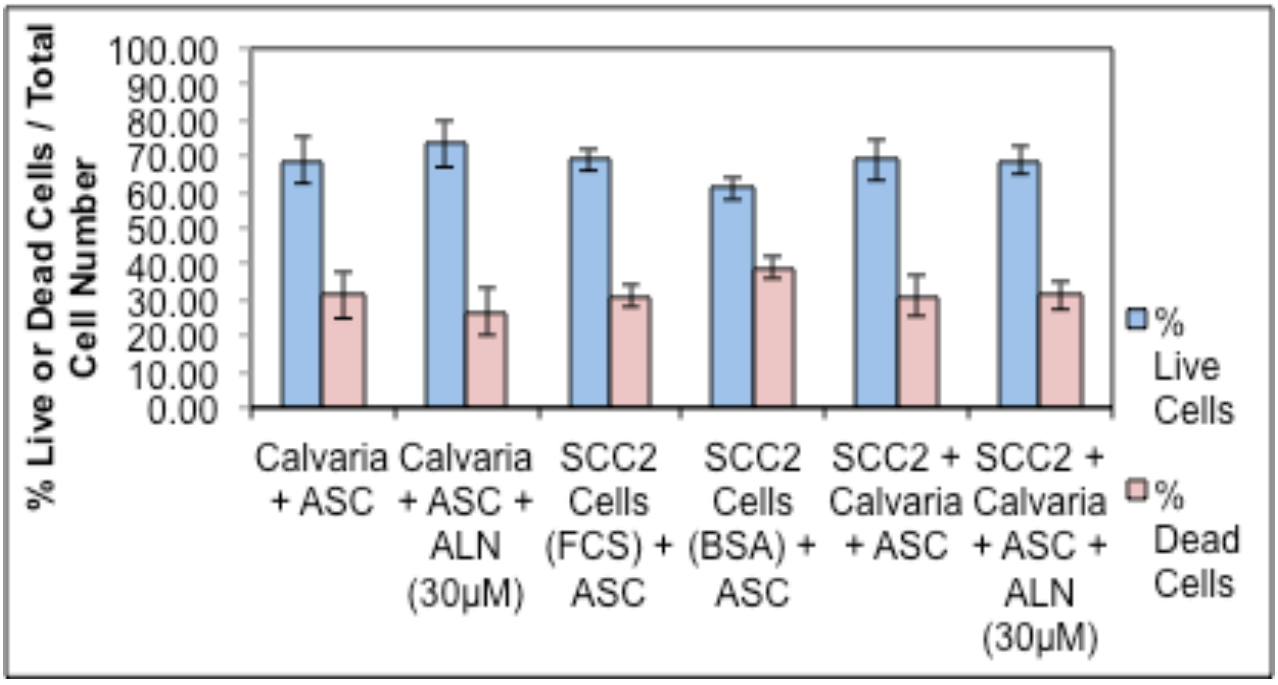
% Live or Dead Cells / Total Cell Number
100.00
90.00
80.00
70.00
60.00
50.00
40.00
30.00
20.00
10.00
0.00
Calvaria + ASC
Calvaria + ASC + ALN (30μM)
SCC2 Cells (FCS) + ASC
SCC2 Cells (BSA) + ASC
SCC2 + Calvaria + ASC
SCC2 + Calvaria + ASC + ALN (30μM)
% Live Cells
% Dead Cells

**Figure 38 - Quantitative Evaluation of the Tumor Colony and Cancer Cell Viability for ASC-Stimulated Bone Formation Model: Control Groups, Calvaria Co-culture with SCC2 Cells in the Absence and Presence of ALN.** Quantitative analysis of total cell number, amount of cells in the media, on the roller tube and calvarial bone, and overall cell viability. (A) SCC2 cells in BSA media had significantly lower number of cells attached to roller tube. When compared with calvaria ASC control, calvaria co-cultured with SCC2 cells + ASC + 30 μM ALN showed significant increase in total cell number, number of cells suspended in media, and cells on calvaria. Results are expressed as a mean ± S.D. (*, $p<0.05$, **, $p<0.001$, Two-tailed t test with equal variance compared with calvaria ASC control); (B) There is no significant difference in cell viability between SCC2 cells in FCS media and BSA media, and no significant difference in cell viability between the calvaria ASC control and calvaria co-cultured with SCC2 cells + ASC in the absence and presence of ALN.

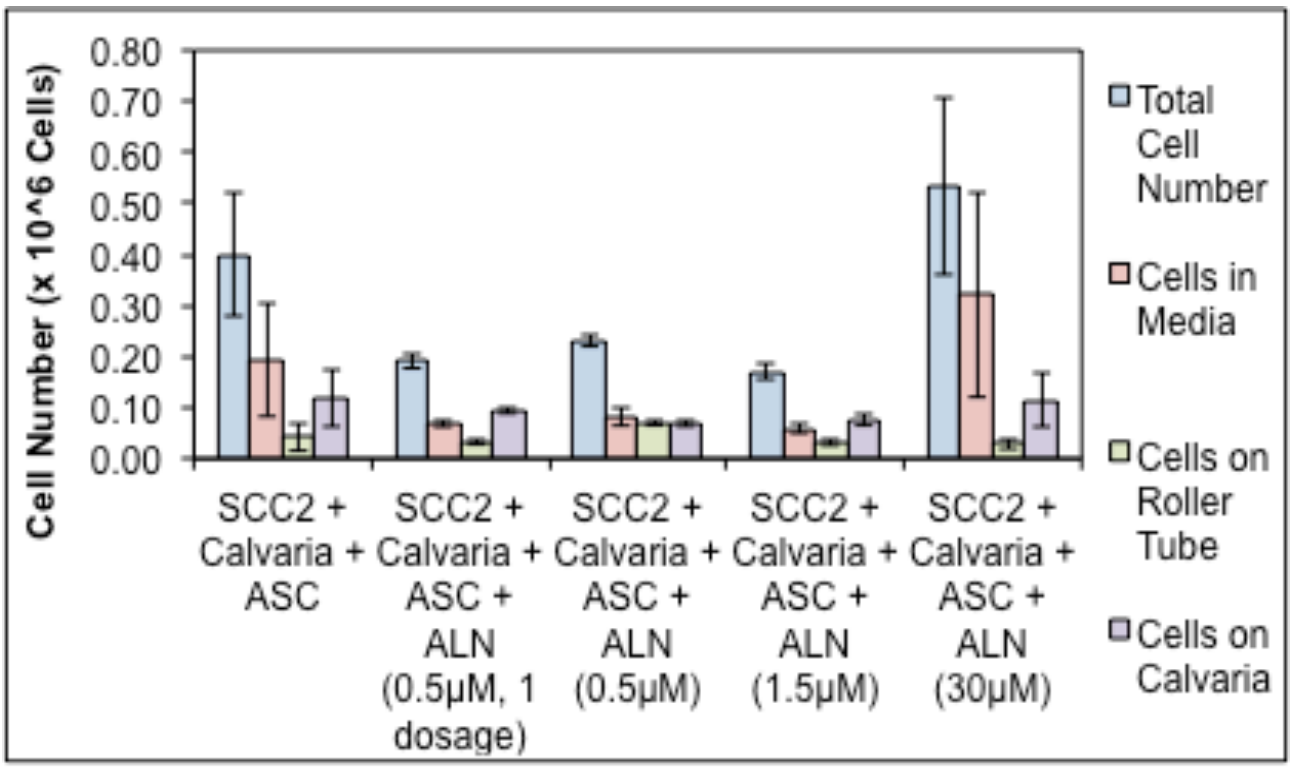
Cell Number (x 10^6 Cells)
0.80
0.70
0.60
0.50
0.40
0.30
0.20
0.10
0.00
SCC2 + Calvaria + ASC
SCC2 + Calvaria + ASC + ALN (0.5μM, 1 dosage)
SCC2 + Calvaria + ASC + ALN (0.5μM)
SCC2 + Calvaria + ASC + ALN (1.5μM)
SCC2 + Calvaria + ASC + ALN (30μM)
Total Cell Number
Cells in Media
Cells on Roller Tube
Cells on Calvaria

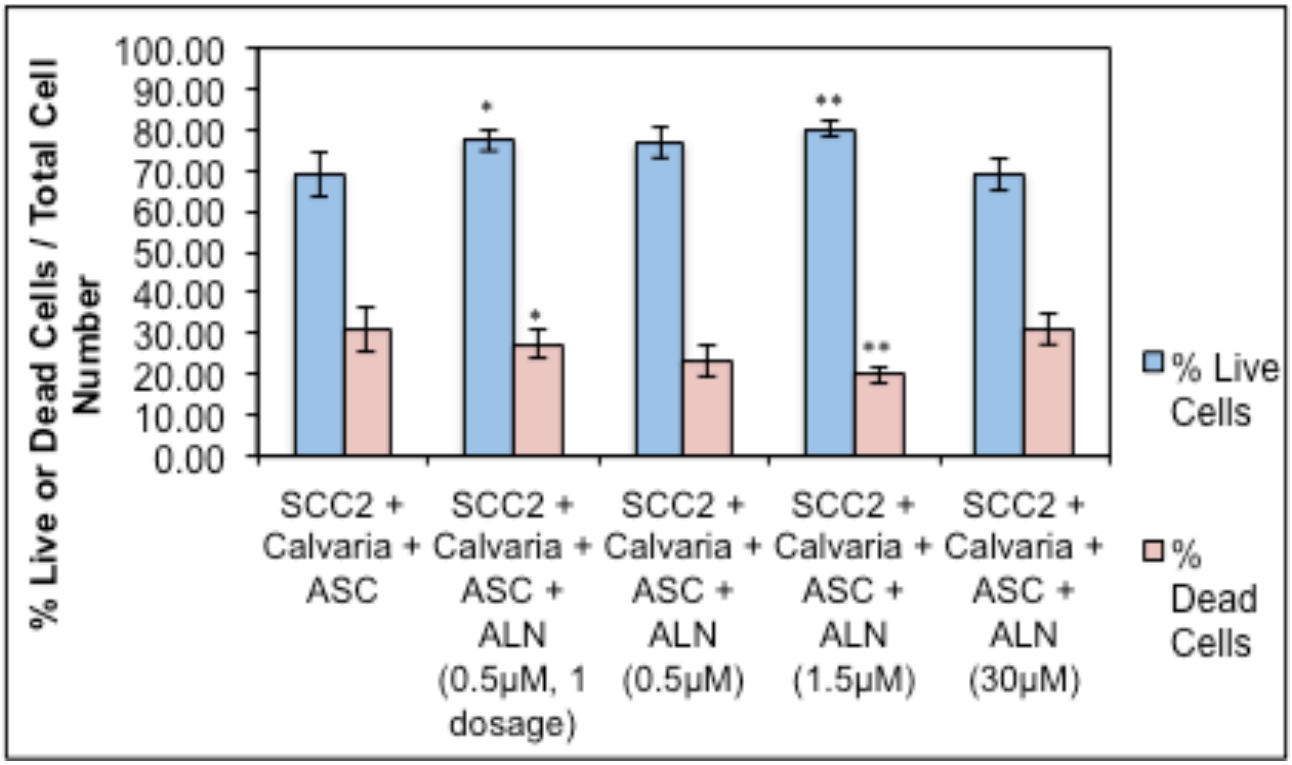
% Live or Dead Cells / Total Cell Number
100.00
90.00
80.00
70.00
60.00
50.00
40.00
30.00
20.00
10.00
0.00
*
*
**
**
SCC2 + Calvaria + ASC
SCC2 + Calvaria + ASC + ALN (0.5μM, 1 dosage)
SCC2 + Calvaria + ASC + ALN (0.5μM)
SCC2 + Calvaria + ASC + ALN (1.5μM)
SCC2 + Calvaria + ASC + ALN (30μM)
% Live Cells
% Dead Cells

**Figure 39 - Quantitative Evaluation of the Tumor Colony and Cancer Cell Viability for ASC-Stimulated Bone Formation Model: Calvaria Co-culture with SCC2 Cells and Different ALN Concentrations.** Quantitative analysis of total cell number, amount of cells in the media, on the roller tube and calvarial bone, and overall cell viability. (A) When quantitative evaluation for calvaria co-cultured with SCC2 cells + ASC are compared with that of calvaria co-cultured with SCC2 cells + ASC and different ALN concentrations (single dosage of 0.5 μM ALN, 0.5 μM ALN, 1.5 μM ALN and 30 μM ALN), there is no statistical significance in total cell number, number of cells in media, number of cells on roller tube, or number of cells on calvaria. (B) Percentage of live and dead cells for calvaria co-cultured with SCC2 cells + ASC and different ALN concentrations (single dosage of 0.5 μM ALN, 0.5 μM ALN, 1.5 μM ALN and 30 μM ALN). Calvaria co-cultured with SCC2 cells + ASC + single dosage of 0.5 μM AL and calvaria co-cultured with SCC2 cells + ASC + 1.5 μM ALN showed increase in percentage of live cells and decrease in percentage of dead cells. Results are expressed as a mean ± S.D. (*, $p<0.05$, **, $p<0.001$, Two-tailed t test with equal variance compared with calvaria co-cultured with SCC2 cells + ASC).

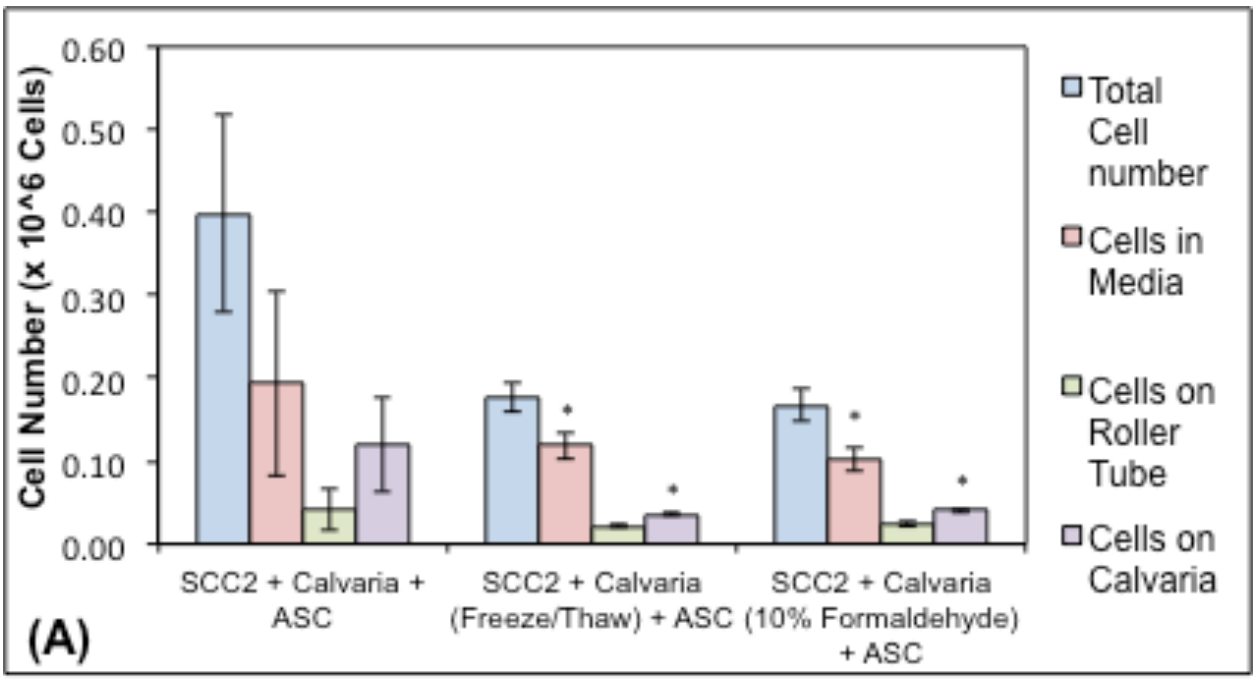
Cell Number (x 10^6 Cells)
0.60
0.50
0.40
0.30
0.20
0.10
0.00
Total Cell number
Cells in Media
Cells on Roller Tube
Cells on Calvaria
SCC2 + Calvaria + ASC
SCC2 + Calvaria (Freeze/Thaw) + ASC
SCC2 + Calvaria (10% Formaldehyde) + ASC
(A)

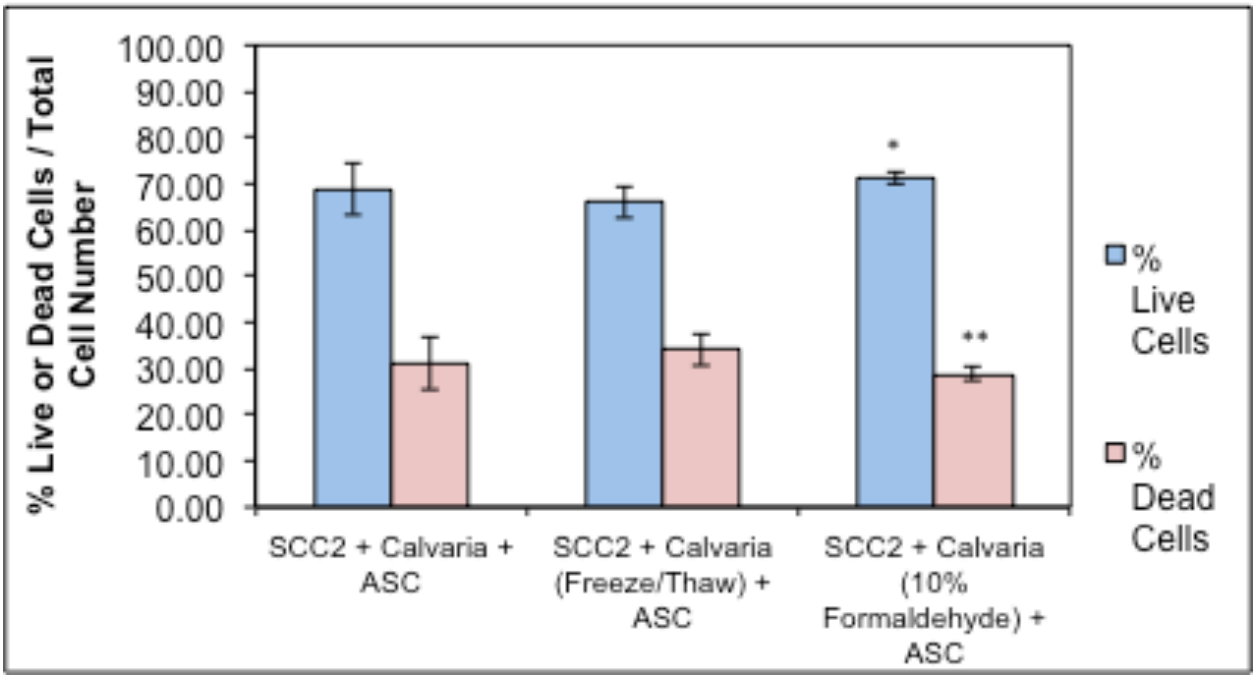
% Live or Dead Cells / Total Cell Number
100.00
90.00
80.00
70.00
60.00
50.00
40.00
30.00
20.00
10.00
0.00
% Live Cells
% Dead Cells
SCC2 + Calvaria + ASC
SCC2 + Calvaria (Freeze/Thaw) + ASC
SCC2 + Calvaria (10% Formaldehyde) + ASC

**Figure 40 - Quantitative Evaluation of the Tumor Colony and Cancer Cell Viability for ASC-Stimulated Bone Formation Model: Calvaria of Reduced Viability Co-cultures with SCC2 Cells.** (A) Calvaria (freeze/thaw) co-cultured with ASC and SCC2 and calvaria treated with 10% formaldehyde co-cultured with SCC2 cells showed significant decrease in amount of cells suspended in media and amount of colonized cells on calvaria compared to calvaria co-cultured with SCC2 + ASC. Results are expressed as a mean ± S.D. (*, $p<0.05$, Two-tailed t test with equal variance compared with calvaria co-cultured with SCC2 cells + ASC). (B) Calvaria treated with 10% formaldehyde co-cultured with ASC and SCC2 cells demonstrated a significant decrease in percentage of live cells and increase in percentage of dead cells. Results are expressed as a mean ± S.D. (*, $p<0.05$, **, $p<0.001$, Two-tailed t test with equal variance, compared with calvaria co-cultured with SCC2 cells + ASC).

## *7.7. Quantitative Analysis of Changes in Media Calcium Concentration and ALP Activity: Effect of ALN and SCC2 Cells Viability on OBs Formation and Bone Formation in Bone Formation Model.*

### *7.7.1. Calcium Uptake Vs. Time*

Calcium uptake of each media over the 8-day culture period for the bone formation model is represented in Figure 41. Similar to the resorption model, media were collected on day 2, 4, 6 and 8 during the culture period. The data represented were corrected for media concentration to obtain net calcium uptake and presented as nmol calcium/10ul media. Calvaria control and calvaria co-cultured with SCC2 have similar calcium concentration throughout the experiment, with the maximum value on day 6. Calvaria + ASC demonstrated an increase in calcium concentration from day 4 to day 8. Calvaria + ASC + 30 μM ALN have the lowest calcium concentration out of all the experimental groups, suggesting a decrease in calcium release (Figure 41 (A)).

Calvaria co-cultured with SCC2 cells + ASC + single dosage of 0.5 μM ALN, 0.5 μM ALN and 1.5 μM ALN all demonstrated higher calcium concentration than the calvaria control throughout the entire experiment. All 3 experimental groups experienced a decrease in calcium concentration level from day 6 to day 8, suggesting bone formation between day 6 and day 8 (Figure 41 (B)).

Calvaria (freeze/thaw) co-cultured with SCC2 cells + ASC, and calvaria treated with 10% formaldehyde co-cultured with SCC2 cells + ASC showed calcium concentration level lower than calvaria control with gradual increase of

calcium release that peaked on day 6 of experiment, and decreased between day 6 and day 8 (Figure 41 (C)).

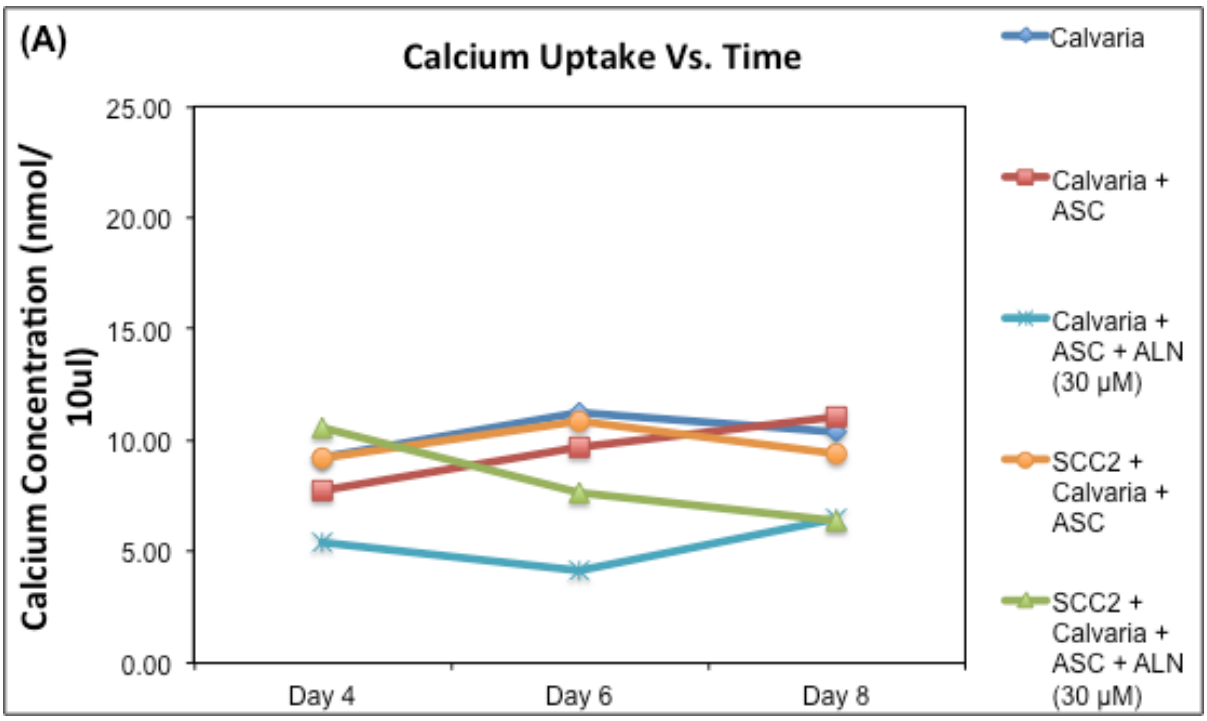
(A)
Calcium Uptake Vs. Time
Calcium Concentration (nmol/ 10ul)
25.00
20.00
15.00
10.00
5.00
0.00
Day 4
Day 6
Day 8
Calvaria
Calvaria + ASC
Calvaria + ASC + ALN (30 µM)
SCC2 + Calvaria + ASC
SCC2 + Calvaria + ASC + ALN (30 µM)

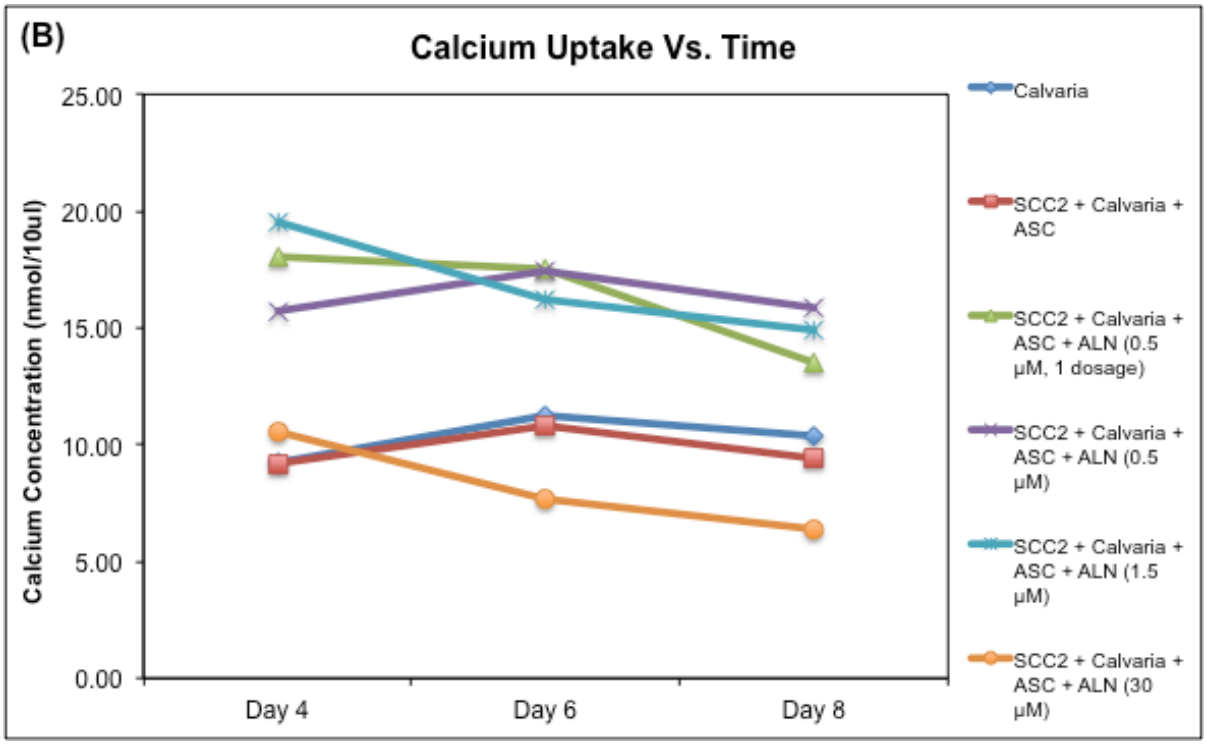
(B)
Calcium Uptake Vs. Time
Calcium Concentration (nmol/10ul)
25.00
20.00
15.00
10.00
5.00
0.00
Day 4
Day 6
Day 8
Calvaria
SCC2 + Calvaria + ASC
SCC2 + Calvaria + ASC + ALN (0.5 µM, 1 dosage)
SCC2 + Calvaria + ASC + ALN (0.5 µM)
SCC2 + Calvaria + ASC + ALN (1.5 µM)
SCC2 + Calvaria + ASC + ALN (30 µM)

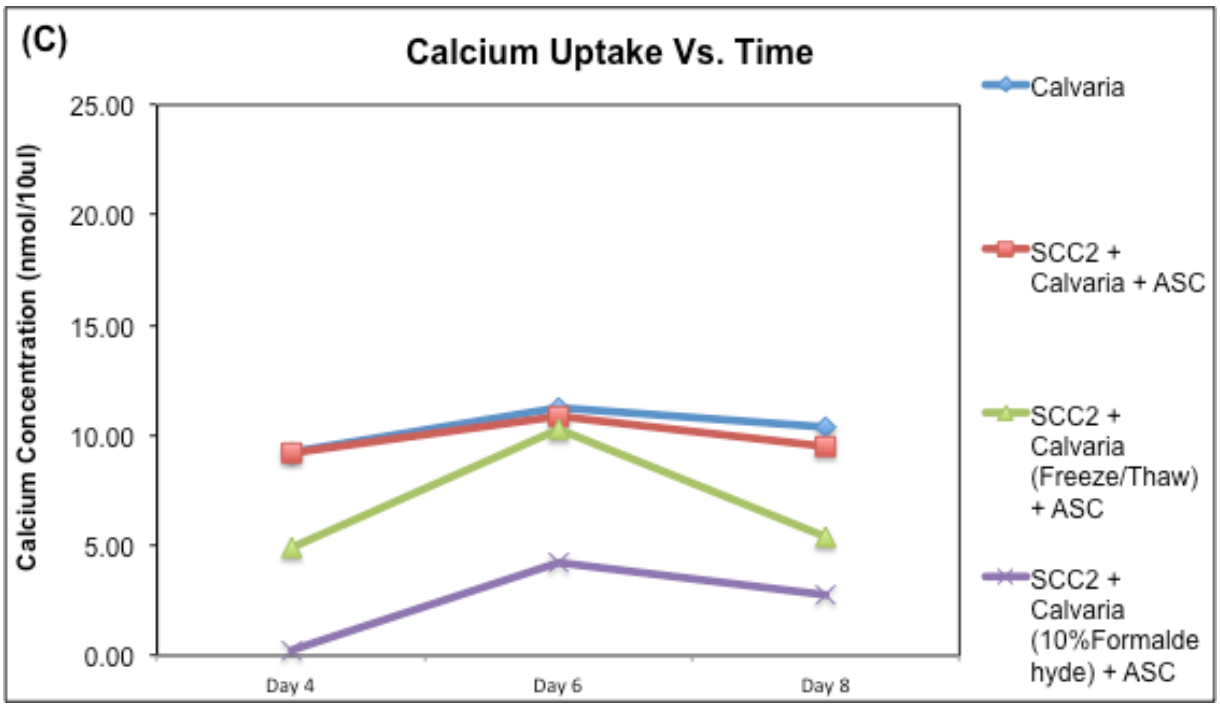
(C)
Calcium Uptake Vs. Time
Calcium Concentration (nmol/10ul)
25.00
20.00
15.00
10.00
5.00
0.00
Day 4
Day 6
Day 8
Calvaria
SCC2 + Calvaria + ASC
SCC2 + Calvaria (Freeze/Thaw) + ASC
SCC2 + Calvaria (10%Formaldehyde) + ASC

**Figure 41 - Bone Formation Model: Calcium Uptake Vs. Time.** Calcium concentration in collected media plotted as a function of time in the bone formation model. Calvaria control and calvaria co-cultured with SCC2 cells + ASC have similar calcium concentrations throughout the experiment; both groups experienced a slight increase in calcium release between day 4 and day 6, and decrease in calcium concentration between day 6 and day 8. Calvaria + ASC showed increase in calcium concentration between day 4 and 8, suggesting bone formation during day 2 and 4. Calvaria + ASC + 30 μM ALN showed substantial decrease in calcium concentration between day 4 and day 6, with gradual increase in calcium release between day 6 and 8. Calvaria co-cultured with SCC2 cells + ASC + 30 μM ALN demonstrated a gradual decrease in calcium concentration throughout the experiment (Figure 41 (A)). Calvaria co-cultured with SCC2 cells + ASC + single dosage of 0.5 μM ALN, 0.5 μM ALN and 1.5 μM ALN all demonstrated higher calcium concentration than the calvaria control throughout the entire experiment. All 3 experimental groups experienced a decrease in calcium concentration level from day 6 to day 8, suggesting bone formation between day 6 and day 8 (Figure 41 (B)). Calvaria (freeze/thaw) and calvaria (10% formaldehyde) both showed calcium concentration level lower than calvaria control throughout the experiment. Both groups demonstrated an increase in calcium release between day 4 to day 6, with decrease in calcium concentration between day 6 to day 8 (Figure 41 (C)).

### 7.7.2. Cumulative Calcium Uptake & ALP Activity

Total cumulative calcium uptake and ALP activity for each experimental group over the 8 day culture period for the bone formation model are represented in Figures 42-44. Surprisingly calvaria + ASC + 30 μM ALN showed decreased calcium release and significant increase in ALP activity ($p$<0.001) (Figure 42 (A) and (B)). Calvaria co-cultured with SCC2 cells + ASC demonstrated an increase in cumulative calcium concentration and showed a significant decrease in ALP activity ($p$<0.001). A significant decrease of cumulative calcium concentration was noted between calvaria co-culture with SCC2 cells + ASC and calvaria co-cultured with SCC2 cells + ASC + 30 μM ALN, but both experimental groups demonstrated similar ALP activity level (Figure 42 (A) and (B)). Calvaria co-cultured with SCC2 cells + ASC + different ALN concentrations (single dosage of 0.5 μM ALN, 0.5 μM ALN, 1.5 μM ALN) all showed significantly increased calcium release ($p$<0.05) and significantly decreased ALP activity ($p$<0.05 for single dosage of 0.5 μM ALN and 0.5 μM ALN; $p$<0.001 for 1.5 μM ALN), (Figure 43 (A) and (B)). Calvaria (freeze/thaw) co-cultured with ASC and SCC2 cells and calvaria (10% formaldehyde) co-culture with SCC2 cells + ASC both showed reduced calcium release, and calvaria treated with10% formaldehyde have significant lower calcium concentration when compared with that of calvaria (freeze/thaw) ($p$<0.05) (Figure 44 (A)). Figure 44 (B) demonstrated significant decrease in ALP activity for both calvaria (10% formaldehy) ($p$<0.001) and calvaria (freeze/thaw) ($p$<0.05).

**Figure 42 – Cumulative Calcium Uptake and ALP Activity for ASC-Stimulated Bone Formation Model: Control Groups, Calvaria Co-culture with SCC2 Cells in the Absence and Presence of ALN**

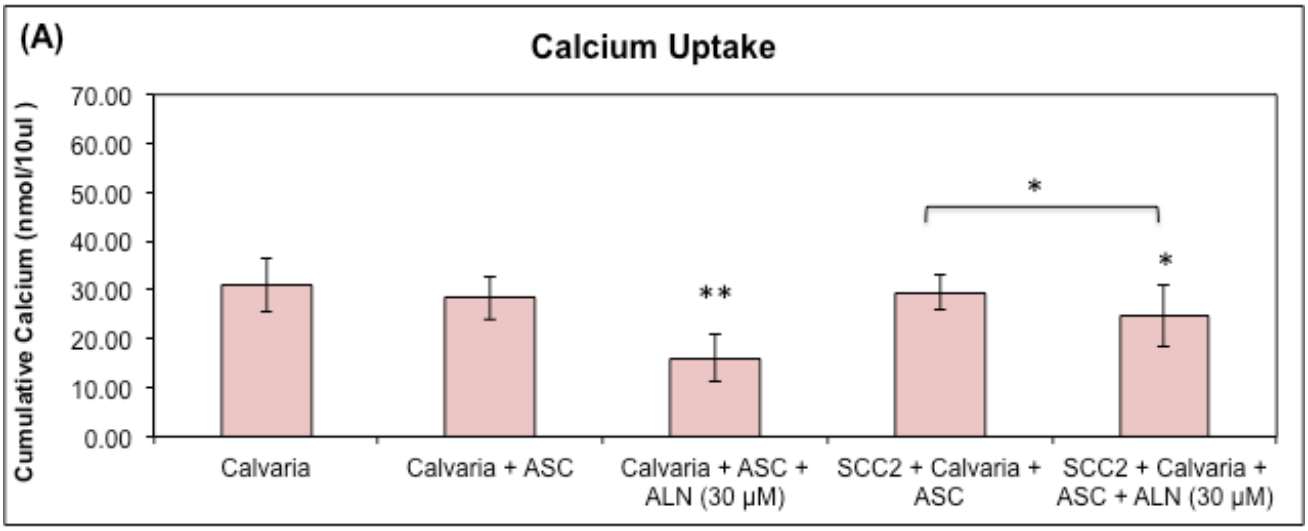


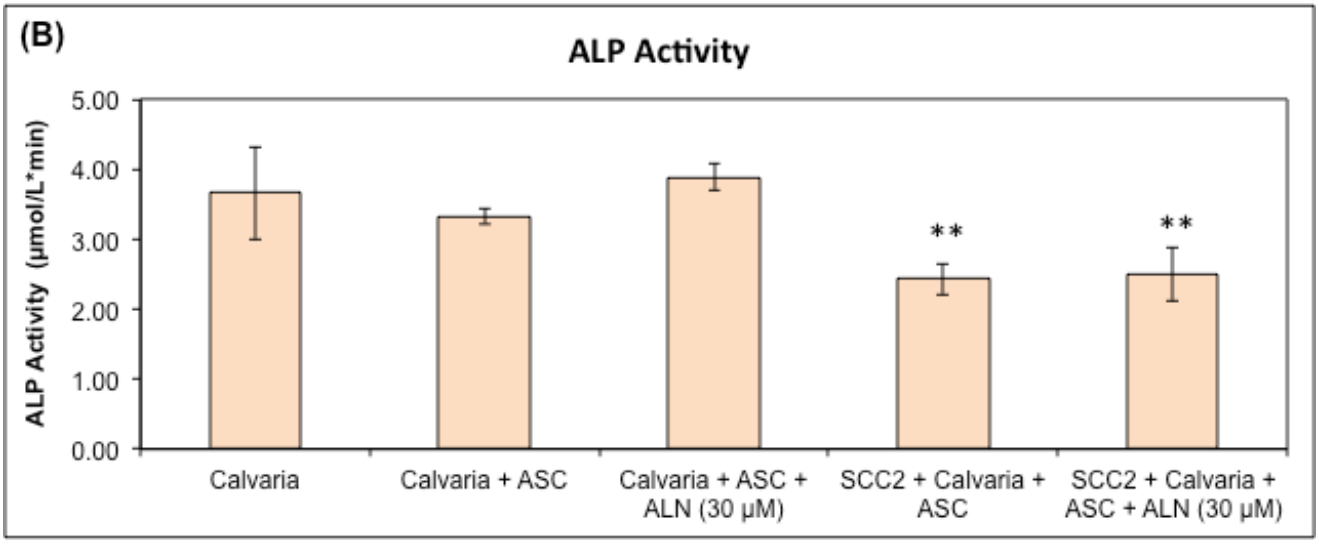

**Figure 43 – Cumulative Calcium Uptake and ALP Activity for ASC-Stimulated Bone Formation Model: Calvaria Co-culture with SCC2 Cells and Different ALN Concentrations**

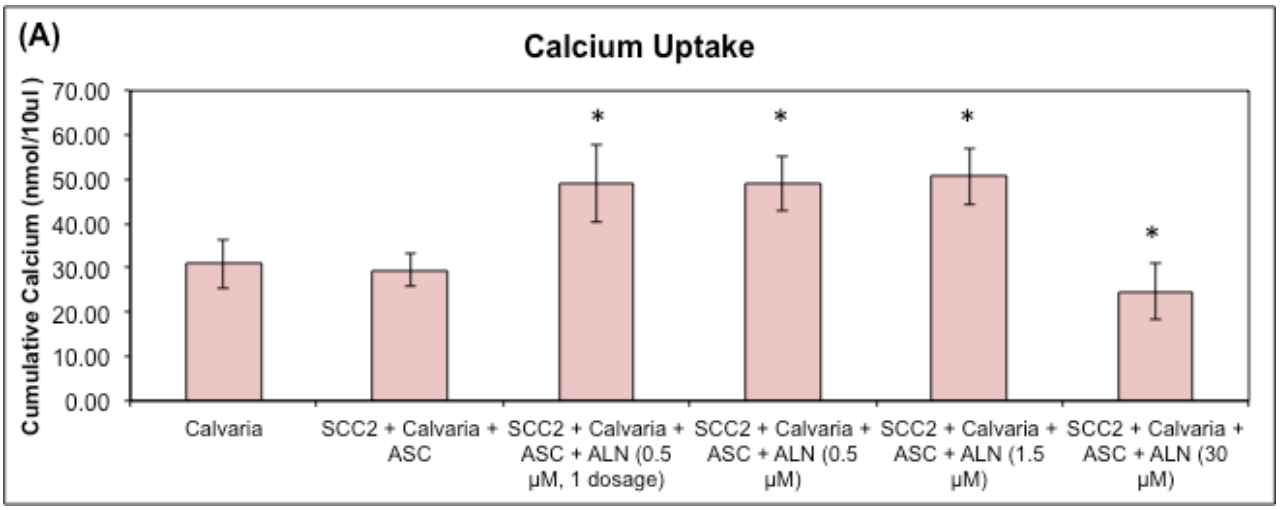


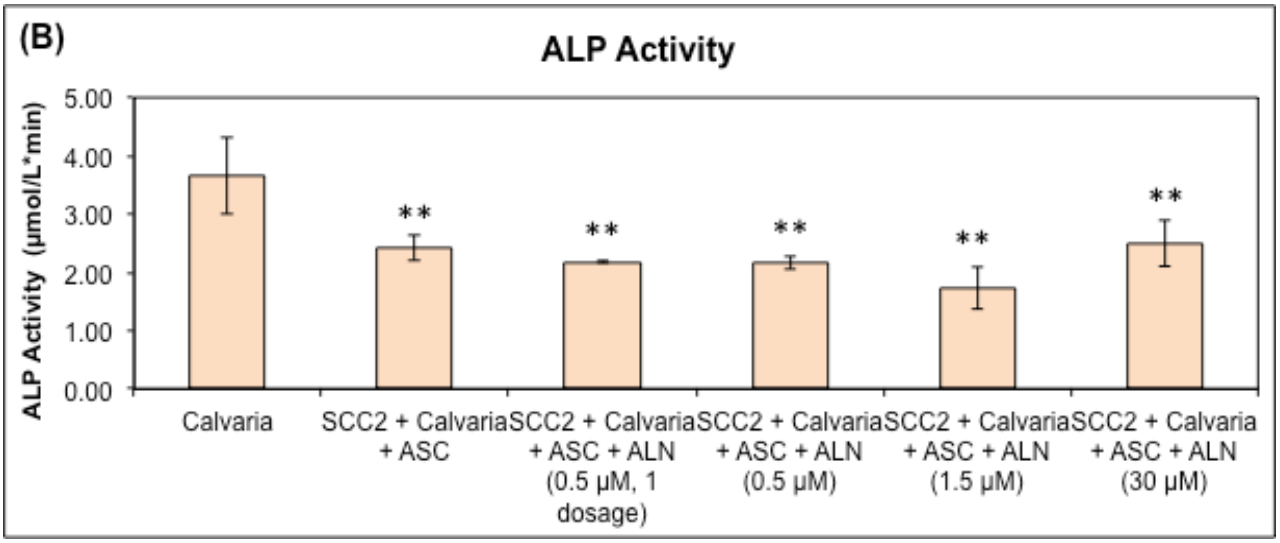

**Figure 44 – Cumulative Calcium Uptake and ALP Activity for ASC-Stimulated Bone Formation Model: Calvaria of Reduced Viability Co-culture with SCC2 Cells**

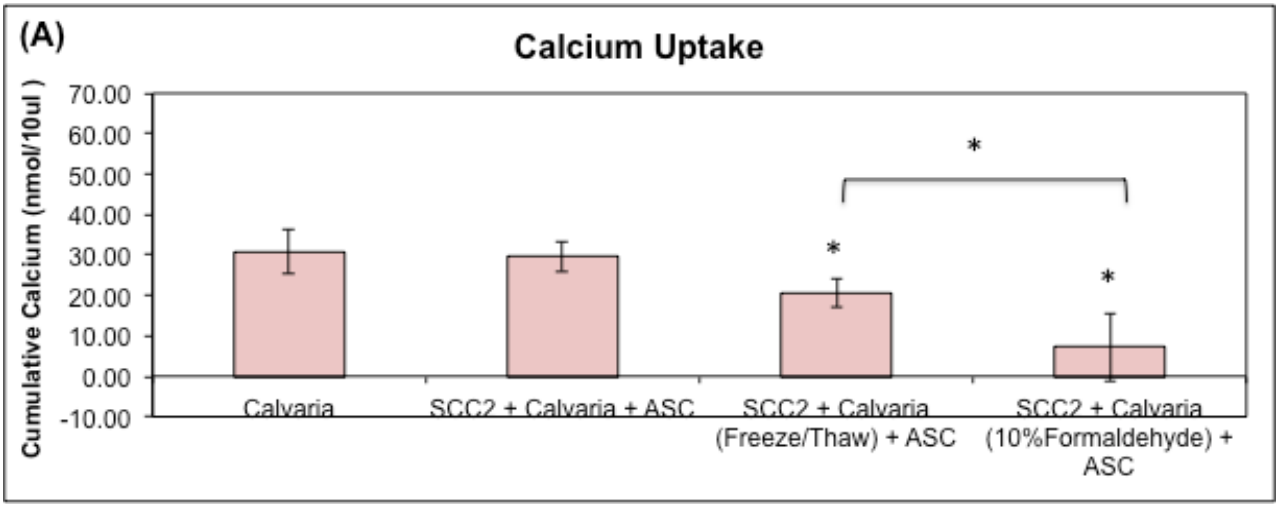


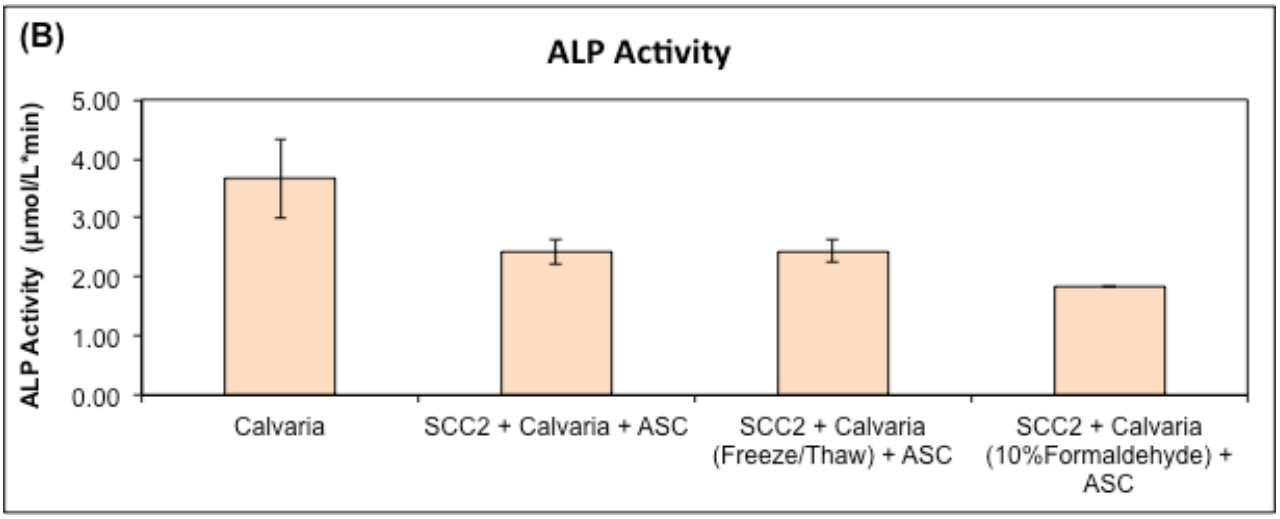

**Figures 42-44 – Quantitative Analysis of Cumulative Calcium Uptake and ALP Activity for ASC-Stimulated Bone Formation Model.** When compared to calvaria control, calvaria + ASC + 30 μM ALN and calvaria co-cultured with SCC2 cells + ASC + 30 μM ALN showed significantly decreased calcium release. Results are expressed as a mean ± S.D. (*, $p<0.05$; **, $p<0.001$, Two-tailed t test with equal variance, compared with calvaria control). Also, there is significant decrease is cumulative calcium concentration between calvaria co-cultured with SCC2 cells + ASC with and without 30 μM ALN ((Figure 42 (A)). Calvaria + ASC + 30 μM ALN showed increased ALP activity when compared to the calvarial control, while calvaria co-cultured with SCC2 cells + ASC, and calvaria co-cultured with SCC2 cells + ASC + 30 μM ALN showed significantly decreased ALP activity (Figure 42 (B)). Results are expressed as a mean ± S.D. (**, $p<0.001$, Two-tailed t test with equal variance, compared with calvaria control). Cumulative calcium release significantly increased in calvaria co-cultured with SCC2 cells + ASC and single dosage of 0.5 μM ALN, 0.5 μM ALN and 1.5 μM ALN, with significant decrease in calcium release for calvaria co-cultured with SCC2 cells and 30 μM ALN (Figure 43 (A)). Results are expressed as a mean ± S.D. (*, $p<0.05$; **, $p<0.001$, Two-tailed t test with equal variance compared with calvaria control). ALP activity for calvaria co-cultured with SCC2 cells + ASC and different ALN concentrations (single dosage of 0.5 μM ALN, 0.5 μM ALN, 1.5 μM ALN and 30 μM ALN) showed significant decrease in ALP activity for calvaria co-cultured with SCC2 cells + ASC and single dosage of 0.5 μM ALN, 0.5 μM ALN and 1.5 μM ALN (Figure 43 (B)). Results are expressed as

a mean ± S.D. (*, $p<0.05$, **, $p<0.001$, Two-tailed t test with equal variance compared with calvarial control). Cumulative calcium uptake for calvaria control, calvaria co-cultured with ASC and SCC2 cells, calvaria that have been frozen/thawed co-cultured with ASC, calvaria treated with 10% formaldehyde co-culture with SCC2 cells + ASC. Both experimental groups showed significant reduction in calcium release, and calvaria treated with 10% formaldehyde have significant lower calcium concentration when compared with that of calvaria (freeze/thaw) (Figure 44 (A)). Results are expressed as a mean ± S.D. (*, $p<0.05$, **, $p<0.001$, Two-tailed t test with equal variance, compared with calvaria control). ALP activity significantly decreased for calvaria (freeze/thaw) co-cultured with ASC and SCC2 cells and calvaria treated with 10% formaldehyde co-cultured with ASC and SCC2 cells (Figure 44 (B)). Results are expressed as a mean ± S.D. (**, $p<0.001$, Two-tailed t test with equal variance compared with calvaria control).

### *7.8. High Resolution 2-Photon Confocal Microscopy for Both Bone Resorption Model and ASC-Stimulated Bone Formation Model*

High-resolution 2-photon confocal microscopy was utilized for 3D visualization of cancer-bone interaction between SCC2 cells and the calvaria. Different fluorescent labels were used to distinguish the mineralized bone matrix, bone cells and SCC2 cells: red-fluorescent BP for the mineralized bone matrix, green-fluorescent human cytokeratin-7 for SCC2 cells and blue-fluorescent DAPI for cell nuclei. Vertical and horizontal recorder of the calvarial ones were performed for both the bone resorption and bone formation model with the horizontal recording captured from endosteum and moving toward the periosteum over a depth of 175 μm at 5 μm intervals with 200x magnification. After the recording, 3D composites of the bone resorption and bone formation model were generated using the ImageJ software and are displayed in Figure 45 (A)-(L). Both the bone resorption and bone formation model showed tumor cell colonization with separation from the mineralized bone matrix by the endosteal cells. No tumor cells were seen on the bone surface in the 3D vertical view in Figure 45 (F) and (I). For the calvaria-cultured with SCC2 cells in the bone resorption model, as in Figure 45 (A)-(C), tumor cells appeared oval in shape and formed a 3-dimensional structure with multiple layers of tumor cells when colonizing the endosteal side of calvaria. Figure 45 (B) showed mineralized bone matrix in red, with endosteal cells as small oval blue nuclei, and tumor cells as larger blue nuclei surrounded by green fluorescence. Distinct bone resorption areas are noted with loss of mineralized bone matrix. Figure (D)-(F) showed

calvaria co-cultured with SCC2 cells + ASC in the bone formation model. Under this condition, the SCC2 cells appeared different morphologically as the cells became more elongated with extended cellular processes. Calvaria co-cultured with SCC2 cells + ALN are displayed in Figure 45 (G)-(I). SCC2 cells appeared ovoid in shapes, and absence of OC-bone resorption area is absent. However, in the presence of ALN, the osteocytes appeared to lose their nuclei and showed degeneration of the mineralized bone matrix. Figure 45 (J)-(L) showed calvaria co-cultured with SCC2 cells + ASC + ALN. Under the formation conditions, SCC2 cells also displayed cellular elongation independent of the presence of ALN. Also, loss of osteocyte nuclei can also be noted in Figure 45 (K) under the bone formation model.

**Figure 45 – High Resolution 2-Photon Confocal Microscopy for Both Bone Resorption Model and Bone Formation Model**

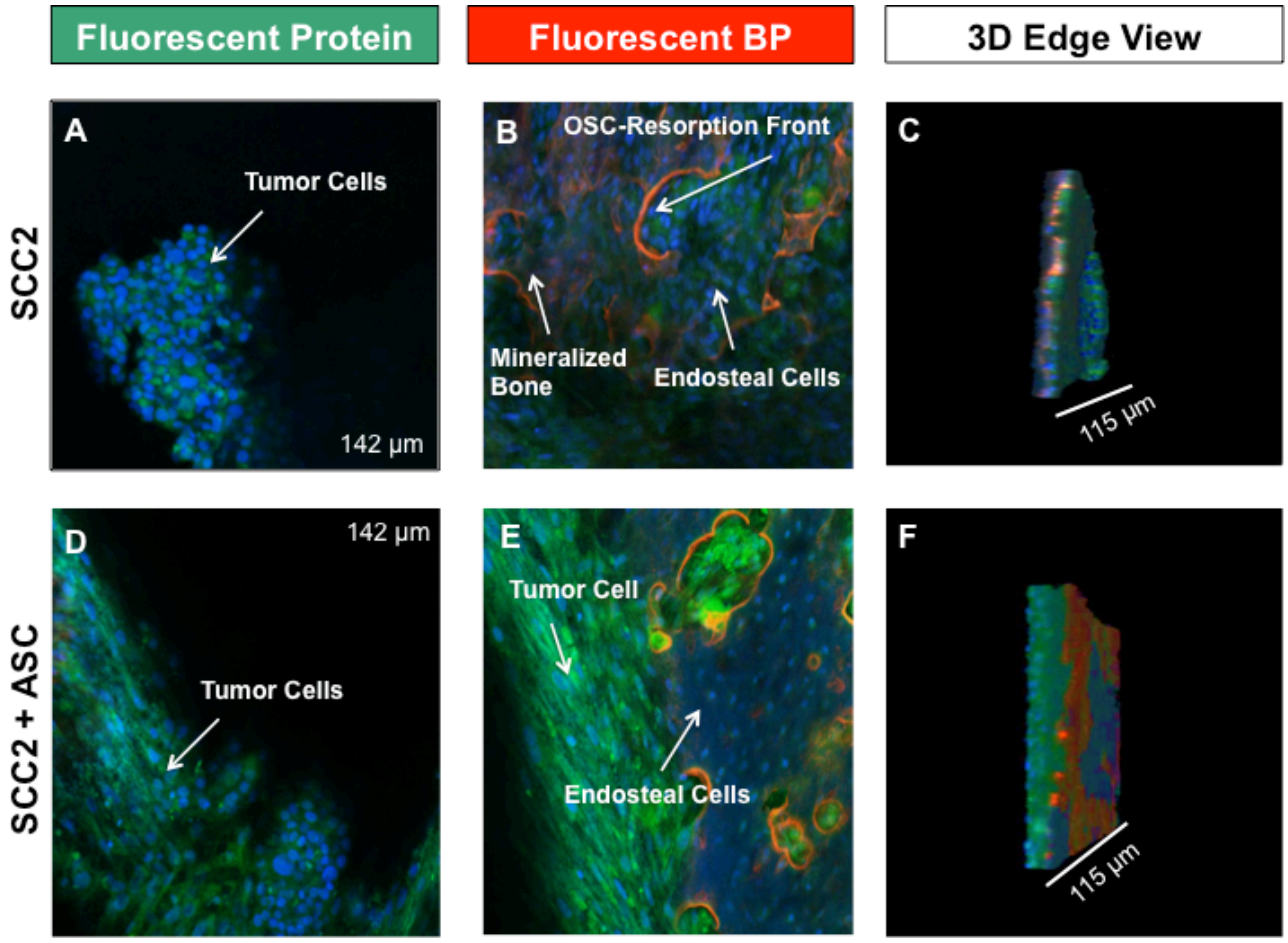

**Figure 45 – High Resolution 2-Photon Confocal Microscopy for Both Bone Resorption Model and Bone Formation Model (Continued)**

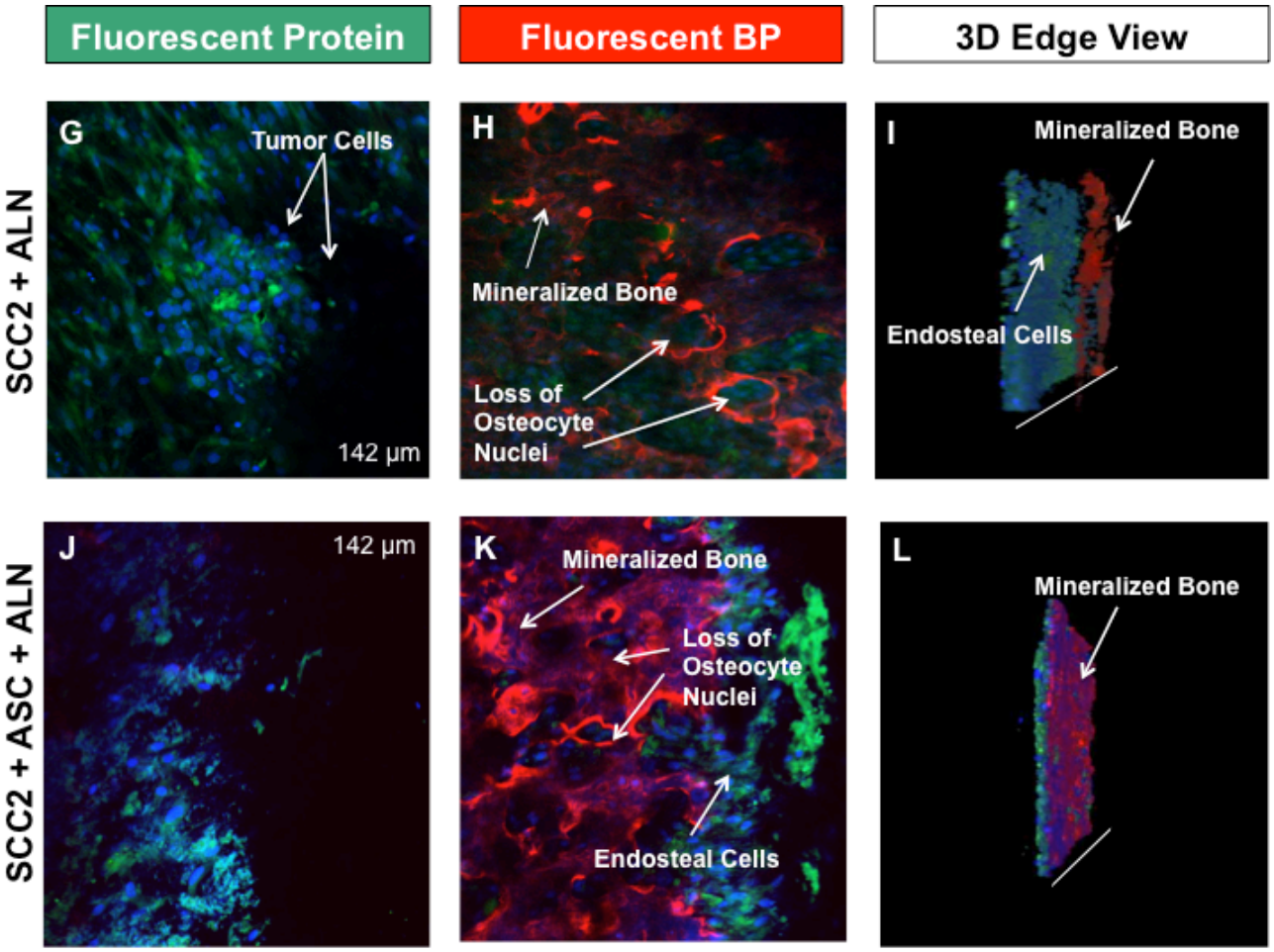

**Figure 45 – High Resolution 2-Photon Confocal Microscopy for Both Bone Resorption Model and Bone Formation Model.** 2-photon high-resolution microscopy of calvaria co-cultured with SCC2 cells under bone formation and bone resorption conditions in the absence and presence of ALN. (A)-(C), composite of calvaria co-cultured with SCC2 cells in bone resorption model, fixed in formalin and fluorescent labeled with red-fluorescent BP for the mineralized bone matrix, green-fluorescent human cytokeratin-7 for SCC2 cells and blue-fluorescent DAPI for cell nuclei. (A), fluorescent composite of BP, human cytokeratin-7 and DAPI of horizontal recording, showing 3D structure of SCC2 cells. (B), fluorescent composite of BP, human cytokeratin-7 and DAPI of horizontal recording, showing endosteal cells separating SCC2 cells from mineralized bone, and presence of OC bone resorption. (C) 90°side view of the 3D orientation of the cancer cells-bone interactions. (D)-(F), composite of calvaria co-cultured with SCC2 cells + ASC in bone formation condition, fixed in formalin and fluorescent labeled with red-fluorescent BP for the mineralized bone matrix, green-fluorescent human cytokeratin-7 for SCC2 cells and blue-fluorescent DAPI for cell nuclei. (D), fluorescent composite of BP, human cytokeratin-7 and DAPI of horizontal recording, showing 3D structure of SCC2 cells. (E), fluorescent composite of BP, human cytokeratin-7 and DAPI of horizontal recording, showing spatial relationship between SCC2 cells, endosteal cells and the mineralized bone matrix. (F), 90°side view of the 3D orientation of the cancer cells-bone interactions. (G)-(I), composite of calvaria co-cultured with SCC2 cells + ALN in bone resorption condition, fixed in formalin and fluorescent

labeled with red-fluorescent BP for the mineralized bone matrix, green-fluorescent human cytokeratin-7 for SCC2 cells and blue-fluorescent DAPI for cell nuclei. (G), fluorescent composite of BP, human cytokeratin-7 and DAPI of horizontal recording, showing 3D structure of SCC2 cells. (H), fluorescent composite of BP, human cytokeratin-7 and DAPI of horizontal recording, showing loss of osteocyte nuclei and deterioration of mineralized bone matrix. (I),Partial side view of 3D orientation of the cancer cells-bone interactions. (J)-(L), composite of calvaria co-cultured with SCC2 cells + ALN+ ASC in bone resorption condition, fixed in formalin and fluorescent labeled with red-fluorescent BP for the mineralized bone matrix, green-fluorescent human cytokeratin-7 for SCC2 cells and blue-fluorescent DAPI for cell nuclei. (J), fluorescent composite of BP, human cytokeratin-7 and DAPI of horizontal recording, showing 3D structure of SCC2 cells. (K), fluorescent composite of BP, human cytokeratin-7 and DAPI of horizontal recording, showing loss of osteocyte nuclei and deterioration of mineralized bone matrix. (L), Partial side view of 3D orientation of the cancer cells-bone interactions.

## 8. Discussion

Bone is a dynamic and highly vascularized organ that provides an ideal microenvironment for sustaining cancer cells, fostering cancer cell colonization and drug therapy resistance. Bone resorption induced by cancer cell metastasis can release growth factor from the bone matrix that are essential for fostering metastasis development by facilitating proliferation of dormant cancer cells. Over time, the goal of cancer therapy has been shifting from targeting and killing the cancer cells directly to interfering with mechanisms that support cancer cell survival. More than 100 years ago, Stephen Paget proposed the seed-and-soil hypothesis, which suggested that modifying the microenvironment that support cancer cell growth may be a valuable approach of treating cancer cells metastasis (Gnant & Clezardin, 2012).

Based on the concept that cancer-bone metastasis and cancer cell survival are bone resorption-dependent, bisphosphonates (BPs) has been used clinically as an adjunctive anti-cancer medication due to its effect on reducing cancer cells-induced bone resorption and cancer cells survival. In pre-clinical trials, nitrogen-containing bisphosphonate (NBPs) demonstrated anticancer activity by inhibiting the activity of farnesyl diphosphate (FPP) synthase of the mevalonate pathway causing impairment in cancer cell adhesion, migration, and proliferation. Alendronate, clodronate and zoledronic acid have also been found to inhibit cancer cell growth and induce cancer cell apoptosis (Gnant & Clezardin, 2012).

The aim of this study was to determine the effect of ALN on SCC2 cells,

calvarial bone biology, and the interplay between the SCC2 cells and calvarial bone. The results of the 2D SCC2 cells culture demonstrated that when SCC2 cells were cultured alone, ALN interfered with SCC2 cells attachment to the cell culture dish in a dose-dependent manner. Also, increasing ALN concentration resulted in an increase of percentage of dead SCC2 cells in the presence of ASC and BSA in cell-culture media. It should also be noted that when ALN was added to cell-culture media with BSA at seeding, SCC2 cells were not able to attach to the cell-culture dish and proliferate. The results of these studies corresponded to the finding of Donetti in 2014, which stated that ALN affects epithelial cells adhesion and proliferation by decreasing reducing desmoglein 1 and keratin 10 expression and changing morphology of the desmosomes (Donetti et al, 2014). The increased effect of ALN on SCC2 viability in the presence of ASC and BSA in cell-culture media can be explained by the importance of FCS in cell-maintenance (Hemeda et al, 2014) and the anti-cancer effect of ASC that was discovered by Pires et al in 2016, whose study showed ASC can induce anti-proliferative and cytotoxic effect on three colon cancer cell lines, and that ASC can induce cell death through oxidative stress (Pires et al, 2016).

The present study provided multiple insights into the nature of cancer cells-bone interaction. First of all, the result demonstrated that cancer cells-bone metastasis is not dependent on osteoclast-mediated bone resorption. Through histologic study, it was apparent that exposure of live calvarial bone to SCC2 cancer cells led to cancer cells colonization on the calvarial endosteal surface, and subsequent activation of the osteoclast-mediated bone resorption. In

addition, calvaria co-cultured with SCC2 cells and ALN resulted in cancer cells colonization in the presence of reduced bone resorption. Furthermore, in the ASC-induced bone formation model new osteoid formation was activated and cancer cell colonization on calvarial endosteal surface was noted despite the absence of osteoclastic bone resorption. The above observations lead to the conclusion that SCC2 cells do not depend on osteoclastic bone resorption for cancer-bone metastasis to occur.

The difference between the 2D cancer cell-culture and the 3D roller tube calvaria-cancer cell co-culture also demonstrated bone-mediated resistance of SCC2 cancer cells to ALN therapy. In the absence of calvarial bone addition of 30 μM ALN led to significant increase of SCC2 cell detachment from the cell-culture dish and percentage of dead SCC2 cells in the presence of BSA and ASC in cell-culture media. However, because of ALN's high affinity to mineralized tissue, there is no difference in the number of SCC2 cells attached to calvaria bone in the presence and absence of 30 μM ALN, and there is no significant difference in SCC2 cells viability in the presence and absence of ALN and ASC, even though the calvaria-SCC2 cells co-cultured was carried out in media containing BSA. Our results are in contrast to the results of other studies that showed NBP able to reduce tumor burden on bone and decrease cancer cells metastasis (Daubine et al, 2007), and varied from the belief that cancer cells require osteoclast-mediated bone resorption to release bone-derived growth factors in order to survive in bone (Clezardin, 2011).

The result from the resorption model showed that calvaria co-cultured with

SCC2 cells resulted in significant increase in cumulative calcium release and TRAP enzyme activity, a marker for osteoclast activity, compared to calvaria alone. These observations also corresponded to the histologic study and NR staining showing multinucleated osteoclasts and osteoclast-mediated bone resorption. When calvaria was co-cultured with SCC2 cells and 30 μM ALN, significant decreases in cumulative calcium release and TRAP activity were observed compared with calvaria co-cultured with SCC2 cells along with absence of multinucleated osteoclast on the NR staining and reduced bone resorption on the histologic study. These results clearly demonstrate and are consistent with various studies which have suggested that addition of ALN can decrease the number and resorptive activity of OCs and inhibit differentiation of osteoclastic lineage cells (Clezardin, 2013; Liu, 2014). When calvaria were co-cultured with SCC2 cells and smaller dosage of ALN (single dosage 0.5 μM, 0.5 μM or 1.5 μM), no significant difference in cumulative calcium release and TRAP activity was noted compared to calvaria co-cultured with SCC2 cells. This result was consistent with NR staining and histologic study which showed multinucleated osteoclasts and bone resorption. This is consistent with a previous study (Daubine et al, 2007), which showed that a single dose of zoledronic acid and dosage lower than clinical dosage had no significant effect on bone destruction caused by cancer cell metastasis.

In the formation model when calvaria was co-cultured with SCC2 cells in the presence of ASC new bone formation was noted on the histologic study, corresponding to a significant decrease in cumulative calcium release and an

increase in ALP activity. On the other hand, when calvaria was co-cultured with SCC2 cells and 30 μM ALN in the presence of ASC, the bone was unable to undergo osteoblast differentiation as no new osteoid formation was noted on the histologic study, and a decrease in ALP activity was noted compared to calvaria + ASC alone. Similarly, co-culture of calvaria with SCC2 cells and lower dosage of ALN (single dosage 0.5 μM, 0.5 μM or 1.5 μM) in the presence of ASC showed histologically no new osteoid formation. This was accompanied with significant increase in cumulative calcium release for all three groups along with decrease in ALP activity compared to calvaria control. The results of this experiment were consistent with previous study from this laboratory (Alasmari et al, 2016), which showed that bone treated with ALN was unable to undergo new bone formation in the presence of ASC. Importantly, the present study using SCC2 cells instead of prostate (PC3) and breast (MDA-231) cancer cells also demonstrated that simultaneous co-culture of calvaria + SCC2 cells + ALN in the presence and absence of ASC that inhibition of osteoclastic bone resorption is achieved at the stage of OC differentiation. In the formation model it is evident from the 2-photon confocal microscopy images that ALN elicited degeneration of osteocytes when calvaria are stimulated to undergo OB differentiation and new osteoid formation. Therefore, ALN's regulation of OC at the differentiation level resulted in impaired function of OB and osteocytes which are responsible for synthesis of RANKL that is essential for the differentiation of macrophages to OCs.

The current study in addition also investigated the phenomenon of whether cancer-bone interaction and bone colonization was dependent on live bone and

bone lining cell layers. The impact of devitalizing bone and bone cells was evaluated by subjecting the bone to formaldehyde fixation and/or repeat freezing approaches. Formaldehyde is commonly used as tissue fixative by cross-linking amino groups in proteins with nearby nitrogen atoms while freezing and thawing calvarial bone would induce osteocytes, osteoblasts and bone lining fibroblasts to burst and die. On the histologic photomicrograph, calvaria co-cultured with SCC2 cells in the presence and absence of ASC showed reduced number of periosteal and endosteal cells, and majority of osteocytes present did not have nuclei present. Such bone organs co-cultured with cancer cells showed no cancer cell colonization neither in resorption nor formation model system, indicating that dead bone can not support cancer cell attachment, colonization and growth. This observation corresponded to the decreased in cumulative calcium release and TRAP/ALP activity as bone resorption was reduced due to lack of cancer cells colonization as a result of reduce calvarial cells viability. When bone treated with 10% formaldehyde was co-cultured with SCC2 cells in the presence and absence of ASC histologic study showed intact osteocyte nuclei and preserved periosteal and endosteal cells. But similar to bone that has been frozen/thawed no cancer cell colonization was noted in the resorption or formation model. Decrease in cumulative calcium release and TRAP activity was noted in the resorption model, while a significant decrease in calcium release was noted in the formation model with decrease in ALP activity. This decrease in cumulative calcium release in the bone formation model may be due to increased mineral deposition of the hydroxyapatite in the presence of the protein-

crosslinking caused by the formaldehyde treatment. Observations from both experimental groups suggested that bone with reduced viability would not be able to support cancer cells therefore cancer cells metastasis to bone would be affected negatively in the presence of bone injury, bone toxicity and bone cell-death.

Some limitations of the experiment include small sample size and short culture period. Certain experimental groups in this study only contain three or four samples; therefore increasing sample size in the future may ensure consistency in the result and accuracy in the statistical analysis. Extending the culture period may allow us to investigate the long-term effect of ALN has on SCC2 cells, calvarial bone and the calvaria-SCC2 cell interaction. Future direction of our study will continue with investigation of other BPs' and their impact on SCC2 cells and cancer-bone cells interactions.

## 9. Bibliography


Alasmari, A., Lin, S.C., Dibart, S., Salih, E. (2016). "Bone Microenvironment-Mediated Resistance of Cancer Cells to Bisphosphonates and Impact on Bone Osteocytes/Stem Cells." *Clinical & Experimental Metastasis.* **33**(6): 563-88.

Allen, M.R., Burr, D.B. (2009). "The Pathogenesis of Bisphosphonate-related Osteonecrosis of the Jaw: So Many Hypotheses, So Few Data." *Journal of Oral and Maxillofacial Surgery.* **1**(5 Suppl): 61-70.

Amin, D., Cornell, S. A., Perrone, M.H., Bilder, G.E. (1996). "1-Hydroxy-3-(methylpentylamino)-propylidene-1,1-bisphosphonic Acid As A Potent Inhibitor of Squalene Synthase." *Arzneimittel-Forschung.* **46**(8): 759-62

Berenson, J.R. (2011). "Antitumor Effects of Bisphosphonates: From the Laboratory to the Clinic." *Current Opinion in Supportive and Palliative Care.* **5**(3): 233-40

Buckwalter, J.A., Glimcher, M.J., Cooper R.R., Recker, R. (1996). "Bone Biology I: Structure, Blood Supply, Cells, Matrix, and Mineralization." *Instructional Course Lectures.* **45**: 371-86.

Carlson, E.R., Ord, R.A. (2002). "Vertebral Metastases From Oral Squamous Cell Carcinoma." *Journal of Oral and Maxillofacial Surgery.* **60**(8): 858-62.

Coleman, R.E. (2008). "Risks and Benefits of Bisphosphonates." *British Journal of Cancer.* **98**(11): 1736-40

Clezardin, P. (2011). "Bisphosphonates' Antitumor Activity: An Unraveled Side of a Multifaceted Drug Class." *Bone.* **48**(1): 71-9.

Curtin, P., Youm, H., Salih, E. (2012). "Three-Dimensional Cancer–Bone Metastasis Model Using ex vivo Co-cultures of Live Calvarial Bones and Cancer Cells." *Biomaterials.* **33**(4): 1065–1078.

D'Aoust, P., McCulloch, C.A., Tenebaum, H.C., Lekic, P.C. (2000). "Etidronate (HEBP) Promotes Osteoblast Differentiation and Wound Closure in Rat Calvaria." *Cell and Tissue Research.* **302**(3): 353-363.

de Groen, P.C., Lubbe, D.F., Hirsch, L.J., Daifotis, A., Stephenson, W., Freedholm, D., Pryor-Tillotson, S., Seleznick, M.J., Pinkas, H., Wang, K.K. (1996). "Esophagitis Associated with the Use of Alendronate." *New England Journal of Medicine.* **335**(14): 1016-21.

Daubine, F., Le Gall, C., Gasser, J., Green, J., Clezardin, P. (2007). "Antitumor Effects of Clinical Dosing Regiments of Bisphosphonates in Experimental Breast Cancer Bone Metastasis." *Journal of the National Cancer Institute.* **99**(4): 322-30.

Donetti, E., Gualerzi, A., Sardela, A., Lodi, G., Carrassi, A., Sforza, C. (2014). "Alendronate Impairs Epithelial Adhesion, Differentiation, and Proliferation in Human Oral Mucosa." Oral Diseases. **20**(5): 466-72.

Dorogi, P.L. (1984). "Kinetics and Mechanism of Ca2+ Binding to Arsenazo III and Antipyrylazo III." *Biochimica et Biophysica Acta (BBA)-General Subjects.* **799**(1): 9-19.

Eastell, R., O'Neill, T.W., Hofbauer, L.C., Langdahi, B., Reid, I.R., Gold, D.T., Cummings, S.R. (2016). "Postmenopausal Osteoporosis." *National Review Disease Primers.* **29**(2): 1-16

Fan, T.M. (2007). "The Role of Bisphosphonates in the Management of Patients That Have Cancer." *Veterinary Clinics of North America: Small Animal Practice.* **37**(6): 1091-1110.

Fleisch, H. (2000). Bisphosphonates in Bone Disease – From the Laboratory to the Patient. San Diego, Academic Press.

Fleisch, H., Maerki, J. and Russell, R.G. (1966). "Effect of Pyrophosphate on Dissolution of Hydroxyapatite and Its Possible Importance in Calcium Homeostasis." *Proceedings of the Society for Experimental Biology and Medicine.* **122**(2): 317-20.

Franzen, A. and Heinegard, D. (1985). "Isolation and Characterization of Two Sialoproteins Present Only in Bone Calcified Matrix." *Biochemical Journal.* **232**(3): 715-724.

Giuliani, N., Pedrazzoni, M., Negri, G., Passeri, G., Impicciatore, M., Girasole, G. (1998). "Bisphosphonates Stimulate Formation of Osteoblast Precursors and Mineralized Nodules in Murine and Human Bone Marrow Cultures in vitro and Promote Early Osteoblastogenesis in Young and Aged Mice in vivo." *Bone.* **22(**5): 455-61.

Gnant, M., Clezardin, P. (2012). "Direct and Indirect Anticancer Activity of Bisphosphonates: A Brief Review of Published Literature." *Cancer Treatment Reviews.* **35**(5): 407-415.

Hemeda, H., Giebel, B., Wagner, W. (2014). "Evaluation o Human Platelet Lysate Versus Fetal Bovine Serum for Culture of Mesenchymal Stromal Cells." *Cytotherapy.* **16**(2): 170-80.

Idris, A.I., Rojas, J., Greig, I.R., Van't Hof, R.J., Ralston, S.H. (2008). "Aminobisphosphonates Cause Osteoblast Apoptosis and Inhibit Bone Nodule Formation in vitro." *Calcified Tissue International.* **82**(3): 191-201.

Kowalski, L.P., Carvalho, A.L., Martins Priante, A.V., Magrin, J. (2005). "Predictive Factors for Distant Metastasis From Oral and Oropharyngeal Squamous Cell Carcinoma." *Oral Oncology.* **41**(5): 534-41.

Kruger T.B., Herlofson, B.B., Landin, M.A., Reseland J.E. (2016). "Alendronate Alters Osteoblast Activities." *Acta Odontologica Scandinavica.* **74**(7): 550-7.

Liu, J. L. J. (2014). "Biological Actions of Nitrogen-Containing Bisphosphonates on Bone Remodeling Using an Ex-vivo Live Calvarial Bone Organ Model System (Master's Thesis)." Boston University Henry M. Goldman School of Dental Medicine, Boston, United States of America.

Marshall, C.J. (1993). "Protein Prenylation: A Mediator of Protein-Protein Interactions." Science. **259**(5103): 1865-1866.

Nanci, A. (2008). Ten Cate's Oral Histology: Development, Structure and Function. Saint Louis, Elsevier.

Neville, B.W. (2008). Oral and Maxillofacial Pathology. Saint Louis, Elsevier.

Pan, B., Farrugia, A.N., To, L.B., Findlay, D.M., Green, J., Lynch, K., Zannettino, A.C. (2004). "The Nitrogen-Containing Bisphosphonate, Zoledronic Acid, Influences RANKL Expression in Human Osteoblast-like Cells by Activating TNF-alpha Converting Enzymes (TACE)." *Journal of Bone and Mineral Research.* **19**(1): 147-54.

Pires, A.S., Marques, C.R., Encarnacao, J.C., Abrantes, A.M., Mamede, A.C., Laranjo, M., Goncalves, A.C., Sarmento-Ribeiro, A.B., Botelho, M.F. (2016). "Ascorbic Acid and Colon Cancer: An Oxidative Stimulus to Cell Death Depending on Cell Profile." *European Journal of Cell Biology.* **95**(6-7): 208-18.

Plotkin, L., Weinstein, R.S., Parfitt, A.M., Roberson, P.K., Manolagas, S.C., Bellido, T. (1999). "Prevention of Osteocyte and Osteoblast Apoptosis by Bisphosphonates and Calcitonin." *Journal of Clinical Investigation.* **104**(10): 1363-74.

Ridley, A.J., Paterson, H.F., Johnston, C.L., Diekmann, D., Hall, A. (1992). "The Small GTP-binding Protein Rac Regulates Growth Factor-Induced Membrane Ruffling." *Cell.* **70**(3): 401-410.

Roelofs, A.J., Ebetino, F.H., Reszka, A. A., Russell, R. G. G., Rogers, M.J (2008). Bisphosphonates. Principles of Bone Biology. Saint Louis: Elsevier.

Rogers, M.J., Crockett, J.C., Coxon, F.P., Monkkonen, J. (2011). "Biochemical and Molecular Mechanisms of Action of Bisphosphonates." *Bone.* **49**(1): 34-41.

Ross, F.P., Christiano, A.M. (2006). "Nothing But Skin and Bone." *Journal of Clinical Investigation.* **116**(5): 140-9.

Russell, R.G., Bisaz, S., Fleisch, H., Currey, H.L., Rubinstein, H.M., Dietz, A.A., Boussina, I., Micheli, A., Fallet, G. (1970). "Inorganic Pyrophosphate in Plasma, Urine, and Synovial Fluid of Patients with Pyrophosphate Arthropathy (Chondrocalcinosis or Pseudogout)." *The Lancet.* **2**(7679): 899-902.

Sato, M., Grasser, W., Endo, N., Akins, R., Simmons, H., Thompson, D.D., Golub, E., Rodan, G.A. (1991). "Bisphosphonate Action. Alendronate Localization in Rat Bone and Effects on Osteoclast Ultrastructure." *Journal of Clinical Investigation.* **88**(6): 2095-2105.

Schenk, R., Eggli, P., Fleisch, H., Rosini, S. (1986). "Quantitative Morphometric Evaluation of the Inhibitory Activity of New Aminobisphosphonates on Bone Resorption in the Rat." *Calcified Tissue International.* **38**(6): 342-49.

Sunberg, R.J., Mosher, E.F., Roof, C.F. (1991). "Designing Drugs for Stronger Bones." *Chemtech.* **21**: 304-09

Takes, R.T., Rinaldo, A., Silver, C.E., Haigentz, M. Jr., Woolgar, J.A., Triantafyllou, A., Mondin, V., Paccagnella, D., de Bree, R., Shaha, A.R.,

Hartl, D.M., Ferlito, A. (2012). "Distant Metastases From Head and Neck Squamous Cell Carcinoma. Part I. Basic Aspects." *Oral Oncology.* **48**(9): 775-9.

Takahama ,A Jr., Correa, M.B., de Almeida, O.P., Lopes, M.A. (2014). "Oral Squamous Cell Carcinoma Metastasizing to the Skull Bone: A Care Report and Literature Review." *General Dentistry.* **62**(2): 59-61.

Tatevossian, A. (1973). "Effect of Parathyroid Extract on Blood Calcium and Osteoclast Count in Mice." *Calcified Tissue International.* **11**(3): 251-7.

Tenenbaum, H.C., Torontali, M., Sukhu, B. (1992). "Effects of Bisphosphonates and Inorganic Pyrophosphate on Osteogenesis in Vitro." *Bone.* **13**(3): 249-55.

Tsuchimoto, M., Azuma, Y., Higuchi, O., Sugimoto, I., Hirata, N., Kiyoki, M., Yamamoto, I. (1994). "Alendronate Modulates Osteogenesis of Human Osteoblastic Cells in vitro." *The Japanese Journal of Pharmacology.* **66**(1): 25-33.

Vescovi, P., Merigo, E., Meleti, M., Manfredi, M., Guidotti, R., Nammour, S. (2012). "Bisphosphonates-Related Osteonecrosis of the Jaws: A Concise Review of the Literature and a Report of a Single-Centre Experience with 151 Patients." *Journal of Oral Pathology and Medicine.* **41**(3): 214-21.

Viereck, V., Emons, G., Lauck, V., Frosch, K.H., Blaschke, S., Grundker, C., Hofbauer, L.C. (2002). "Bisphosphonates Pamidronate and Zoledronic Acid Stimulate Osteoprotegrin Production by Primary Human Osteoblasts." *Biochemical and Biophysical Research Communications.* **291**(3): 680-6.

Wang, J., Glimcher, M.J., Mah, J., Zhou, H.Y., Salih, E. (1998). "Expression of Bone Microsomal Casein Kinase II, Bone Sialoprotein, and Osteopontin During the Repair of Calvarial Defects." *Bone.* **22**(6): 621-28

Zerial, M., Stenmark, H. (1993). "Rab GTPAses In Vesicular Transport." *Current Opinion in Cell Biology.* **5**(4): 613-620.

## CURRICULUM VITAE